STATE OF RHODE ISLAND AND PROVIDENCE PLANTATIONS
ENERGY FACILITY SITING BOARD

IN RE: INVENERGY THERMAL DEVELOPMENT LLC	:	
APPLICATION TO CONSTRUCT AND	:	SB-2015-06
OPERATE THE CLEAR RIVER ENERGY	:	
CENTER, BURRILLVILLE, RHODE ISLAND	:	

PRE-FILED DIRECT TESTIMONY OF ELLEN G. COOL

Rhode Island Office of Energy Resources
One Capitol Hill
Providence, RI 02908

EXECUTIVE SUMMARY

Ellen G. Cool, Ph.D, is a Vice President and Principal of Levitan & Associates, Inc. and testifies as the sponsor for the Advisory Opinion of the Rhode Island Office of Energy Resources ("OER") dated September 12, 2016 ("OER's Advisory Opinion"). She testifies as to the impact the Clear River Energy Center ("CREC" or the "Facility" or the "Project") will have on regional greenhouse gas ("GHG") emissions, specifically, carbon dioxide ("CO_2"), the primary GHG associated with operation of a power plant. Ms. Cool testifies for purposes of updating certain findings in OER's Advisory Opinion based on information that has become available since the filing of OER's Advisory Opinion, and to address several issues raised by the Conservation Law Foundation's witness, J. Timmons Roberts. Dr. Cool, based on her expertise and experience, opines that the updated information does not alter the overall conclusion in OER's Advisory Opinion that the operation of CREC will contribute to lowering CO_2 emissions, on a consumption-accounting basis for Rhode Island.

STATE OF RHODE ISLAND AND PROVIDENCE PLANTATIONS
ENERGY FACILITY SITING BOARD

IN RE: INVENERGY THERMAL DEVELOPMENT LLC APPLICATION TO CONSTRUCT AND OPERATE THE CLEAR RIVER ENERGY CENTER, BURRILLVILLE, RHODE ISLAND	: : : :	SB-2015-06

RHODE ISLAND OFFICE OF ENERGY RESOURCES'
PRE-FILED DIRECT TESTIMONY OF ELLEN G. COOL

Q. Please state your name, title, and business address.

A. I am Ellen G. Cool, Ph.D, Vice President and Principal of Levitan & Associates, Inc. ("LAI"), and my business address is 100 Summer Street, Suite 3200, Boston, Massachusetts, 02110.

Q. Please summarize your educational background and professional experience.

A. I have an A.B. degree in geological sciences from Harvard University, and an M.S. and Ph.D. in geological sciences from the University of Washington. From 1985 to 1999 I was an environmental consultant for several environmental engineering firms, attaining the level of principal and regional manager. I am currently a Vice President and Principal at LAI, which I joined in 1999. I have 30 years of consulting experience in the energy and environmental industries. I have advised clients on competitive procurement options for wholesale power supply, including high-voltage, direct current ("HVDC") transmission projects, natural gas-fired plants, and renewable generation projects. My experience includes advising clients on environmental compliance strategies and liability assessments, siting and permitting of generation, transmission, and pipeline projects, cogeneration development, contract restructuring, acquisition of deregulated energy service companies and the net environmental impact of new and repowered generation projects. A detailed description of my experience and educational background is in my curriculum vitae which was filed with the Rhode Island Energy

Facility Siting Board ("EFSB") on September 12, 2016.

Q. Please describe LAI.

A. LAI is a management consulting firm specializing in power market design, power and fuel project evaluations, pipeline infrastructure, and competitive energy economics. Since its founding in 1989, LAI has conducted numerous assignments in New England and other markets throughout the United States and Canada on diverse matters pertaining to generation and transmission project evaluations, wholesale energy and capacity price forecasts, retail price impacts, competitive power market design, asset valuation, bulk power security, power and fuel procurements, contract structures, gas/electric interdependencies, natural gas infrastructure, and risk management. LAI's clients include utilities, generators, Independent System Operators ("ISOs"), Regional Transmission Organizations ("RTOs"), end-users, state regulatory commissions, and financial institutions.

Q. Have you previously testified before the EFSB?

A. No.

Q. Have you previously provided expert testimony before any regulatory commission, board, or agency?

A. Yes. I have testified before the Massachusetts Energy Facilities Siting Board on the economic benefits, environmental impacts, and non-transmission alternatives of a new 345 kilovolt ("kV") transmission line in southeast Massachusetts, and I testified before the New Jersey Board of Public Utilities regarding the environmental impact, including greenhouse gas ("GHG") emissions, associated with the proposed construction of three proposed gas-fired combined-cycle plants. I have also testified frequently before the Connecticut Public Utilities Regulatory Authority regarding the integrity of procurements for standard service supplies, as well as procurements for renewable and conventional generation projects.

Q. On whose behalf are you testifying?

A. My testimony is on behalf of the Rhode Island Office of Energy Resources ("OER").

Q. What is your role in this proceeding?

A. LAI was engaged by OER to provide technical assistance in developing the Advisory Opinion of the Rhode Island Office of Energy Resources dated September 12, 2016 ("OER's Advisory Opinion"). I am the designated sponsor of OER's Advisory Opinion.[1]

Q. What was the subject matter of OER's Advisory Opinion?

A. Consistent with the EFSB's directives found on page 17 of the Preliminary Decision and Order dated March 10, 2016, OER's Advisory Opinion examined the impacts of the Clear River Energy Center ("CREC" or the "Facility" or the "Project") on anticipated GHG emissions and whether the Facility will conform to the requirements and provisions of the Resilient Rhode Island Act, R.I. Gen. Laws § 42-6.2-1 et seq. (the "Act"), and other state energy policies.

Q. What was your role in preparing OER's Advisory Opinion?

A. LAI's role is described in Section II of OER's Advisory Opinion. In summary, I along with colleagues at LAI analyzed the data and other information provided by the applicant, Invenergy Thermal Development LLC ("Invenergy"), through its application filed with the EFSB on October 29, 2015 ("Application"), and through its responses to data requests issued by OER and other parties. I developed findings that were provided in OER's Advisory Opinion regarding the impact of the Project on regional GHG emissions, and consistency of the Project with respect to Rhode Island energy policy.

---

[1] The EFSB requested "that each such agency … [providing an informational advisory opinion] prepare to have a representative appear at the final hearing of the [EFSB] to sponsor the informational advisory opinion, as well as to sponsor and enter into evidence any information outside of the record of this docket that is relied upon in the advisory opinion". [Preliminary Order and Decision dated March 10, 2016, section VII (B)].

Q. What is the purpose of your testimony?

A. The purpose of my testimony is twofold: (1) to update certain findings in OER's Advisory Opinion based on information that has become available since OER's Advisory Opinion was filed, including testimony and updated analyses provided by Invenergy; and (2) to address several issues raised by Professor J. Timmons Roberts, a witness for the Conservation Law Foundation ("CLF"), through CLF's responses to data requests and through Professor Roberts' pre-filed direct testimony.

Q. Did you prepare this testimony yourself?

A. I personally conducted or supervised the work of LAI staff that assisted me in preparing this testimony.

Q. The Office of Energy Resources' Third Set of Data Requests Directed to Invenergy dated April 10, 2017 asked Invenergy to update its analysis of the Project's operation and GHG emissions. Why was this necessary?

A. Invenergy's Application provided a forecast of CREC's impact on the regional electricity markets and on GHG emissions over the period 2019 to 2025. Invenergy acknowledged that the forecast model was based on electricity and fuel market data and other assumptions available to its consultant, PA Consulting Group, Inc. ("PA"), when it ran the model, some time prior to June 2015.[2] The purpose of OER's data request was to assess whether market developments over the past two years may have altered Invenergy's or OER's conclusions regarding GHG impacts ascribable to CREC.

Q. What relevant market developments have occurred over the past two years?

A. There have been four significant market changes that have the potential to materially

[2] PA issued a confidential memorandum describing its model on June 16, 2015, so the model inputs were "locked down" prior to that date.

change the GHG impact results: (i) A decrease in the price of natural gas over the forecast period, and more specifically, a decrease in natural gas price relative to coal and oil; (ii) An increase in the penetration of new renewable resources over the forecast period, attributable in part to an expansion of distributed renewable generation across the region, and pending procurement of renewable resources under long term contracts conducted by Rhode Island, Massachusetts and Connecticut; (iii) An increase in energy efficiency and behind-the-meter solar photovoltaic ("PV") resources over the forecast period; and (iv) A decrease in forecasted net load, as evident by a comparison of the load forecast data in the 2015 Capacity, Energy, Loads, and Transmission ("CELT") report issued by the Independent System Operator – New England ("ISO-NE") versus the 2017 CELT report.

Q Did PA's revised model utilize updated market information?

A. The model appears to have utilized the most currently available market information at the time that the modeling work was undertaken. Through supplemental response 3-2 of Invenergy Thermal Development LLC's Supplemental Responses to the Office of Energy Resources' Third Set of Data Requests dated June 23, 2017 ("OER-DR-3-2"), Invenergy provided information regarding the market assumptions used by PA in its May 2017 update to the electric market simulation model. Natural gas prices were based on NYMEX futures prices on April 28, 2017, which are reasonably current. For New England, PA utilized the load data from the 2017 CELT report, which appropriately updates the load forecast for the region and was released by ISO-NE on May 15, 2017. For New York, PA used the 2017 Load and Capacity Data Report, the most recent forecast publicly available released on April 1, 2017. PA's carbon dioxide ("CO_2") emission allowance price forecast was also updated based on more recent Regional Greenhouse Gas Initiative ("RGGI") auction results, including the March 8, 2017 auction.

Q. Were there any other significant updates to the input assumptions in PA's model?

A. The buildout of renewable resources in New England increased by 665 megawatts ("MW") (151%) on a nameplate capacity basis in the 2017 model update, reflecting an expected increase in the penetration of renewable resources across the region.

Q. What were PA's conclusions regarding changes in GHG emissions based on the updated analysis?

A. In his pre-filed direct testimony, filed June 30, 2017, Mr. Ryan Hardy reported that over the first five years of CREC's operation, 2020 through 2024, CREC would lead to an annual average CO_2 emissions reduction of 0.95% for the New England and New York Region (p. 21, lines 20-25).

Q. Is this statement consistent with more detailed model results provided by Invenergy in its response to OER-DR-3-2?

A. Yes, I confirmed this percent reduction from the data provided in Confidential Exhibit B to OER-DR-3-2.

Q, How do the updated model results compare with the model findings presented in the Application?

A. On a percentage basis, this emission reduction resulting from the updated analysis is generally consistent with PA's results presented in the Application (p. 120). The Application concluded that operation of CREC would produce a 1.01% reduction in CO_2 emissions across the New England and New York region, on an average annual basis between 2019 and 2025, just slightly higher.

Q. Did the 2017 updated model reveal any other changes to the forecast of regional emissions?

A. Yes. If I compare the forecast of total regional emissions of CO_2 across New England and New York between PA's updated model and PA's 2015 model, CO_2 emissions decreased by approximately 10% on an average annual basis in the 2017 updated model, regardless of whether CREC was included in the model.

Q. Why do you believe that the modeled CO2 emissions have decreased across the region between the 2015 analysis and the 2017 update?

A. I believe that there are three contributing factors. First, from 2015 to 2017, ISO-NE's forecast of net load across New England has decreased, reducing the demand for electricity. The decreased net load forecast is due, in large part, to the increase in energy efficiency and behind-the-meter PV. Dispatchable fossil-fuel fired resources would run less in response to decreased demand for energy, reducing CO2 emissions. Second, a decrease in natural gas prices relative to coal prices would cause gas-fired resources to displace coal, which is a more carbon-intensive fuel. I noted that coal generation in the 2017 updated model results has decreased by 88% relative to the 2015 model results. Third, the increase in renewable resources in the 2017 updated model results would also contribute to reducing CO_2 emissions.

Q. Does the decrease in overall CO_2 emissions in the 2017 updated model alter your conclusion about the impact of CREC's operation on CO_2 emissions?

A. No. As previously stated, on a percentage reduction basis, the 2017 model results are consistent with the model results presented in the Application. Because the total emissions across the region is reduced in the 2017 update, a 0.95% average annual decrease in regional emissions ascribable to the addition of CREC is equal to approximately 644,000 short tons per year of avoided CO_2 emissions when both CREC units are in service. The comparable value presented in the Application was approximately 1,058,500 short tons. That is, the updated model indicates that operation of CREC still results in a decrease in CO_2 emissions, but the magnitude of the decrease on a short tons per year basis is smaller.

Q. Mr. Hardy's pre-filed direct testimony and Invenergy's response to OER-DR-3-2 presented only model results from 2020 through 2024. In his testimony (page 41, lines 10-11), Mr. Hardy stated that he "would expect continued emissions and ratepayer energy costs savings over a much longer timeframe." Is it reasonable to draw conclusions about the impacts of CREC's operation over the long term based on only five years of model results?

A. Without model results beyond 2024, it is not possible to quantify CREC's contribution to emissions reductions across the New England and New York region. I do, however, concur that it is reasonable to expect that CREC will continue to contribute to regional CO_2 emissions reductions beyond 2024, relative to a future without CREC. As discussed in OER's Advisory Opinion (page 20-21), because CREC would be one of the most efficient gas-fired resources in the region, it will continue to displace energy from less efficient and higher emitting fossil-fired resources. I anticipate that clean energy policies of New England states will continue to promote increased development and penetration of renewable resources and energy efficiency in order to achieve states' greenhouse gas reduction targets. As a consequence, over time the region will rely less on the incumbent fossil-fired resources, including CREC, and therefore CREC's contribution to reducing regional CO_2 emissions will diminish.

Q. Are you aware that Invenergy has submitted an Addendum to its Major Source Permit Application, in which Invenergy proposes to reduce the number of days per year that the Facility would be permitted to burn ultra-low sulfur distillate ("ULSD") as a backup fuel when the primary fuel, natural gas, is not deliverable due to pipeline

constraints?

A. Yes. Invenergy's Application states that it requested the Rhode Island Department of Environmental Management ("DEM") to issue an air permit that would allow it to run each of the two combustion turbine units for 30 days per year on ULSD. I am aware that the Addendum that Invenergy subsequently filed on September 15, 2016 proposed to revise the limit to 15 days per year on ULSD for each unit. The Addendum also stated that ULSD would be used only for oil system readiness testing, if gas is curtailed, or if the pipeline declares a force majeure event. Table 1 of the Major Source Permit Addendum also provides an update to the potential emissions summary data for the Facility.

Q. Would the change from 30 days per year to 15 days per year on ULSD for each unit change any of the findings in OER's Advisory Opinion?

A. Yes. On page 15 of OER's Advisory Opinion, I calculated that burning ULSD for 30 days for each unit would emit 415,440 tons of CO_2 during those days, or an increase of approximately 128,000 tons per year over burning natural gas. If the allowable days of ULSD usage were reduced to 15 days per year for each unit, the Project would emit 209,736 tons of CO_2 during those days, or an increase of approximately 75,850 tons of CO_2 over burning natural gas. This calculation utilizes the updated emission rate information provided in Table 1 of the Major Source Permit Addendum.

Q. How would burning oil for 15 days each year affect PA's updated model results, which concluded that operation of CREC would reduce regional CO_2 emissions by 0.95% on an annual average basis between 2020 and 2024?

A. I cannot quantify this from the available information, since an event that would trigger ULSD usage was not modeled. Plants with dual fuel capability can switch to burning oil when there are constraints on the gas pipeline system. This typically occurs during cold snaps, when the lion share of gas pipeline capacity is used by the local gas distribution companies to deliver gas for their core heating load, driving up the delivered price of natural gas. While CREC might switch to ULSD during cold snaps, other plants in the region would do so as well. Since oil is a more CO_2-intensive fuel than natural gas, emissions would increase across the region, relative to a case where there are no gas pipeline constraints. However, I would expect that emissions with CREC in operation would be less than without CREC in operation, since even when burning ULSD CREC will be one of the most efficient plants in the region.

Q. Are there any other findings in OER's Advisory Opinion that would change?

A. Yes. On page 19 of OER's Advisory Opinion, I calculated that burning ULSD for the maximum of 30 days per year for each unit would result in an average annual CO_2 emission rate of approximately 815 pounds per megawatt-hour ("MWh"). If the annual limit is reduced to 15 days per year for each unit, and using the emission rate data in the Major Source Permit Addendum, the average annual CO_2 emission rate falls to approximately 776 pounds per MWh.

Q. Would these changes alter the conclusion in OER's Advisory Opinion that operation of CREC would contribute to lowering CO_2 emissions, on a consumption-accounting basis, for Rhode Island?

A. No. Using ULSD for 15 days per year for each unit rather than 30 days per year for each unit would reduce the overall GHG emissions from the Project all else remaining the same, since ULSD is a more carbon-intensive fuel than natural gas.

Q. According to Invenergy's Application, 67 acres will be acquired from Spectra Energy to construct the Facility. The Application (at page 9) indicates that the property is forested. Recognizing that trees and other vegetation sequester carbon, shouldn't clearing

of vegetation to construct the Facility be accounted for in the GHG impact analysis of CREC?

A. Removal of trees and other vegetation from the site has no direct impact on electric sector GHG accounting for Rhode Island. However, it is possible to estimate the CO_2 equivalent that would otherwise be sequestered in the biomass each year if the vegetation were not cleared.

Q. Would this be a material offset to the CO_2 emission reduction that Invenergy's consultant, PA, attributes to CREC?

A. No. The available measurements of carbon content in forests indicate that removing trees and other vegetation from the CREC site would not be a significant offset to the CO_2 emissions reduction ascribable to the operation of CREC. I relied on a metastudy conducted by S. Luyssaert and others, which compiled a global database of CO_2 data for various types of forests.[3] The mass of CO_2 that is sequestered in forests varies widely depending on the type and age of trees and the climate. For temperate deciduous forests found in the Northeast, measurements of the uptake of CO_2 average approximately 5.1 short tons of CO_2 per acre per year. Conservatively, assuming that all 67 acres of the property would be cleared, this would result in 341 tons per year of CO_2 that would not be sequestered by forest growth. This incremental quantity represents a very small offset to the approximately 644,000 short tons per year of avoided CO_2 based on the 2017 model update.

Q. What about the CO_2 content of the trees and vegetation currently on the property?

A. Assuming that the trees and other vegetation currently on the property would all be combusted or allowed to biodegrade, I computed the total CO_2 equivalent content across the property. I relied on a study by Thurner and others, who measured carbon content and carbon

---

[3] Luyssaert, S., et al, 2007, "CO_2 balance of boreal, temperate, and tropical forests derived from a global database," Global Change Biology, 13, 2509–2537. A copy is attached as Exhibit ECG-1.

density in temperate forests in the Northern Hemisphere.[4] They found that temperate broadleaf and mixed forests in the Northern Hemisphere store on average approximately 95 short tons of CO_2 equivalent per acre. This equates to approximately 6,400 tons of CO_2 equivalent for the entire 67-acre CREC site. That is, if we suppose that all of this vegetation on the site is cleared and either used as biomass fuel or allowed to naturally decompose, it would emit 6,400 tons of CO_2. We could account for this as either a single year's release or spread out over the life of the plant. Either way, it is clear that the CO_2 emission reduction ascribable to the operation of CREC would dwarf the incremental CO_2 release from clearing the vegetation across the property.

Q. Are you aware of the changes to the Invenergy Water Supply Plan?

A. Yes. I understand that Invenergy submitted on January 11, 2017 a revised Water Supply Plan under which water would be transported by truck to the site.

Q. Does the revised Water Supply Plan alter your findings in OER's Advisory Opinion submitted in September?

A. No. However, it would be reasonable to include tailpipe emissions associated with delivery of water, fuel, and other supplies to the Facility. Based on my analysis, I conclude that the tailpipe emissions would be a minor offset and not enough to materially change the findings of OER's Advisory Opinion.

Q. Please explain the basis for this conclusion.

A. I estimated the CO_2 emissions that would result from the water deliveries based on the revised Water Supply Plan filed on January 11, 2017 and information submitted by Invenergy on February 14, 2017 through Invenergy's Responses to the Town of Burrillville's 22nd Set of Data

[4] Thurner, M, et al., 2014, "Carbon stock and density of northern boreal and temperate forests," Global Ecology and Biogeography, 23, 297-310. A copy is attached as Exhibit ECG-2.

Requests. Appendix E to Invenergy's revised Water Supply Plan contains a traffic analysis and provides expected truck travel routes. Based on Invenergy's Response to the Town of Burrillville's Data Request 22-13, it is expected that two to three water trucks per day would be needed on a daily basis when the Facility is fueled by gas, but up to five trucks per day may be needed occasionally. Invenergy proposed the trucks be filled with water at a station in Johnston, Rhode Island and transported to the Spectra Energy Algonquin Compressor Station site on Wallum Lake Road in Burrillville, which by way of US-44 and RI-100 is approximately 40 miles roundtrip. The tailpipe emissions rate for diesel-fueled trucks is 22.4 pounds of CO_2 per gallon burned, based on information from the U.S. Energy Information Administration.[5] Assuming gas mileage for heavy-duty trucks that utilize diesel fuel ranges from four to eight miles per gallon, truck deliveries of water would result in an additional 41 to 205 tons of CO_2 emissions per year ascribable to CREC, depending on the number of daily roundtrips and the truck fuel efficiency, assuming that the plant operates on natural gas year-round. Relative to the annual average avoided emissions ascribable to CREC of 644,000 tons per year, this is a small offset.

Q. How would the tailpipe emissions from water trucks change if ULSD is burned for 15 days a year?

A. According to the Water Supply Plan (page 14), each day of an oil firing will require 724,320 gallons of water from the on-site water tank, which would be replenished after an oil-firing event. The water delivery trucks are expected to have a capacity of 8,000 gallons. Thus, for 15 days of oil usage, 1,358 truck round trips would be needed to replenish 10,864,800 gallons of water used. The water replenishment trucks following 15 days of ULSD use would contribute an incremental 152 tons of CO_2 in tailpipe emissions, conservatively assuming a truck fuel

[5] Based on U.S. Energy Information Administration, Carbon Dioxide Emissions Coefficients by Fuel, https://www.eia.gov/environment/emissions/co2_vol_mass.php

efficiency of only 4 miles per gallon. On an annual basis, assuming ULSD is burned for 15 days per year and natural gas for the remaining days, the total tailpipe emissions from water supply trucks would be a maximum of 357 tons of CO_2 per year ascribable to CREC.

Q. Are there other truck deliveries that should be accounted for?

A. Yes. In addition to water deliveries, Invenergy's Response to the Town of Burrillville's Data Request 22-1 ("Burrillville-22-1") and 22-2 ("Burrillville 22-2") indicate that there will be an estimated 15 ammonia trucks making trips to the CREC site per month, and typically one demineralizer trailer per month.

CREC does not yet have a contractual agreement with any suppliers for the plant's delivery of ammonia, demineralization, or ULSD, but several potential suppliers have been contacted. Based on Invenergy's response to the Town of Burrillville's 27th Set of Data Requests, Request 27-6 ("Burrillville-27-6") and 27-7 ("Burrillville-27-7"), I computed the approximate round trip mileage for the ammonia trucks and demineralizer trailer, each from two separate potential suppliers. The potential ammonia truck routes will range from 86.4 to 104.6 miles roundtrip, and would result in 22 to 53 tons of CO_2 emissions per year ascribable to CREC, depending on the selected supplier and truck fuel efficiency. The potential demineralizer trailer routes range from 116 to 117 miles roundtrip, and would result in an additional 2 to 4 tons of CO_2 emissions per year ascribable to CREC, depending on the selected supplier and truck fuel efficiency. According to Burrillville 22-8, two additional trucks for ammonia, demineralization, and/or wastewater may be required following oil firing. Additionally, following an oil firing event, ammonia and demineralizer trucks would contribute an additional 0.31 to 0.62 tons of CO_2 per day. Assuming one day of replenishment for each day of oil firing, and a full 15 days of ULSD usage per year, tailpipe emissions associated with ammonia and demineralizer deliveries would contribute in approximately 4.7 tons to 9.3 tons on an annual basis.

No supplier has been contacted yet for the delivery of hydrogen tube trailers, so I am unable to provide emission estimates for these trucks at this time I would expect, however, that it would be a small adjustment and not alter my conclusions.

Q. Did you estimate the tailpipe emissions associated with delivery of ULSD?

A. Yes. According to Exhibit 27-7 to Burrillville-27-7, the truck route from the potential ULSD supplier is approximately 54.4 miles roundtrip. Based on the maximum unit heat input rate for ULSD provided in Table A-2 of the Major Source Permit Addendum, I estimated that the Facility could burn a maximum of 19,000,000 gallons per year if both units burned ULSD for the full 15 days per year. The capacity of oil tank trailers is not specified, but for the purpose of this analysis I assumed the capacity would be 8,000 gallons, which is a typical size. If the ULSD is delivered in 8,000-gallon capacity trailers, this would require a total of 2,377 round trips per year, resulting in approximately 181 to 362 tons of tailpipe CO_2 emissions per year, depending on truck fuel efficiency. Larger trailers would require fewer trips.

Q. Based on your estimates, what would be the maximum tailpipe emissions associated with deliveries to the Facility?

A, Conservatively, the total contribution of tailpipe CO_2 emissions from the water, ULSD, ammonia, and demineralization trucks, assuming a full 15 days of ULSD burn, would be approximately 785 tons CO_2 per year. This represents only a 0.122 percent offset to the 644,000 tons annual average avoided emissions ascribable to operation of CREC.

Q. What would be the maximum annual GHG burden ascribable to CREC if you included all the tailpipe emissions and the impact from clearing all of the vegetation on the site?

A. The sum of my estimate of the total tailpipe emissions plus the impact of land clearing would be 1,446 tons per year, assuming that the vegetation initially cleared from the property decomposes over 20 years. This is only 0.22 percent of the expected annual average CO_2 emissions.

Q. Is there any other information included in OER's Advisory Opinion which should be updated?

A. Yes. Figure 1 on page 13 of OER's Advisory Opinion compares the forecast of CO_2 allowance prices produced for the RGGI 2016 Program Review, to the CO_2 allowance price forecast utilized by PA. The RGGI 2016 Program Review produced a range of forecast trajectories, corresponding to a range of assumptions regarding the stringency of the RGGI annual CO_2 cap and other future regulations. On June 27, 2017, the RGGI Program Review released a draft 2017 policy scenario overview that unveiled nine new forecast scenarios that collectively replace the scenarios used in the 2016 RGGI Program Review and in OER's Advisory Opinion. The new scenarios feature three policy cases: Policy Case 1 has a 2.5% cap decline from 2021-2030; Policy Case 2 has a 3.5% cap decline from 2021-2030; and Policy Case 3 has a 6.52% cap reduction in 2019 and a cap that declines 3.0% from 2021-2030. The different Policy Cases were run with alterative scenarios that incorporate differing assumptions regarding a national CO_2 program. The range of the new RGGI forecast scenarios, shown in the figure below, result in overall price trajectories that are generally lower than the forecast range illustrated in Figure 1 of OER's Advisory Opinion.

Figure 1

2017 RGGI Policy Scenario Forecast Range[6]

---

[6] RGGI Program Review materials may be accessed at: http://www.rggi.org/design/2016-program-review/rggi-meetings

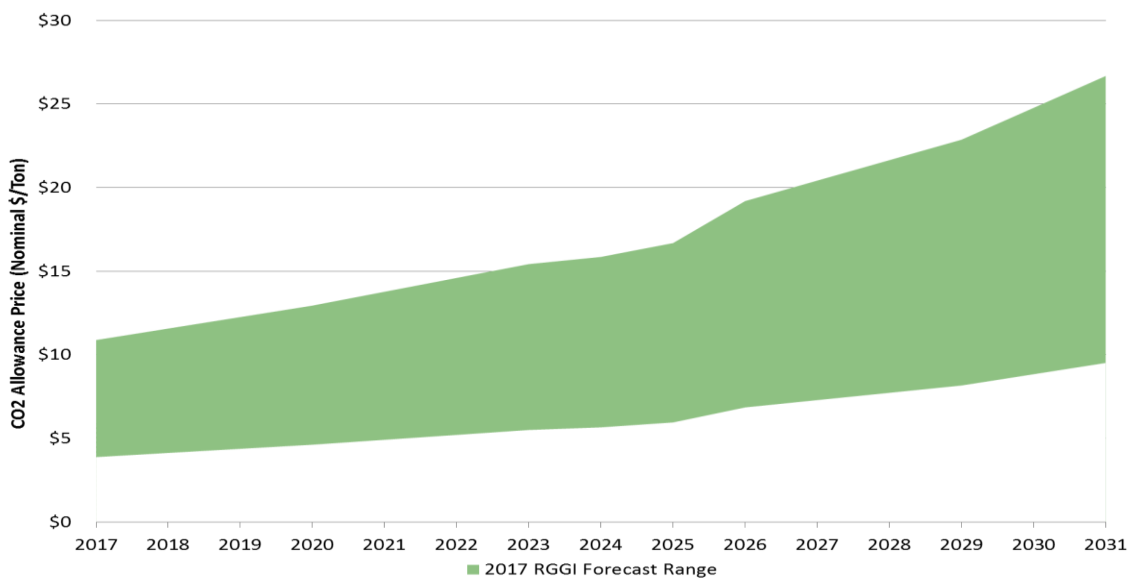

Q. **Does the change in the RGGI forecast change the findings in OER's Advisory Opinion?**

A. No. OER's Advisory Opinion noted that PA's RGGI allowance forecast is low compared to all of the RGGI 2016 Program Review scenario forecasts, but that using a low forecast conservatively estimates the output of the Facility and the system-wide CO_2 emission reductions. PA's updated allowance price forecast remains at or below the lowest of the RGGI scenario forecasts.

Q. How do these forecasts compare with recent RGGI auction clearing prices?

A. Quarterly RGGI auction clearing prices from 2014 through the most recent auction on June 7, 2017 have ranged from $2.53/ton to $7.50/ton, with an average of $4.78/ton.

Q. Are you familiar with the pre-filed direct testimony offered by Professor J. Timmons Roberts in this docket, on behalf of CLF?

A. Yes, I am.

Q. On page 16 of his pre-filed direct testimony, Professor Roberts predicts that CREC would likely run on backup ULSD during heat waves during the summer and compound

the GHG emissions impacts. Do you agree with this assertion?

A. No, I do not.

Q. Why not?

A. In the Northeast, the demand for natural gas is highest on very cold winter days when homes and businesses rely on gas for heating. On those days, the interstate pipelines that transport gas into and through the region operate at full capacity, or very nearly so. Local gas distribution companies ("LDCs") that deliver gas to homes and businesses have primary firm contractual rights to the capacity on the pipelines. Most gas-fired electric generators take interruptible service on the pipelines, which is a lower priority right, and so they can only schedule gas to the extent that there is spare pipeline capacity not used by the LDCs. On very cold winter days when pipelines are most constrained, interruptible service customers are most likely to be curtailed, and electric generators that are permitted to use backup fuel oil are likely to switch to oil. During the summer, when residential, commercial, and industrial customers' gas demand is low and gas demand for electric generation is highest, there is typically sufficient pipeline capacity for interruptible service customers, and electric generators do not need to rely on backup fuel oil.

Q. Do you have any data that supports your expectation of electric generators' use of backup fuel in summer versus winter?

A. Yes. I examined the recent operating history of the three gas-fired electric generators in Rhode Island that are permitted to use backup fuel oil: Manchester Street, Ocean State Power, and Pawtucket Power. Manchester Street and Ocean State Power are directly connected to the Algonquin pipeline system, the same pipeline on which CREC proposes a direct connection. Pawtucket Power is located behind the citygate of the LDC, National Grid.

I analyzed a database of plant emissions that is maintained by the U.S. Environmental Protection Agency ("EPA") and publicly available on the EPA's website. Most fossil-fueled electric generators are required to report to the EPA hourly emissions data collected by their continuous emission monitoring systems ("CEMS"). This information is used by regulators to determine whether fossil-fueled electric generators are operating within their emission limits for regulated pollutants. Because the CO_2 emission rate when a unit is burning natural gas is quite different from the rate when burning oil, it is possible to distinguish which fuel was burned in each hour the unit is producing electricity. I used the CEMS hourly CO_2 emissions data to determine whether the individual units at these three plants were burning gas or oil during each hour of the peak summer months (July and August) and the peak winter months (December, January, and February). Review of CEMS data was performed for the peak months in 2013 through February 2017.

Exhibit EGC-3 shows the percentage of hours that each Manchester Street, Ocean State Power, and Pawtucket Power unit burned oil during these months. The results show that Manchester Street and Ocean State Power burned oil only during the winter, and none during any of the peak summer months, 2013 through 2016. Pawtucket Power burned oil nearly all of the time it operated in January and February, but only during 2% of the time that it operated during one of the summer months, August 2015. These findings are consistent with the statement in CREC's air permit application that "the gas turbines would primarily fire ULSD during the winter months."[7]

Q. Is it reasonable to look back at recent historic emissions in gauging CREC's potential use of oil going forward?

[7] Major Source Permit Application Addendum. Clear River Energy Center – Burrillville, Rhode Island. ESS Group. Page 3.

A. Yes. The historic data are illuminating in regard to fuel use at existing and proposed generation in Rhode Island. In January 2017, Enbridge (formerly Spectra Energy) completed a 342 MDth/d expansion of its mainline route system in New York, Connecticut and Rhode Island to serve increased LDC loads through the Algonquin Incremental Market ("AIM") project. If, say, all AIM capacity were available for power generation during the summer, the equivalent power generation output at full load would be sufficient to support 1,900 MW. While AIM capacity is fully subscribed by LDCs in Rhode Island, Connecticut, and Massachusetts, and likely fully or near fully utilized by the LDCs during the peak heating season, it will not be fully utilized during the non-heating season, a time when LDC loads constitute a small percentage of peak demand. The majority of the AIM capacity will therefore be available to generators in southern New England during the summer, thereby reducing the demand for backup oil for electricity generation across the Algonquin pipeline system. Enbridge is also currently in the process of adding an incremental 132.7 MDth/d of pipeline capacity to its system between Mahwah, NJ and downstream points including an interconnection with the Maritimes & Northeast pipeline in Beverly, MA, through the Atlantic Bridge project. Similar to the AIM project, the capacity associated with the Atlantic Bridge project has been contracted by LDCs and industrial customers. The market effects of the project will therefore be similar to those described above. The facilities associated with the project are now under construction for a November 1, 2017 target in-service date.

Q. Why did Pawtucket Power burn any oil in the summer?

A. I do not know exactly why. Since Pawtucket Power is not directly connected to an interstate pipeline, it must rely on National Grid for the last leg of the supply chain from the pipeline citygate to the generator gate station. LDC tariffs governing interruptible transportation can sometimes include costly imbalance resolution charges, penalties for non-ratable use, as well as significant volumetric charges. These restrictive tariff provisions sometimes favor oil use rather than natural gas. Also, LDCs typically conduct local maintenance during the summer, which may cause oil use. The CEMS data show that Pawtucket Power relied on backup fuel oil almost entirely during the peak winter months. Oil use during the summer of 2014 and 2015 was a relatively negligible amount and oil was not used at all during the summer of 2016.

Q. Has Invenergy stated whether it will contract for interruptible or firm gas transportation service?

A. Invenergy has indicated that it would rely on firm gas transportation service for at least a portion of its natural gas requirements. See page 119 of Invenergy's Application and response 3-5 of Invenergy Thermal Development LLC's Responses to the Division of Public Utilities and Carriers Third Set of Data Requests in Docket Number 4609 before the Rhode Island Public Utilities Commission. If CREC acquires a primary firm entitlement to mainline capacity on Algonquin for a portion of its maximum daily requirement ("MDQ"), then at least a portion of its generating capacity could be scheduled on natural gas throughout the winter, even on extremely cold winter days. Use of firm gas transportation service for all or a portion of CREC's MDQ would lessen CREC's potential reliance on ULSD.

Q. Are firm service customers ever curtailed?

A. Yes, firm customers can be curtailed, but such curtailments are rare and almost always require the pipeline to declare a force majeure event. A force majeure event is associated with an operating contingency or emergency that requires the pipeline operator to take whatever action is necessary to ensure the safety and security of the pipeline system. Last resort measures can include isolation of a route segment or the reduction in pressure and flow to firm service customers along the route segment where the incident occurred.

Q. On page 2 of the Conservation Law Foundation's Response to Town of Burrillville's First Data Requests, CLF states that CREC would emit more carbon than the current New England average when it burns gas or oil. Please comment on this statement.

A. I agree that CREC's expected annual average CO_2 emission rate, whether it burns only natural gas or all of its permitted ULSD each year, would be somewhat higher than the average New England-wide CO_2 emission rate. However, it is misleading and incorrect to simply compare the average CREC emission rate to the average New England system-wide emission rate. This is because CREC's emissions are not additive to the average emissions of all of the other existing plants in the region. Consistent with the way that ISO-NE, the regional grid operator, dispatches available generating resources to minimize system-wide production costs, the energy that CREC generates would replace energy that would otherwise be generated from less efficient and more carbon-intensive plants. By adding CREC to the region's resource mix, the average annual emission rates will therefore decrease. Over the long term, as the generation fleet becomes increasingly cleaner and more efficient, energy from CREC will in turn be displaced by more efficient gas-fired plants, if they are constructed, and by renewable resources, which have no fuel costs and little to no emissions.

Q. What is the appropriate ISO-NE system-wide emission rate that the CREC emission rate should be compared to?

A. As discussed on pages 15 through 19 of OER's Advisory Opinion, since operation of CREC will displace less efficient and higher-emitting dispatchable resources, the appropriate comparison is to ISO-NE's marginal emission rate. When OER's Advisory Opinion was filed, the most up-to-date information from ISO-NE was the "2014 ISO New England Electric

Generator Air Emissions Report." ISO-NE has since released the results of its 2015 analysis.[8] The 2015 data indicates that the system-wide marginal emission rate in 2015 was 857 lb/MWh. Although the ISO-NE marginal emissions rate dropped by 9% from 2014 to 2015, it remains significantly above the average CREC emission rate of 760 lb/MWh on natural gas. Even if ULSD is burned for the maximum of 15 days per year for each unit, the calculated average CO_2 emission rate of 776 lb/MWh previously stated is still less than the 2015 ISO-NE marginal emission rate of 857 lb/MWh. I note that over the same period of time, the average ISO-NE system-wide emission rate increased by 2.9%, from 726 lb/MWh in 2014 to 747 lb/MWh in 2015.

Q. On page 10 of his testimony, Professor Roberts states that "carbon emission levels today are significantly above 1990 levels." Have you seen any data that supports that statement?

A. No, the available data is not consistent with Professor Roberts' assertion. In this portion of his testimony, he is addressing the economy-wide carbon reduction goals set forth in the Act. The Act requires the Rhode Island Executive Climate Change Coordinating Council ("EC4") to submit to the Governor and General Assembly a plan that includes strategies, programs, and actions to meet specific targets for GHG emissions reductions: 10% below 1990 levels by 2020; 45% below 1990 levels by 2035; and 80% below 1990 levels by 2050. Since filing his testimony, the EC4 issued its Greenhouse Gas Emissions Reduction Plan ("GHG Plan")[9], which identifies proposed strategies, programs, and actions to meet the targets for GHG emissions reductions established in the Act. Figure 2 on page 9 of the GHG Plan displays the state's

---

[8] ISO New England, Inc. System Planning, "2015 ISO New England Electric Generator Air Emissions Report," January 2017. Available at: https://www.iso-ne.com/static-assets/documents/2017/01/2015_emissions_report.pdf

[9] The Rhode Island Greenhouse Gas Emissions Reduction Plan by the EC4, December 2016 may be accessed at: http://www.planning.ri.gov/documents/climate/EC4%20GHG%20Emissions%20Reduction%20Plan%20Final%20Draft%202016%2012%2029%20clean.pdf

historic GHG emissions, and a projection of emissions under a "business-as-usual" scenario, relative to the 1990 baseline and relative to the emissions reduction targets for 2020, 2035, and 2050. It is clear from the figure, which is reproduced herein as Figure 2, that the current emissions are significantly below the 1990 baseline. Importantly, the data demonstrate that Rhode Island is on track to achieve the 2020 emissions reduction target, due to the success of current GHG reduction policies and programs.

Figure 2

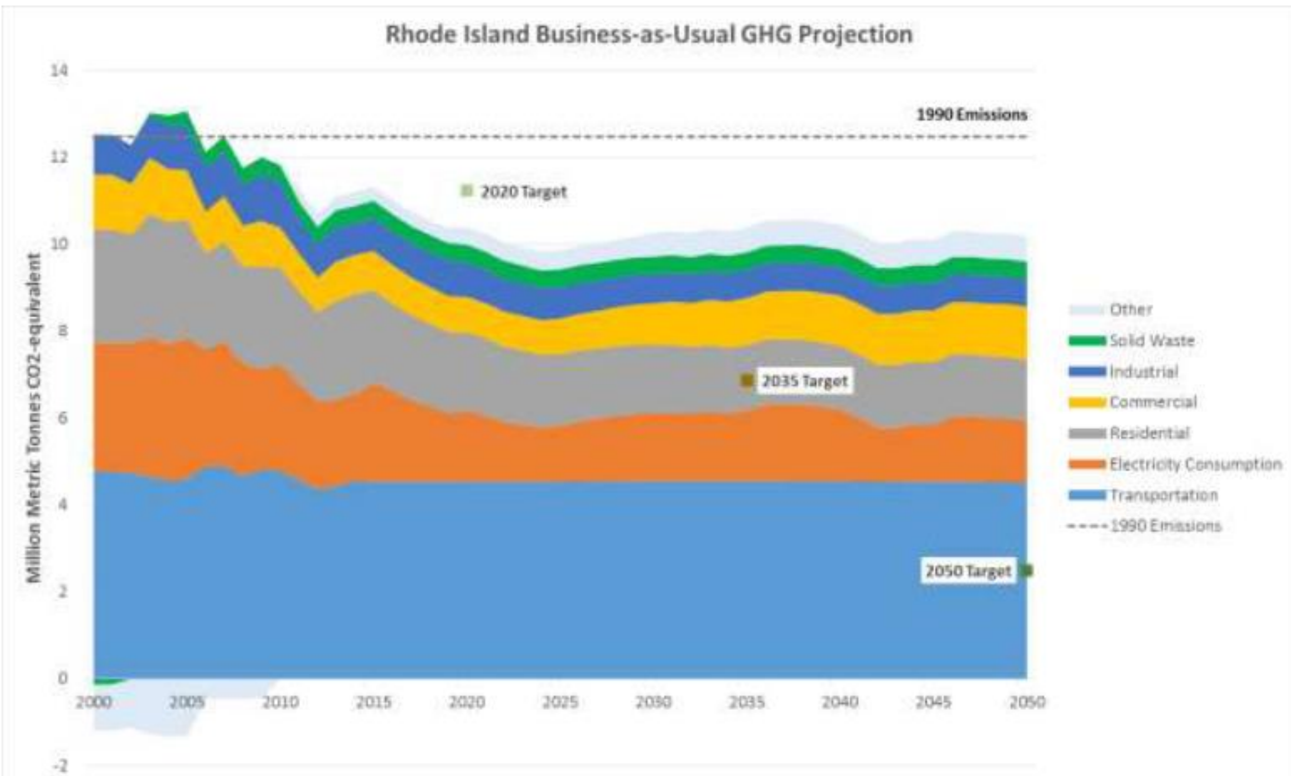

Q Do you disagree with any other statements in Professor Roberts' testimony?

A. Yes, I do. On page 15 of his testimony, he states that "The plant will have to be used, or there will be huge stranded costs for the firm and the state." As New England's generation fleet evolves and is modernized over time, with more efficient resources displacing and replacing less efficient generation resources, it is true that CREC may in the future be dispatched only sparingly by ISO-NE. There may be a point in time when revenues from the electricity markets administered by ISO-NE are insufficient to cover CREC's fixed and variable operating costs, and CREC may decide to mothball or retire the plant. However, the risk of financial losses is borne entirely by Invenergy and its investors, and not by electric customers in Rhode Island or elsewhere in New England.

Q. On page 17 of his testimony, Professor Roberts states, "Having a surplus of natural gas-fired electricity here in the state will decrease the incentive to make the competing long-term investments that will be needed for new renewables." Do you agree with this statement?

A. No, I do not. Gas-fired generation plants and renewable resources are not directly competing investments. Investments in gas generation by the private market do not have a direct impact on the public policy motivation of decision-makers to promote renewable energy through mandates or incentives. An investor seeking to develop a new power plant will develop a pro forma analysis of the projected investment returns, based on a forecast of project revenues and all fixed and variable costs, including all financing costs, taxes, and depreciation. Project revenues for natural gas-fired plants consist of revenues from the ISO-NE energy, capacity, and ancillary services markets. While the overnight capital costs for renewable resources such as wind and solar may be somewhat higher than for gas-fired simple or combined cycle plants, renewable resources have an additional revenue stream in the form of Renewable Energy Credits ("RECs"), and in some cases, favorable tax treatment. RECs represent the value of the environmental attributes associated with renewable energy generation. One MWh of energy generated by a qualified renewable resource produces one REC. All the New England States, including Rhode Island, have implemented a renewable portfolio standard ("RPS"), termed renewable energy standard, or RES, in Rhode Island, which requires all load serving entities to either purchase renewable energy or RECs up to a specified percentage of their annual load. Rhode Island, along with several other New England states, have also required the state's electric distribution companies ("EDCs") to solicit proposals and enter into long term contracts for renewable resources. A firm demand for RECs under the RPS, coupled with long term contracts with EDCs, support financing of new renewable projects. Regardless of the total capacity of the gas-fired fleet in Rhode Island or across the region, New England states have legislative and policy tools that promote the development of renewable resources to achieve state's GHG reduction and renewable energy goals.

Q. You previously mentioned the GHG Plan issued by the EC4 in December 2016. The GHG Plan identifies mitigation options for Rhode Island to achieve the GHG reduction targets set forth in the Act. Would the development and operation of CREC hinder Rhode Island's ability to implement the proposed mitigation options?

A. No, it would not.

Q. Please explain why development and operation of CREC would not hinder or impair Rhode Island's ability to implement the GHG mitigation options.

A. The GHG Plan identifies ten major mitigation options available to Rhode Island to meet its economy-wide GHG reduction targets. These include options that pertain to the transportation, industrial processes, and building heating sectors, as well as electricity. There are several options that are relevant to the electricity sector: energy efficiency, utility-scale renewable energy, distributed generation, clean energy imports, and relicensing of the Millstone nuclear units. Except for preservation of the nuclear units, each of these mitigation options can be implemented, at least in part, through policy tools that are available to Rhode Island, and that build upon existing state programs such as Least Cost Procurement, the RES, the Renewable Energy Growth Program, the Long Term Contracting Standard for Renewable Energy, and the Affordable Clean Energy Security Act. The GHG Plan also recognizes that achieving the GHG reduction targets will also require actions outside of the State's direct control. These may include expansion of clean energy resources throughout New England and contracting for imports of clean energy such as hydropower from outside of the region. Indeed, the Plan acknowledges that "Reaching the levels of GHG reduction in 2050 implied by the Act would require existing stocks of conventional technologies (e.g., fossil fuel generating resources, heating equipment, and vehicles) to be largely replaced with alternative, carbon-free technologies by 2050." These tools available to Rhode Island and the other states in the region will continue to increase the percentage of energy sold in Rhode Island that is derived from clean energy resources. Thus the demand for energy from incumbent fossil-fired resources including CREC will diminish, regardless of how much fossil-fueled capacity remains in the region's fleet. CREC's operation would contribute to lowering GHG emissions in the near term until a decreased demand for fossil-fueled generation leads to its output being replaced by lower and zero carbon emitting resources in the long term.

Q. Does this conclude your testimony?

A. Yes.

EXHIBIT EGC-1

Global Change Biology (2007) **13**, 2509–2537, doi: 10.1111/j.1365-2486.2007.01439.x

CO_2 balance of boreal, temperate, and tropical forests derived from a global database

S. LUYSSAERT*†, I. INGLIMA‡, M. JUNG§, A. D. RICHARDSON¶, M. REICHSTEIN§, D. PAPALE‖, S. L. PIAO**, E. -D. SCHULZE§, L. WINGATE††, G. MATTEUCCI‡‡, L. ARAGAO§§, M. AUBINET¶¶, C. BEER§, C. BERNHOFER‖‖, K. G. BLACK***†††, D. BONAL‡‡‡, J. -M. BONNEFOND§§§, J. CHAMBERS¶¶¶, P. CIAIS**, B. COOK‖‖‖, K. J. DAVIS****, A. J. DOLMAN††††, B. GIELEN*, M. GOULDEN‡‡‡‡, J. GRACE††, A. GRANIER§§§§, A. GRELLE¶¶¶¶, T. GRIFFIS‖‖‖‖, T. GRÜNWALD‖‖, G. GUIDOLOTTI‖, P. J. HANSON*****, R. HARDING†††††, D. Y. HOLLINGER‡‡‡‡‡, L. R. HUTYRA§§§§§, P. KOLARI¶¶¶¶¶, B. KRUIJT‖‖‖‖‖, W. KUTSCH§, F. LAGERGREN******, T. LAURILA††††††, B. E. LAW†, G. LE MAIRE**, A. LINDROTH******, D. LOUSTAU§§§, Y. MALHI§§, J. MATEUS§§§§§§, M. MIGLIAVACCA¶¶¶¶¶¶, L. MISSON‖‖‖‖‖‖, L. MONTAGNANI*******, J. MONCRIEFF††, E. MOORS‖‖‖‖‖, J. W. MUNGER§§§§§, E. NIKINMAA¶¶¶¶¶, S. V. OLLINGER¶, G. PITA§§§§§§, C. REBMANN§, O. ROUPSARD‡‡‡‡‡‡, N. SAIGUSA§§§§§§§, M. J. SANZ¶¶¶¶¶¶¶, G. SEUFERT‖‖‖‖‖‖‖, C. SIERRA†, M. -L. SMITH‡‡‡‡‡, J. TANG‖‖‖, R. VALENTINI‖, T. VESALA******** and I. A. JANSSENS*

**Department of Biology, University of Antwerp, Universiteitsplein 1, B-2610 Wilrijk, Belgium, †College of Forestry, Oregon State University, Corvallis, OR 97331-5752, USA, ‡Department of Environmental Sciences, Second University of Naples, Via Vivaldi 43, 81100 Caserta, Italy, §Max Planck Institute for Biogeochemistry, PO Box 100164, 07701 Jena, Germany, ¶Complex Systems Research Center, University of New Hampshire, Morse Hall, 39 College Road, Durham, NH 03824, USA, ‖Department of Forest Science and Environment, University of Tuscia, 01100 Viterbo, Italy, **LSCE, Orme des Merisiers, 91191 Gif-sur-Yvette, France, ††Institute of Atmospheric and Environmental Science, School of GeoSciences, The University of Edinburgh, Edinburgh, EH9 3JN Scotland, UK, ‡‡CNR-ISAFOM, Via Cavour 4-6, 87036 Rende, Italy, §§Environmental Change Institute, Oxford University Centre for the Environment, South Parks Road, Oxford OX1 3QW, UK, ¶¶Unit of Physics, Faculté Universitaire des Sciences Agronomiques de Gembloux, 8 Avenue de la Faculté, 5030 Gembloux, Belgium, ‖‖Department of Meteorology, Institute of Hydrology and Meteorology, Technische Universität Dresden, Pienner Strasse 23, 01737 Tharandt, Germany, ***School of Biology and Environmental Science, University College Dublin, Belfield, Dublin 4, Ireland, †††Irish Council for Forest Research and Development (COFORD), Arena House, Arena Road, Sandyford, Dublin 18, Ireland, ‡‡‡INRA Kourou – UMR Ecofog, PO Box 709, 97387 Kourou Cedex, French Guiana, §§§INRA, Research Unit EPHYSE, Centre de Bordeaux, BP 81, F-33883, Villenave d'Ornon, France, ¶¶¶Ecology and Evolutionary Biology, Tulane University, 310 Dinwiddie Hall, New Orleans, LA 70118, USA, ‖‖‖Department of Forest Resources, University of Minnesota, 1530 Cleveland Ave. N, St Paul, MN 55108, USA, ****Department of Meteorology, The Pennsylvania State University, 512 Walker Building, University Park, PA 16802, USA, ††††Department of Hydrology and Geo-environmental Science, Vrije Universiteit Amsterdam, 1081 HV Amsterdam, The Netherlands, ‡‡‡‡Department of Ecology and Evolutionary Biology, University of California, Irvine, CA 92697, USA, §§§§INRA EEF, 54280 Champenoux, France, ¶¶¶¶Department for Ecology and Environmental Research, Swedish University of Agricultural Sciences, PO Box 7042, SE-750 07 Uppsala, Sweden, ‖‖‖‖Biometeorology, University of Minnesota, 55108 St Paul, MN, USA, *****Environmental Sciences Division, Oak Ridge National Laboratory, Oak Ridge, TN 38731-6422, USA, †††††Center of Ecology and Hydrology Edinburgh, Bush Estate, Penicuik, Midlothian EH26 0QB, UK, ‡‡‡‡‡USDA Forest Service, 271 Mast Rd., Durham, NH 03824, USA, §§§§§Department of Earth and Planetary Sciences, Harvard University, Cambridge, MA, USA, ¶¶¶¶¶Department of Forest Ecology, University of Helsinki, PO Box 27, FI-00014, Finland, ‖‖‖‖‖Alterra, PO Box 47, 6700 AA Wageningen, The Netherlands, ******Physical Geography and Ecosystems Analysis, Lund University, Sölvegatan 12, SE-223 62 Lund, Sweden, ††††††Finnish Meteorological Institute, PO Box 503, FI-00101 Helsinki, Finland, §§§§§§Departamento de Engenharia Mecânica, Instituto Superior Técnico, Ave. Rovisco Pais 1, 1049 Lisbon, Portugal, ¶¶¶¶¶¶Dipartimento di Scienze dell'Ambiente e del Territorio, Università degli Studi di Milano, Bicocca, Italy, ‖‖‖‖‖‖CNRS-CEFE, 1919 route de Mende, 34293 Montpellier, France, *******Autonomous Province of Bolzano, Agency for the Environment, Via Amba Alagi 5; Forest Services, Via Brennero 6, 39100 Bolzano, Italy, ‡‡‡‡‡‡CIRAD, UPR-80 ETP, avenue d'Agropolis, 34398, Montpellier, Cedex 05, France, §§§§§§§National Institute*

Correspondence: S. Luyssaert, Department of Biology, University of Antwerp, Universiteitsplein 1, B-2610 Wilrijk, Belgium, tel. +32 3820 2289, e-mail: Sebastiaan.Luyssaert@ua.ac.be *of Advanced Industrial Science and Technology, AIST Tsukuba West, Tsukuba 305-8569, Japan, ¶¶¶¶¶¶¶CEAM, Parque Tecnológico, c/Charles H. Darwin 14, 46980 Paterna Valencia, Spain, ||||||||||||||Joint Research Centre, Via E. Fermi 1, I-21020 Ispra (VA), Italy, ********Department of Physical Sciences, University of Helsinki, PO Box 64, 00014 Helsinki, Finland*

Abstract

Terrestrial ecosystems sequester 2.1 Pg of atmospheric carbon annually. A large amount of the terrestrial sink is realized by forests. However, considerable uncertainties remain regarding the fate of this carbon over both short and long timescales. Relevant data to address these uncertainties are being collected at many sites around the world, but syntheses of these data are still sparse. To facilitate future synthesis activities, we have assembled a comprehensive global database for forest ecosystems, which includes carbon budget variables (fluxes and stocks), ecosystem traits (e.g. leaf area index, age), as well as ancillary site information such as management regime, climate, and soil characteristics. This publicly available database can be used to quantify global, regional or biome-specific carbon budgets; to re-examine established relationships; to test emerging hypotheses about ecosystem functioning [e.g. a constant net ecosystem production (NEP) to gross primary production (GPP) ratio]; and as benchmarks for model evaluations. In this paper, we present the first analysis of this database. We discuss the climatic influences on GPP, net primary production (NPP) and NEP and present the CO_2 balances for boreal, temperate, and tropical forest biomes based on micrometeorological, ecophysiological, and biometric flux and inventory estimates. Globally, GPP of forests benefited from higher temperatures and precipitation whereas NPP saturated above either a threshold of 1500 mm precipitation or a mean annual temperature of 10 °C. The global pattern in NEP was insensitive to climate and is hypothesized to be mainly determined by nonclimatic conditions such as successional stage, management, site history, and site disturbance. In all biomes, closing the CO_2 balance required the introduction of substantial biome-specific closure terms. Nonclosure was taken as an indication that respiratory processes, advection, and non-CO_2 carbon fluxes are not presently being adequately accounted for.

Nomenclauture:

DOC = dissolved organic carbon;
fNPP = foliage component of NPP;
GPP = gross primary production (GPP > 0 denotes photosynthetic uptake);
mNPP = missing component of NPP;
NBP = net biome production (NBP > 0 denotes biome uptake);
NECB = net ecosystem carbon balance (NECB > 0 denotes ecosystem uptake);
NEE = net ecosystem exchange (NEE > 0 denotes ecosystem uptake);
NEP = net ecosystem production (NEP > 0 denotes ecosystem uptake);
NPP = net primary production (NPP > 0 denotes ecosystem uptake);
R_a = autotrophic respiration ($R_a > 0$ denotes respiratory losses);
R_e = ecosystem respiration ($R_e > 0$ denotes respiratory losses);
R_h = heterotrophic respiration ($R_h > 0$ denotes respiratory losses);
rNPP = root component of NPP;
R_s = soil respiration ($R_s > 0$ denotes respiratory losses);
VOC = volatile organic compounds;
wNPP = wood component of NPP

Keywords: carbon cycle, CO_2, forest ecosystems, global database, gross primary productivity, net ecosystem productivity, net primary productivity

Received 21 September 2006; revised version received 8 June 2007 and accepted 11 May 2007

Introduction

By sequestering large amounts of atmospheric carbon, forests play an important role in the global carbon cycle and are thought to offer a mitigation strategy to reduce global warming (Schimel *et al*., 2001). The awareness that fossil fuel burning has perturbed the carbon cycle, with feedbacks to global climate, has inspired researchers and funding agencies worldwide to invest in carbon cycle research. Hence, many more data on carbon cycling in forests have become available in recent decades. Knowledge of global patterns in net primary production (NPP) improved substantially during the 1970s thanks to the International Biological Program (IBP; Jager *et al*., 2000). More recently, additional insight in global NPP was gained by analyses of updated comprehensive data summaries (Scurlock & Olson, 2002; Ciais *et al*., 2005), as well as by modelling studies, such as the Potsdam NPP model intercomparison study (Cramer *et al*., 1999). Global patterns (both spatial and temporal) in gross primary production (GPP) and respiration (R_e) are mainly based on modelling exercises (i.e. Schimel *et al*., 2001). Exceptions include analyses of NEP and GPP measurements from eddy covariance flux networks (Valentini *et al*., 2000; Janssens *et al*., 2001; Law *et al*., 2002; Reichstein *et al*., 2003) and a synthesis of the CO_2 balance of a boreal, temperate and tropical forest site (Malhi *et al*., 1999).

Because the wide spread application of the eddy covariance technique our understanding of the magnitude, temporal, and spatial variability of CO_2 cycling in terrestrial ecosystems has evolved quickly (Baldocchi, 2003). However, considerable uncertainties remain regarding the current status of terrestrial sinks and the fate of the carbon sequestered by the terrestrial biosphere over both short and long timescales. The flow of carbon between the different components of forest ecosystems and its eventual allocation to long-term storage pools (wood and soil organic matter) is likely to vary across forests of different growth strategies (deciduous vs. evergreen), age, management regime, and climate. The relevant data are collected at many sites around the world, but need to be synthesized to address the remaining uncertainties. Therefore, we have assembled a comprehensive global database for forest ecosystems, which includes carbon budget variables (fluxes and stocks), ecosystem traits (e.g. leaf area index, age), as well as ancillary site information such as management regime, climate, and soil characteristics. This publicly available database is dedicated to quantifying the global and biome-specific carbon budget of the forests, re-examination of previously hypothesized global relationships, testing emerging hypotheses about ecosystem functioning, and providing benchmarks for ecosystem model evaluations. The database will be updated as additional data become available.

The objectives of this manuscript are to (1) present the database structure, explain data consistency and quality control mechanisms, (2) identify data gaps, (3) present global patterns in GPP, NPP and NEP, and (4) establish forest carbon budgets by biome.

Components of the C-balance

GPP of an ecosystem represents the gross uptake of CO_2 that is used for photosynthesis. The synthesis of new plant tissue from CO_2, water and nutrients and the maintenance of living tissues are energy demanding processes (Penning de Vries *et al*., 1974; Amthor, 2000). Hence, some photo-assimilated compounds are lost from the ecosystem as autotrophic respiration (R_a) due to the costs associated with growth and maintenance of foliage, wood, and roots. The amount of photosynthates that is not used for respiration and is available for other processes is defined as NPP and relates to GPP and R_a as

$$\mathrm{GPP} = \mathrm{NPP} + R_a. \quad (1)$$

The bulk of NPP is allocated to the production of biomass in different ecosystem components: foliage (fNPP), wood (wNPP; including branches and stems), and root (rNPP; including coarse and fine roots) production. In addition to these measurable components, NPP also includes a variety of additional components and processes that are more difficult to measure and often ignored. In this manuscript, these components were called mNPP and include the carbon invested in understory plant growth and in reproductive organs (flowers, seeds, fruits), as well as carbon lost through herbivory, emitted as volatile organic compounds (VOC) and methane (CH_4), and exuded from roots or transferred to mycorrhizae. The global average of production and losses contained in mNPP was estimated to be 11% (Randerson *et al*., 2002) but can easily amount to 20% of the sum of fNPP, wNPP, and rNPP in tropical forests (Clark *et al*., 2001). Thus,

$$\mathrm{NPP} = \mathrm{fNPP} + \mathrm{wNPP} + \mathrm{rNPP} + \mathrm{mNPP}. \quad (2)$$

The residence time of carbon, which is the time between fixation in photosynthates and the return to the atmosphere following respiration or chemical transformation into VOC, exudates or CH_4, differs among NPP components. Carbon incorporated in wood, which is physiologically dead, has a residence time within the living tree of years to centuries, whereas the carbon deposited in foliage and fine roots has residence times of months to years. Each year part of the standing biomass is transferred to litter- and/or soil layer carbon pools (each of which has different residence times). These carbon pools are subjected to decomposition by microbial activity, a process defined as heterotrophic respiration (R_h). The decomposition processes that contribute to R_h include decomposition of current year biomass, but also contain decomposition of organic matter that accumulated in the ecosystem during the last decades, centuries or millennia. The imbalance between NPP and R_h is the NEP

$$\mathrm{NPP} = \mathrm{NEP} + R_h. \quad (3)$$

The sum of R_h and R_a represents the total ecosystem respiration (R_e) and the sum of the belowground fraction of R_a and R_h is the soil respiration (R_s). NEP is determined by the difference between GPP and R_e and differs from the net rate of organic carbon accumulation in ecosystems (Schulze *et al.*, 2000).

$$\mathrm{GPP} = \mathrm{NEP} + R_e. \quad (4)$$

The carbon fluxes observed in experiments differ from the long-term carbon balance mainly because non-CO_2 losses and nonrespiratory CO_2 losses, which occur at a range of timescales, are typically ignored. Shortly (<1 year) after uptake, synthesized compounds are lost from the ecosystem as VOCs (Guenther *et al.*, 1995) or as plant-produced CH_4 (Keppler *et al.*, 2006). On longer timescales (>1 years), part of the annually accumulated NEP leaves the ecosystem as dissolved organic carbon (DOC) or microbially produced CH_4. In addition, all or part of the carbon that has been built up over the years by the accumulation of the annual NEP can leave the ecosystem and eventually return to the atmosphere as nonrespiratory CO_2 fluxes by forest fires, harvests and/or erosion (Randerson *et al.*, 2002; Amiro *et al.*, 2006). Therefore, non-CO_2 and nonrespiratory CO_2 losses should be accounted for in Eqn (4) to obtain the carbon balance. The net ecosystem carbon balance (NECB) is the term applied to the total rate of organic carbon accumulation (or loss) from ecosystems (Chapin *et al.*, 2006) and balances NEP as follows:

$$\begin{aligned}\mathrm{NECB} =\ & \mathrm{NEP} \\ & - \text{nonrespiratory } CO_2 \text{ losses} - \text{non-}CO_2 \text{ losses} \\ & + \text{import from bordering ecosystems}.\end{aligned} \quad (5)$$

GPP, NPP, NEP, and NECB may all represent carbon sinks or sources (except GPP which is always a sink) but the relevance of the sink or source depends on the temporal and spatial scale one wants to study. Where the carbon sink in GPP is only sustained for minutes, the sink or source quantified as the NECB equals the long-term carbon-sequestration by ecosystems. When integrated over time and space the NECB equals the net biome production (NBP; Schulze & Heimann, 1998; Buchmann & Schulze, 1999). It is the NBP that is reflected in the long-term atmospheric concentration of CO_2, CH_4 and other atmospheric carbon-compounds.

Materials and methods

Database

A comprehensive relational database structure was designed to store information on carbon fluxes, ecosystem properties, and site information of forest stands. Data entries originated from peer-reviewed literature, established databases (e.g. Olson *et al.*, 2001; Papale *et al.*, 2006) and personal communications with research groups involved in Fluxnet (Baldocchi *et al.*, 2001). The high quality of the database is ensured by several features: (1) referential integrity is ensured by the structure of the database, (2) data selection is based on strict methodological criteria, (3) consistency of the NPP data is ensured by a hierarchical framework, (4) uncertainty of the fluxes are estimated in a consistent manner accounting for the methodological approach and the length of the time series, (5) the uncertainty of aggregated fluxes is estimated, and (6) a variety of observed and/or modelled meta-data is included in the database.

Structure of the database. The database is structured by site. A site is a forest or a stand with a known geographical location, biome (US Department of Agriculture biome classification; Reich & Eswaran, 2002), tree species composition and management regime. Hence, different treatments within an experimental forest or different aged stands that form a chronosequence were recorded as different sites. Each site in the database is linked to at least one carbon balance component and each component is further linked to the methodology that was used to estimate it. Owing to its structure, the database can contain multiple estimates of the same flux for the same year (i.e. if these estimates were reported in different studies or estimated with different measurement techniques). Because data from different sources or references are stored as different entries, the structure of the database, thus ensures referential integrity.

Selection criteria. Flux estimates were included in the database when they were based on direct measurements (NPP, NEP, R_s, R_h, and R_a), derived from single or multiple direct measurements (GPP, NPP, NEP, R_e, R_h, and R_h) or modelled (GPP, NPP, NEP, R_e, R_s, R_h, and R_a).

NPP estimates were included in the database when they were based on direct measurements of the main components of NPP (Clark *et al.*, 2001) if these were obtained as follows: the net annual production of leaves or needles was determined by collecting leaf/needle fall throughout the year; annual stem and branch increment were determined using species- and region-specific allometric equations relating aboveground woody biomass increment to the change in basal area of individual trees in the plot; and coarse-root production was determined through species- and region-specific allometric equations relating root mass to basal area and fine-root production was determined by repeated soil coring, isotopic estimates of fine-root turnover combined with biomass measurements, upscaled root-length production observed in minirhizotrons or the soil respiration and litterfall constraint formulated by Raich & Nadelhoffer (1989). Furthermore, to be included in the database, foliage, stem, branch, coarse and fine root biomass increment had to be corrected for the annual litterfall of these components. When available, we also included estimates of NPP which accounted for: the NPP of the understory vegetation through destructive harvests (available for 30% of the sites with NPP estimates); fruit and seed production (availability: <4%); herbivory (availability: <4%); emissions of volatile compounds (availability: 0%) and leaching of root exudates (availability: 0%). However, availability of these NPP components was not a necessary criterion for inclusion.

Direct measurements of annual and multiple-year NEP were included in the database when based on continuous measurements with a tower-based eddy covariance system. NEP estimates were accepted when data gaps due to system failure, stable atmospheric conditions or data rejection were filled by means of standardized methods (Falge *et al.*, 2001; Reichstein *et al.*, 2005) to provide complete data sets. These data, however, do not include corrections for possible effects of advection, which may lead to a systematic underestimation of night-time respiration even at high turbulence.

Biometric NEP estimates were included in our database when they were based on the difference between biomass production and heterotrophic respiration (e.g. Hanson *et al.*, 2003) or repeated biomass inventories and soil respiration measurements (e.g. Law *et al.*, 2004).

Estimates of R_s and its heterotrophic component R_h were included in the database when based on subtracting chamber measurements from undisturbed plots from measured and up-scaled root respiration (Hanson *et al.*, 2000) or chamber measurements after trenching or girdling. Directly measured estimates of R_a were included in the database when the estimate was based on up-scaled chamber measurements of foliage, stem and root respiration (e.g. Ryan *et al.*, 1996).

Half-hourly eddy covariance measurements can be used to derive an estimate of R_e and GPP. At night there is no photosynthesis, so the site-specific relationship between the night-time NEE and soil temperature can be used to estimate the half-hourly respiration during the day given the daytime soil temperature. However, due to below-canopy CO_2 storage and advection, nocturnal NEE measured on calm nights (u^* threshold) is not used to estimate R_e. These rejected data were treated as gaps and filled by means of standardized methods (Falge *et al.*, 2001). Only measured data were used to fit a relationship between night-time NEE and soil temperature, from which daytime respiration was estimated. The relationship can be fitted with constant parameter values (Falge *et al.*, 2001) or with variable parameter values (Reichstein *et al.*, 2005). Respiration estimates from either method of fitting were included in the database. Applying Eqn (4) results in half-hourly estimates of GPP that must be integrated over the course of a year to obtain an estimate of the annual GPP. On sites affected by advection, GPP and R_e are both likely to be underestimated.

When data are available for at least two flux components, the identities given by Eqns (1)–(4) can be used to estimate a missing flux (e.g. R_a can be calculated from the difference between R_e and R_h). Flux estimates obtained by applying these equations were also included in the database. However, modelled GPP, NPP, NEP, R_e, R_s, R_h, and R_a estimates were only included when a mechanistic process model driven by daily or more detailed climatological input variables was used, and when the model was calibrated with site-specific parameters and/or validated against site-specific measurements such as biomass, NEP, etc.

Consistency of the flux data. Despite the strict selection criteria there are still inconsistencies between methodological approaches (i.e. an eddy covariance-based estimate of GPP includes the understory, whereas most process models limit the GPP to the photosynthesis of the overstory vegetation). Depending on the methodological approach, respiration by mycorrhizae may be included either in R_a or in R_h. These inconsistencies contribute to the observed variation among sites, but given the small contribution of understory and mycorrhizal fluxes are unlikely to have severely affected the results presented below.

More problematic are the inconsistencies in NPP. Although NPP data are more widely available than other carbon-flux estimates, there are considerable problems of consistency among NPP studies. Reported NPP values can range from the NPP of a single component (e.g. foliage NPP) to the complete NPP of the ecosystem. The database accounted for these inconsistencies by combining 11 components and nine aggregation levels of NPP in a hierarchical framework (Fig. 1). At the lowest level, stem and foliage NPP were recorded. When both components were measured, the lowest possible level of aboveground NPP (ANPP_1; foliage + stem NPP) was calculated. The next level included branch NPP. If branch NPP was measured, wood NPP (stem + branch NPP) and ANPP_2 (foliage + stem + branch NPP or foliage + wood NPP) were calculated. Coarse and fine root NPP were recorded as separate components and summed to obtain the belowground NPP (BNPP_1; coarse + fine roots NPP). If all required low-level components were available, the total NPP (TNPP_1) was calculated as ANPP_2 + BNPP_1. If the understory NPP was measured, the next level of total NPP was calculated (TNPP_2). Adding estimates of the NPP of the reproductive parts, herbivory, root exudation and VOC's and CH_4 resulted in TNPP_3, TNPP_4, TNPP_5, and TNPP_6, respectively. The framework was considered hierarchical because a certain level of NPP was calculated only when all underlying components were measured. For example, TNPP_4 was not calculated unless TNPP_3 was available and NPP consumed by herbivores was measured. There was, however, one exception: NPP calculated from the difference between GPP and R_a or the sum of NEP and R_h was set to TNPP_5 despite the absence of lower-level NPP estimates. The imbalance between GPP and R_a was

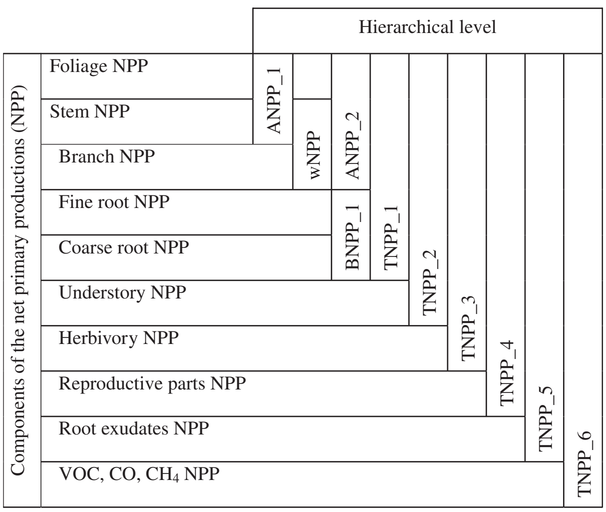

Fig. 1 Hierarchical framework for net primary production (NPP) where 11 components of the NPP are hierarchically combined in nine aggregation levels of NPP.

assigned to TNPP level 5 instead of level 6 because most often GPP and NEP were estimated on the basis of eddy covariance measurements which do not capture VOC's and CH_4 losses.

Given this careful processing and quality evaluation of data for each site, the NPP data are consistent when a single level of NPP data is used. For the majority of the sites, only a few components were reported such that TNPP_1 was the most common estimate for total NPP. It should be noted that minor inconsistencies remain within an individual component (i.e. the use of different cut-off diameters between coarse and fine roots). However, the variation due to these inconsistencies is expected to disappear when NPP estimates of a higher level are used [i.e. the variation due to different cutoff diameters are expected to disappear when total belowground NPP (BNPP_1) is used].

Uncertainty of the measured CO_2 fluxes. Although recently efforts have been made to quantify the uncertainties of eddy covariance measurements (Hollinger *et al.*, 2004; Hollinger & Richardson, 2005; Richardson *et al.*, 2006; Black *et al.*, 2007), uncertainty of CO_2-flux estimates are only rarely reported in the literature and when reported it is often unclear whether the given value denotes instrumental, spatial, temporal and/or other sources of variability. Therefore, we ignored the reported uncertainty and instead estimated the total uncertainty for every component flux contained in the database. The uncertainty was estimated in a uniform way based on expert judgment. We could not identify prior information that could constrain the absolute range of the estimated NEP. Without measurements or prior information, experts agreed that the NEP of a forest most likely ranges from -100 to $600\,g\,C\,m^{-2}\,yr^{-1}$. The absolute range of the NEP estimate is, thus, $\pm 350\,g\,C\,m^{-2}\,yr^{-1}$ (this manuscript). However, all methodological approaches contained in the database used site-specific observations and are therefore expected to reduce the uncertainty surrounding the NEP estimates. Consequently, the uncertainty was reduced with a method-specific factor (i.e. when NEP was determined by eddy covariance measurements), the precision was thought to be 30% of 350 or $105\,g\,C\,m^{-2}\,yr^{-1}$. This estimate is similar to those presented by Griffis *et al.* (2003), Richardson & Hollinger (2005) and Oren *et al.* (2006). For tropical forest, where night-time measurements are often problematic the absolute range of the NEP estimate was set to $\pm 700\,g\,C\,m^{-2}\,yr^{-1}$. The applied method-specific reduction factors (i.e. 30% for eddy covariance, are given in Table 1). When a flux was a multiple-year mean value, its value is less prone to interannual variability and, therefore, its uncertainty

Table 1 Method-specific reduction factors for GPP, NPP, NEP, R_e, R_s, R_h and R_a determined by expert judgment

Method	GPP	NPP	NEP	R_e	R_s	R_h	R_a	Reduction factor
Eddy covariance and data assimilation	x		x					0.2
Eddy covariance	x		x	x	x			0.3
Measured increment and litterfall		x						0.3
Chamber based					x			0.4
Measured and modelled increment and litterfall		x						0.6
Process-model based	x	x	x	x				0.6
Chamber + girdling						x		0.8
Chamber + root excised						x		0.8
Chamber + trenching						x		0.8
Radiocarbon						x		0.8
Chamber based							x	0.8
Alkali absorption					x			0.8
Chamber + gap based						x		0.9
Process-model based					x	x	x	1.0
Flux component based	x	x	x	x	x	x	x	1.0

The reduction factors account for the precision of a method and are multiplied with the absolute range of the uncertainty of the fluxes (Table 2) to get the uncertainty of a specific observation.
NPP, net primary production; NEP, net ecosystem production; GPP, gross primary production.

Table 2 Absolute range ($g\,C\,m^{-2}\,yr^{-1}$) of GPP, NPP, NEP, R_e, R_s, R_h and R_a under the assumption that measurements are absent

Component flux	Uncertainty
GPP	500 + 7.1 × (70–latitude)
NPP	350 + 2.9 × (70–latitude)
NEP	350 if latitude > 23
	700 if latitude < 23
R_e	500 + 7.1 × (70–latitude)
R_s	200 + 8.6 × (70–latitude)
R_h	100 + 2.9 × (70–latitude)
R_a	100 + 4.3 × (70–latitude)

Values determined by expert judgment.
NPP, net primary production; NEP, net ecosystem production; GPP, gross primary production.

(s_{ij}) was further reduced by accounting for the length of the time series. Thus,

$$s_{ij} = (p_i \times RF_j) \Big/ \sqrt{l_{ij}},$$

where p_i is the initial uncertainty for site i in the absence of measurements according to Table 2 and RF_j is the reduction factor for method j according to Table 1 and l_{ij} is the length of the time series (in years) for site i for which the fluxes where estimated with method j.

A similar approach was followed to estimate the uncertainty of GPP, NPP, R_e, R_a, R_h, and R_s. However, for these fluxes the latitude of the site contained prior information regarding their absolute range [i.e. GPP at a boreal site likely ranges from 0 to 1000 $g\,C\,m^{-2}\,yr^{-1}$, whereas GPP at a tropical site likely ranges from 2000 to 4000 $g\,C\,m^{-2}\,yr^{-1}$ (this manuscript)]. Consequently, the absolute range for GPP in the absence of measurements depends on the latitude (Table 2). For each site contained in the database the latitude was known and as such, the absolute range in the absence of measurements could be estimated. This initial uncertainty was then reduced by the method-specific factor (Table 1) and further adjusted for the length of the time series.

Aggregated fluxes and their uncertainty. According to the planned analysis, differently structured tables can be extracted from the database (e.g. for low-resolution model comparison, the data should be aggregated by latitudinal and longitudinal cells whereas for analyzing C balances of different forests the data should be aggregated by site). For a given site or cell (i), the flux component (F) was determined with k different methods j. The average flux component determined by method j for site or cell i was then given as F_{ij}. The average flux component across methods (F_i) was calculated as the weighted mean:

$$F_i = \frac{\sum_{j=1}^{k} l_{ij} \times F_{ij}}{\sum_{j=1}^{k} l_{ij}}.$$

The uncertainty of the weighted mean was calculated by means of error propagation:

$$s_i = \sqrt{\frac{\sum_k l_{ij} \times (s_{ij})^2}{\sum_k l_{ij}}} \Big/ \sqrt{n_i},$$

where n_i is the total number of observations for the flux component F_i for site or cell i and l_{ij} is the number of observations determined with method j. Hence, the obtained uncertainty (s_i) is a proxy for the uncertainty surrounding the mean annual flux for the site or cell.

Site description data. Additional site information related to stand characteristics, standing biomass, leaf area index and growing environment were added to the database as separate tables (see Appendix A). Stand characteristics such as basal area, mean tree diameter, mean tree height, mean tree density and mean stand age are available for many sites. Also, the observed standing biomass and its major components, the maximal observed leaf area index, and some methodological details of the leaf area measurement technique were available and stored in the database for many sites. A description of stand management was also included in the database. Among sites, information on management was of variable quality and detail. Therefore, a coarse classification, distinguishing managed (when the description contained a reference to planting, thinning or harvesting), unmanaged (when no management had occurred during the last 50 years), recently burned (when burned in the last 25 years), recently clear cut (when clear cut in the last 25 years) and fertilized and irrigated sites (when the site was fertilized or irrigated often as part of an experimental set-up). Finally, the growing environment was characterized by the observed mean annual temperature and annual precipitation.

For almost all sites, soil texture expressed as the volumetric percentage of sand, silt and clay was extracted from Global Soil Data Products (Global Soil Data Task, 2000). The spatial resolution is 5 min. Mass percentages were converted to volumetric percentages by dividing the mass percentage by the bulk density (i.e. 1.19 g cm^{-3} for sand and 0.94 g cm^{-3} for clay). The percentage silt was calculated as the difference of the volumetric percentage sand and clay from 100%. The normalized different vegetation index (NDVI) at a spatial resolution of 8×8 km^2 and 15-day interval were acquired from the Global Inventory Monitoring and Modelling Studies (GIMMS) group derived from the NOAA/AVHRR series satellites (NOAA 7, 9, 11 and 14) for the period January 1982 to December 2003 (Tucker *et al.*, 2005). In addition to the direct measurements, monthly precipitation, air humidity and temperature were extracted from the CRU data set (Mitchell & Jones, 2005). The observed temperature and precipitation were strongly correlated to the CRU-derived temperature and precipitation ($r^2 = 0.93$ and 0.70, respectively). However, the CRU data were added to the database and used in the present analysis because these data was more complete and consistent (all from 1990 to 2003) than the observed data. Monthly net solar radiation, absorbed downward longwave radiation, net surface longwave radiation, soil moisture, dry nitrogen deposition, wet nitrogen deposition and ammonia deposition were simulated with the model ORCHIDEE (Krinner *et al.*, 2005).

Biome-specific CO_2 balances

The different biomes were characterized by means of a stand and climate description. The stand description was based on observed values, the climate description was based on the CRU data set (Mitchell & Jones, 2005) and ORCHIDEE model output (Krinner *et al.*, 2005). All data were extracted from the database and mean values with their SD were presented for the different biomes.

For the selected biomes, site-specific GPP, NPP, NEP, R_e, R_a, R_h values and their uncertainty were extracted from the database and aggregated as explained above. Evergreen and deciduous sites were analyzed separately. Flux estimates affected by climatic anomalies such as El Niño events or the 2003 summer drought were included, however, recently cut, burned, fertilized or irrigated sites were excluded from the present analysis (although these are included in the database). Whenever an estimate was available for two of the three respiration components (R_a, R_h, and R_e), the missing component was calculated based on the relationship between the respiration components. A similar procedure was used to calculate R_e when GPP and NEP were measured. The uncertainty of the calculated component was calculated by error propagation. In theory R_a and/or R_h can also be calculated when estimates of GPP and NPP and/or NPP and NEP are available. However, the NPP values that were extracted from the database were not the total NPP but just the sum of foliage, wood and root NPP (TNPP_1). Using Eqns (1)–(4) with only part of the NPP (TNPP_1) instead of the total NPP ($R_a = \text{GPP} - \text{TNPP\_5}$ or $R_h = \text{TNPP\_5} - \text{NEP}$) violates the underlying assumptions of the equations.

Subsequently, the biome-specific weighted mean was calculated for each flux, using the inverse of the uncertainty as the weight. Hence, the mean values are strongly determined by flux estimates from long-term experimental sites and by estimates obtained with more precise measurement techniques (see Table 1). The flux values in the CO_2 balances should be interpreted as the most reliable mean estimates currently available but it should be noted that the balances are only representative for a larger region as far as the sites with the long time series and more precise flux estimates are representative for that region. As with most general patterns, these mean fluxes, which are the result of both spatial and temporal averaging may not apply to specific sites or specific years (Gower *et al*., 1996).

Robustness of the CO_2 balances was tested by removing the lowest and highest observed flux for each component and re-calculating the weighted mean. The weighted mean for the trimmed data set was compared with the weighted mean of the original data set. When, for all flux components, the difference between the original and truncated weighted means was less than $\pm$ 10%, the CO_2 balance was considered robust. CO_2 balances for which none of the weighted means of the trimmed components deviated more than 25% from the weighted means of the original components were considered acceptable. If one of the weighted means deviated more than 25% from its original value, the CO_2 balance was considered sensitive to the available data.

It is conceivable that GPP could be estimated for many years on a site where R_h was not measured or that GPP at a given site was measured with a precise method whereas R_h was measured with a less precise technique. Consequently, the biome-specific CO_2 balances were not necessarily closed. Closure of the balances was enforced by introducing terms that closed the budget. Six closure terms, one for each flux, were introduced to Eqns (1), (3) and (4) introduced. The equations can be rewritten as follows:

$$\mathrm{GPP} + \delta\mathrm{GPP} = \mathrm{NPP} + \delta\mathrm{NPP} + R_a + \delta R_a,$$
$$\mathrm{NPP} + \delta\mathrm{NPP} = \mathrm{NEP} + \delta\mathrm{NEP} + R_h + \delta R_h,$$
$$\mathrm{GPP} + \delta\mathrm{GPP} = \mathrm{NEP} + \delta\mathrm{NEP} + R_e + \delta R_e.$$

The CO_2 balance was further constrained by introducing the soil respiration (R_s). Following the definitions of the respiration components the following inequalities apply:

$$R_a + \delta R_a > R_e + \delta R_e - R_s,$$
$$R_s > R_h + \delta R_h,$$
$$R_e + \delta R_e > R_s,$$
$$R_a + \delta R_a + R_h + \delta R_h > R_s.$$

For the selected biomes, mean biome-specific estimates were available for GPP, NPP, NEP, R_e, R_a, R_h, and R_s. The closure terms were optimized by means of quadratic programming such that the objective function $(|\delta\mathrm{GPP}| + |\delta\mathrm{NPP}| + |\delta\mathrm{NEP}| + |\delta R_e| + |\delta R_a| + |\delta R_h|)^2$ was minimal and the CO_2-balance closed.

The closure terms are a numerical way to approach data quality and flux uncertainty on the biome level. Ideally each individual closure term should be zero; deviations from zero indicate a closure problem. Small deviations indicate a good agreement between the fluxes unless the fluxes were not measured independently. Large closure terms (i.e. beyond uncertainties in measured fluxes) could indicate problems with the accuracy of the measurement technique or missing components in the CO_2 balance but could also be due to a high natural variability within the biome because a different set of sites may have been used to calculate the different carbon fluxes. An underestimation of one flux (i.e. NPP can be accounted for by adding a closure term to NPP but also by decreasing R_a or GPP). Therefore, the sum of the absolute values of the closure terms were discussed instead of individual closure terms.

Mean biome-specific fluxes (weighted by the inverse uncertainty), closure terms and NPP components were calculated for 1000 bootstrap data sets for GPP, NPP, fNPP, wNPP, rNPP, NEP, R_e, R_a, and R_h. Consequently, the SD of the mean fluxes, closure terms and NPP components could be estimated for each biome.

Results and discussion

Available data

In total, 513 forest sites are included in the database: 309 needle-leaved, 181 broadleaved and 23 mixed sites or 345 evergreen, 146 deciduous and 22 mixed sites. The database contains 519 GPP estimates for 133 sites, 298 NPP (TNPP_1) estimates for 244 sites, 714 NEP estimates for 164 sites, 504 R_e estimates for 112 sites, 40 R_a estimates for 21 sites and, 186 R_h estimates for 138 sites. Irrespective of the classification, southern hemisphere ecosystems were highly underrepresented with just 21 sites (Fig. 2). Many common tree species from the southern hemisphere are, therefore, not represented in the database and coverage would greatly benefit from additional southern hemisphere data. However, only part of the data that is collected within the frame of Fluxnet was made available for use at this moment. Therefore, we expect that more GPP, NEP, and R_e data will become available in the near future, especially for South America.

The applied biome classification (Reich & Eswaran, 2002) distinguished eight forest biomes; the database contained 96 boreal humid (13% of the forested biomes vs. 19% of the sites), 38 boreal semiarid (5% area vs. 19% sites), 299 temperate humid (17% area vs. 58% sites), 17 temperate semiarid (10% area vs. 3% sites), 18 mediterranean warm (5% area vs. 4% sites), 0 mediterranean cold (1% area vs. 0% sites), 29 tropical humid (20% area vs. 3% sites) and 16 tropical semiarid sites (28% area vs. 6% sites). Although the temperate humid forest are overrepresented compared with their areal extent, all main climatic regions that support forest growth are present in the database. The lack of data for mediterranean cold forests is considered less essential because these ecosystems account for <1% of the global biomes

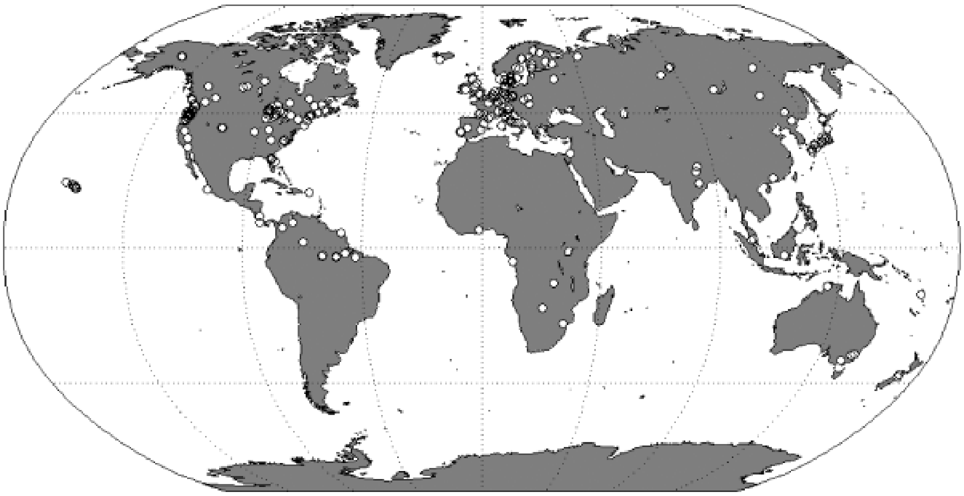

Fig. 2 Geographical distribution of the sites contained in the database.

that support forest growth. Their extent is limited to the Sierra Nevada and Cascade mountain ranges in the western US, the western half of the Russian-Kazakh border and the Caucasian mountain range between eastern Turkey and northwestern Iran (Reich & Eswaran, 2002). Semiarid forests, particularly tropical semiarid forests (covering almost 30% of the global forested biomes) appear under-studied. It is not clear whether the data gaps are the result of a lack of data or whether the data exists but the ecosystems were not classified as forest. The difference between forests, shrublands and savannas is not always clear, and this is especially a problem in semiarid regions where forests are less dense and individual trees are smaller than in more mesic regions.

Beside climatic conditions, growth strategy (i.e. evergreen vs. deciduous) is also expected to influence the CO_2 balance. Therefore, evergreen and deciduous sites were analyzed separately. Highly disturbed sites such as recently cut, burned, fertilized or irrigated sites are included in the database but were excluded from the current analysis. Separation by growth strategy highlighted several data gaps. Subdividing the data according to climate and growth strategy revealed that only the CO_2 balances of temperate humid evergreen, temperate humid deciduous and tropical humid evergreen forests were robust. Our robustness measure quantifies the leverage of individual observations on the overall mean but contains no information concerning the representativeness or the quality of the observations. The robustness of the CO_2 balance for boreal humid evergreen and temperate semiarid evergreen was acceptable and for the other biomes (i.e. boreal semiarid evergreen, boreal semiarid deciduous and mediterranean warm evergreen forests), CO_2 balances were only indicative because the current estimates were highly sensitive to the available data due to smaller sample sizes and greater variability among sites.

Although robustness is not solely a function of the number of sites, we observed a relationship between the number of sites included in the budget calculation and the robustness of individual flux estimates (not shown). Across biomes and fluxes, weighted means calculated from at least 18 sites consistently produced robust flux estimates. In addition, 16% of the R_h and 33% of the R_a were estimated with process models (compared with 10% of the GPP, 3% of NEP, 5% of R_e, and 1% of the NPP). The low number of real observations and the correspondingly high share of modelled values, tend to suggest that more effort should be put into measuring the components of R_e (i.e. R_a and R_h, independently). More direct (and thus less uncertain) observations would increase the robustness of the flux estimates and would also be valuable for testing or improving models of heterotrophic and autotrophic respiration. Even up-scaled measurements of aboveground autotrophic respiration and soil respiration from chamber measurements would be valuable data with which constraints on R_a and R_h could be improved. For all biomes, data of non-CO_2 and nonrespiratory CO_2 losses are rare. Consequently, more data are needed before these carbon fluxes can be included in biome-specific balances.

How do climate, stand characteristics and CO_2 fluxes differ among biomes?

Climate and stand characteristics across biomes. Mean climate, stand characteristics and CO_2 fluxes of the biomes are based on the observations contained in the database. Hence, the values given in Tables 3–5 are representative for the sites contained in the database and not necessarily representative for the entire biome. Nevertheless, the well-known climatological contrasts between biomes were obvious across the investigated sites. Going from boreal towards tropical forests, the mean annual temperature at sites in the database increases from −3 to 23 °C and the difference in mean temperature between winter (December, January and February for the northern hemisphere and June, July, and August for the southern hemisphere) and summer (June, July, and August for the northern hemisphere

Table 3 Mean carbon fluxes, NPP components, sum of closure terms [$\Sigma(\delta\text{Flux}) = |\delta\text{GPP}| + |\delta\text{NPP}| + |\delta R_e| + |\delta R_a| + |\delta R_h|$] and their standard deviation for the different biomes. The SD refer to the variability surrounding the mean values

	Boreal humid	Boreal semiarid		Temperate humid		Temperate semiarid	Mediterranean warm	Tropical humid
	Evergreen	Evergreen	Deciduous	Evergreen	Deciduous	Evergreen	Evergreen	Evergreen
GPP	973 ± 83	773 ± 35	1201 ± 23	1762 ± 56	1375 ± 56	1228 ± 286	1478 ± 136	3551 ± 160
NPP	271 ± 17	334 ± 55	539 ± 73	783 ± 45	738 ± 55	354 ± 33	801 ± NA	864 ± 96
fNPP	73 ± 9	47 ± 5	109 ± 11	159 ± 19	235 ± 13	56 ± 11	134 ± NA	316 ± 32
wNPP	205 ± 28	110 ± 20	304 ± 36	280 ± 29	329 ± 47	117 ± 20	389 ± NA	212 ± 52
rNPP	69 ± 9	157 ± 31	112 ± 22	235 ± 14	207 ± 20	172 ± 19	278 ± NA	324 ± 56
NEP	131 ± 79	40 ± 30	178 ± NA	398 ± 42	311 ± 38	133 ± 47	380 ± 73	403 ± 102
R_e	824 ± 112	734 ± 37	1029 ± NA	1336 ± 57	1048 ± 64	1104 ± 260	1112 ± 100	3061 ± 162
R_a	489 ± 83	541 ± 35	755 ± 31	951 ± 114	673 ± 87	498 ± 58	615 ± NA	2323 ± 144
R_h	381 ± 40	247 ± 26	275 ± 31	420 ± 31	387 ± 26	298 ± 16	574 ± 98	877 ± 96
$\Sigma(\delta\text{Flux})$	439 ± 122	176 ± 81	163 ± 90	216 ± 102	206 ± 95	713 ± 314	359 ± 131	774 ± 225
R_e/GPP	0.88 ± 0.09	0.97 ± 0.04	0.86 ± 0.01	0.77 ± 0.03	0.77 ± 0.04	0.87 ± 0.22	0.76 ± 0.07	0.88 ± 0.04
R_e/GPP	0.85 ± 0.14	0.95 ± 0.06	0.86 ± 0.02	0.76 ± 0.04	0.76 ± 0.06	0.96 ± 0.38	0.76 ± 0.10	0.86 ± 0.06

The R_e/GPP ratio was calculated for each bootstrap before and after balance closure.
NPP, net primary production; NEP, net ecosystem production; GPP, gross primary production.

Table 4 Stand climate characterized by the mean ± SD in winter (December, January and February in the northern hemisphere and June, July and August in the southern hemisphere) and summer (June, July and August in the northern hemisphere and December, January and February in the southern hemisphere) for the different biomes

	Boreal humid	Boreal semi-arid		Temperate humid		Temperate semiarid	Mediterranean warm	Tropical humid
	Evergreen	Evergreen	Deciduous	Evergreen	Deciduous	Evergreen	Evergreen	Evergreen
Mean winter temperature (°C)	−9 ± 7	−18 ± 6	−20 ± 8	4 ± 5	2 ± 9	0 ± 5	10 ± 3	23 ± 4
Mean summer temperature (°C)	13 ± 4	13 ± 4	13 ± 4	17 ± 4	20 ± 5	14 ± 3	23 ± 3	24 ± 3
Precipitation sum winter (mm)	205 ± 110	52 ± 33	47 ± 31	449 ± 337	183 ± 164	356 ± 182	239 ± 212	685 ± 664
Precipitation sum summer (mm)	144 ± 88	183 ± 105	156 ± 86	194 ± 234	356 ± 259	81 ± 99	106 ± 127	469 ± 395
Net radiation sum winter ($W\,m^{-2}$)	46 ± 48	46 ± 31	33 ± 29	147 ± 92	150 ± 100	152 ± 141	196 ± 47	361 ± 55
Net radiation sum summer ($W\,m^{-2}$)	216 ± 35	359 ± 102	348 ± 108	473 ± 104	425 ± 78	502 ± 95	550 ± 102	437 ± 47
Mean winter air humidity (%)	86 ± 16	83 ± 19	79 ± 22	84 ± 11	79 ± 11	85 ± 18	74 ± 7	82 ± 4
Mean summer air humidity (%)	72 ± 12	71 ± 6	70 ± 6	67 ± 12	77 ± 5	50 ± 6	60 ± 8	77 ± 6

The temperature, precipitation and air humidity values are based on the CRU data set. Net radiation are model outputs from ORCHIDEE.

Table 5 Stand characteristics for the different biomes

	Boreal humid	Boreal semiarid		Temperate humid		Temperate semiarid	Mediterranean warm	Tropical humid
	Evergreen	Evergreen	Deciduous	Evergreen	Deciduous	Evergreen	Evergreen	Evergreen
Latitude (°)	58 ± 7	59 ± 5	61 ± 5	44 ± 8	44 ± 9	44 ± 2	40 ± 4	14 ± 8
Max LAI ($m^2\,m^{-2}$)	4.1 ± 3.0	3.4 ± 1.8	3.5 ± 1.5	7 ± 2.9	6.1 ± 3.5	1.8 ± 1.0	3.5 ± 1.2	5.2 ± 1.2
Tree height (m)	14 ± 7	8 ± 2	19 ± 5	20 ± 12	19 ± 7	10 ± 5	12 ± 8	28 ± 9
Basal area ($m^2\,ha^{-1}$)	28 ± 12	26 ± 10	28 ± 4	42 ± 24	31 ± 15	8 ± 2	24 ± 14	23 ± 13
Tree density (number ha^{-1})	3767 ± 5652	4230 ± 3018	1451 ± 720	1399 ± 1985	1723 ± 2439	506 ± 326	2136 ± 2815	385 ± 221
Stand age (years)	72 ± 52	121 ± 67	78 ± 31	91 ± 141	75 ± 50	94 ± 86	45 ± 34	> 100
Aboveground biomass ($g\,C\,m^{-2}$)	5761 ± 3708	4766 ± 2498	7609 ± 2438	14 934 ± 13 562	10 882 ± 5670	6283 ± 5554	5947 ± 1808	11 389 ± 5824
Belowground biomass ($g\,C\,m^{-2}$)	1388 ± 836	1604 ± 925	1352 ± 645	4626 ± 4673	2565 ± 2609	2238 ± 1728	3247 ± 2212	2925 ± 2284

The values are the mean ± the standard deviation of the observed values for the sites included in the CO_2-balances

and December, January, and February for the southern hemisphere) decreased from 31 to 1 °C (Table 4). Along the same gradient, the difference in net radiation sum between winter and summer decreased from 315 to 76 W m^{-2}. The annual precipitation sum in boreal semiarid forests was < 400 mm and exceeded 2200 mm in tropical humid forests. In the semiarid forests, the difference in precipitation between winter and summer was more pronounced than in the humid biomes (Table 4). Pronounced differences between winter and summer relative air humidity were only present in the temperate semiarid and mediterranean warm forests.

The distribution of plant species and, thus, forest ecosystems depends on historical events (i.e. ice ages), migrational ability and ability to adapt to present environmental conditions (Schulze, 2005). The mean ecosystem characteristics for each of the selected biomes are given in Table 5. The unexpected high latitude of the tropical forests is caused by the high number of Hawaiian sites with latitude around 20°N. The low leaf area index for temperate semiarid evergreen forests is not robust and most likely due to the low number of observations for this biome. Maximum LAI (in most cases, LAI refers to tree LAI and does not include the LAI of the understory or the herb layer), tree height, basal area, tree density, and biomass do not follow a clear trend but overall higher biomass accumulation is observed in forests from the poles to the equator with the highest accumulation in temperate-humid evergreen forests. Within a climatic zone, forests in the humid biomes accumulate in general more biomass compared with forests in semiarid biomes. Despite the exclusion of recently disturbed sites, there is a 50-year gap between the mean and median age of the trees in the temperate humid evergreen biome, which indicates a skewed age distribution. Unrepresentative sampling in the presence of both intensively managed and old-growth stands (mostly located in the Pacific Northwest of the United States) in this biome likely explains the lower median age of the evergreen biome.

Global patterns in GPP, NPP, and NEP. The global pattern in GPP shows a clear dependency on the climatic conditions (Fig. 3). Temperature and precipitation which are both sensitive to effects of continentality and topography were thought to give a more meaningful representation of climate than latitude, longitude, and elevation. Climatic conditions explain 71 ± 2% of the variability in GPP [$P < 0.01$ for GPP = f(temperature) × f(precipitation), where f is a power function]. In line with the basic ecological principles (e.g. Liebig's 'Law of the Minimum'), the GPP of ecosystems that are already limited by low precipitation sums (< 800 mm) or low mean annual temperatures (< 5 °C) do not benefit from higher mean annual temperatures or precipitation, respectively. Given a sufficient amount of precipitation (> 800 mm), GPP increases with increasing temperatures (Fig. 3, top panel). A similar relationship between temperature

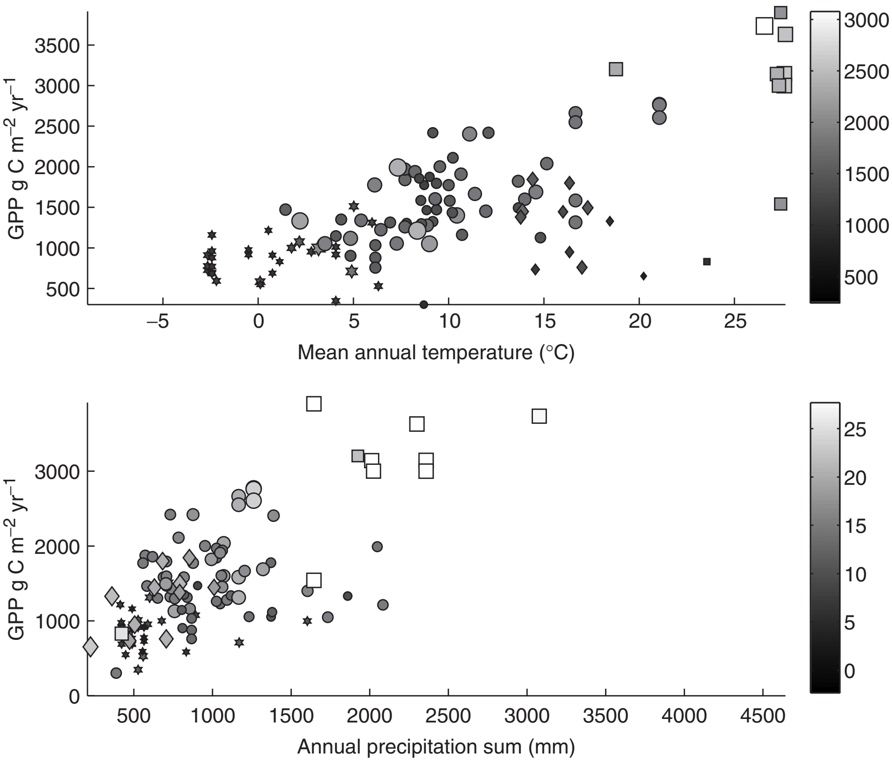

Fig. 3 The top panel shows the gross primary production (GPP) according to the mean annual temperature, the size and color of the marker is a measure for the annual precipitation sum (mm). The bottom panel shows the GPP according to the annual precipitation sum, the size and color of the marker is a measure for the mean annual temperature (°C). Stars, boreal; circles, temperate; diamonds, Mediterranean; and squares, tropical forests.

and GPP has been reported for different types of terrestrial vegetation such as tundra, forest, and grasslands (Law *et al.*, 2002). Given a nonrestrictive mean annual temperature (>5 °C), GPP benefits from higher annual precipitation sums. However, the beneficial effect of precipitation appears to saturate above 1500 mm (i.e. for tropical forests, there was no correlation between precipitation and GPP, see Fig. 3, bottom panel). This apparent saturation could originate from the use of precipitation as the independent variable instead of plant available water. At high precipitation sites, run-off is a major component of the hydrological balance and hence evapotranspiration remains almost constant beyond annual precipitation sums of 1500 mm (Schulze, 2005). At temperatures between 5 and 15 °C, some of the dryer forests even have higher GPP than wetter forests (Fig. 3), likely because the dryer sites experience less cloudiness and hence more sunshine (Table 4).

Although an effort was made to use consistent NPP data (TNPP_1), the observed relationships between climatic variables and NPP are more scattered than earlier reported relationships (Lieth & Whittaker, 1975; Scurlock & Olson, 2002). Some of the scatter in our data set is caused by including chronosequences (i.e. the 'line' at 25 °C or at 1200 mm in Fig. 4, top and bottom panel, respectively) in the analyses. Nevertheless, temperature and precipitation explain 36 ± 5% of the variability in NPP [$P<0.01$ for NPP = *f*(temperature) × *f*(precipitation), where *f* is a power function]. Similar to the results for GPP, the NPP of ecosystems does not respond to increasing temperatures or precipitation when the ecosystem is limited either by precipitation (<800 mm) or temperature (<5 °C), respectively (Fig. 4, top and bottom panel). For mean annual temperatures ranging from 5 to 10 °C, NPP increases with increasing temperature but appears to saturate beyond 10 °C (Fig. 4, top panel). Although low NPP values are observed at sites with low precipitation, there is no clear correlation between NPP and precipitation above precipitation of 1500 mm (Fig. 4, bottom panel). Schuur (2003) reported that NPP decreased beyond the 1500 mm threshold, but our results are not conclusive. This saturation or decrease could be the effect of using precipitation instead of plant available water as the independent variable in the figures. Similar to our observations for GPP, some of the dryer forests at intermediate mean annual temperatures (between 5 and 15 °C) have higher

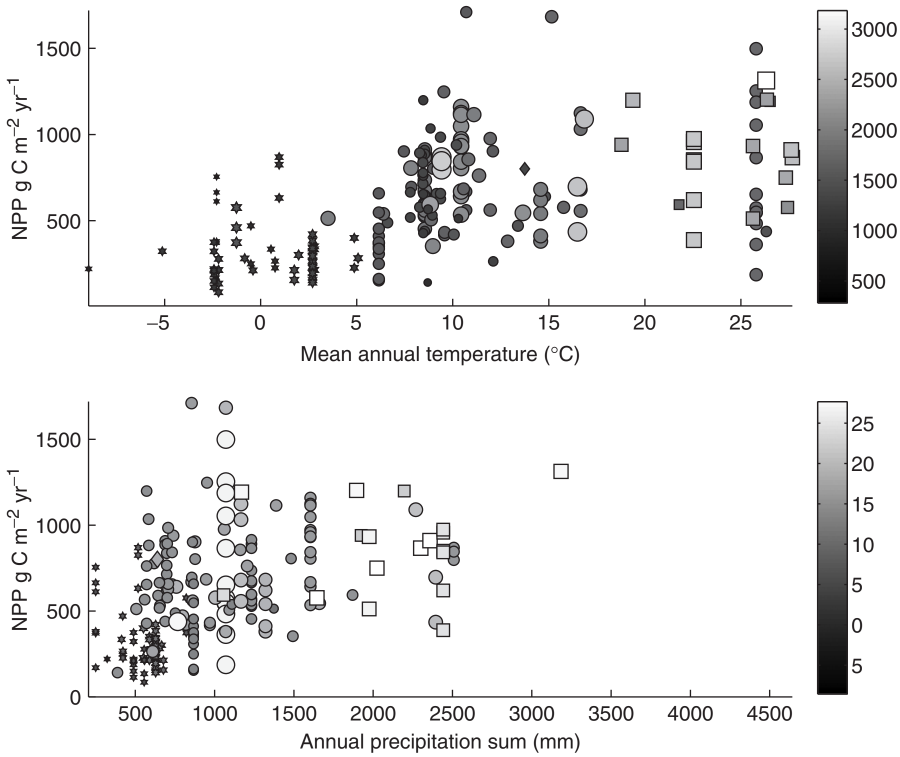

Fig. 4 The top panel shows the net primary production (NPP) according to the mean annual temperature, the size and color of the marker is a measure for the annual precipitation sum (mm). The bottom panel shows the gross primary production (GPP) according to the annual precipitation sum, the size and color of the marker is a measure for the mean annual temperature (°C). Stars, boreal; circles, temperate; diamonds, Mediterranean; and squares, tropical forests.

NPP than wetter forests at similar temperatures, likely because these dryer sites have a higher GPP. Despite tropical forests having the highest observed GPP values, the highest NPP values were observed in the temperate forests. High autotrophic respiration and/or non-CO_2 losses in tropical forests compared with the other biomes could explain this observation, but this then raises the question why these factors are particularly important in tropical humid forests.

Similar to earlier studies (Law *et al.*, 2002), NEP was found independent from the mean annual temperature and precipitation sum (Fig. 5). Climate explained just $5 \pm 1\%$ of the variability in NEP [$P = 0.03$ for NEP $= f$(temperature) $\times f$(precipitation), where f is a power function). However, the highest NEP values are observed in temperate humid forests. This may be related to forest management, which is more intensive in this biome. Forest management targets to increase the production of woody biomass. Therefore, it is to be expected that the effect of forest management is reflected in the CO_2 balance as thinning and harvesting result in a higher wNPP and a lower heterotrophic respiration due to the removal of woody biomass before it dies and decomposes *in situ*. Mean wNPP in temperate humid forests is among the highest values observed (Table 3), which supports the idea that management is the cause of the high-observed NEP values. However, an effect of management on R_h is not seen in the data (Table 3). Although some of the higher NEP values in temperate forests might be due to management, management in itself neither explains the magnitude of the NEP value nor whether the ecosystem is a CO_2 source or sink. The global pattern of NEP values of unmanaged forest across biomes (Fig. 6) is similar to that of forests in general (Fig. 5) and shows that also unmanaged forests are most often carbon sinks. This finding indicates that preservation of unmanaged forest ecosystems could be just as important as reforestation efforts in mitigating climate change through carbon sequestration.

Across European forests, the absence of a latitudinal trend in GPP, in the presence of a latitudinal trend in NEP was the foundation for the hypothesis that respiration was the main determinant of the CO_2 balance at the regional scale (Valentini *et al.*, 2000). However, the current analysis at larger spatial scale shows exactly the opposite (i.e. a global pattern in GPP in the absence of a global pattern in NEP). Our

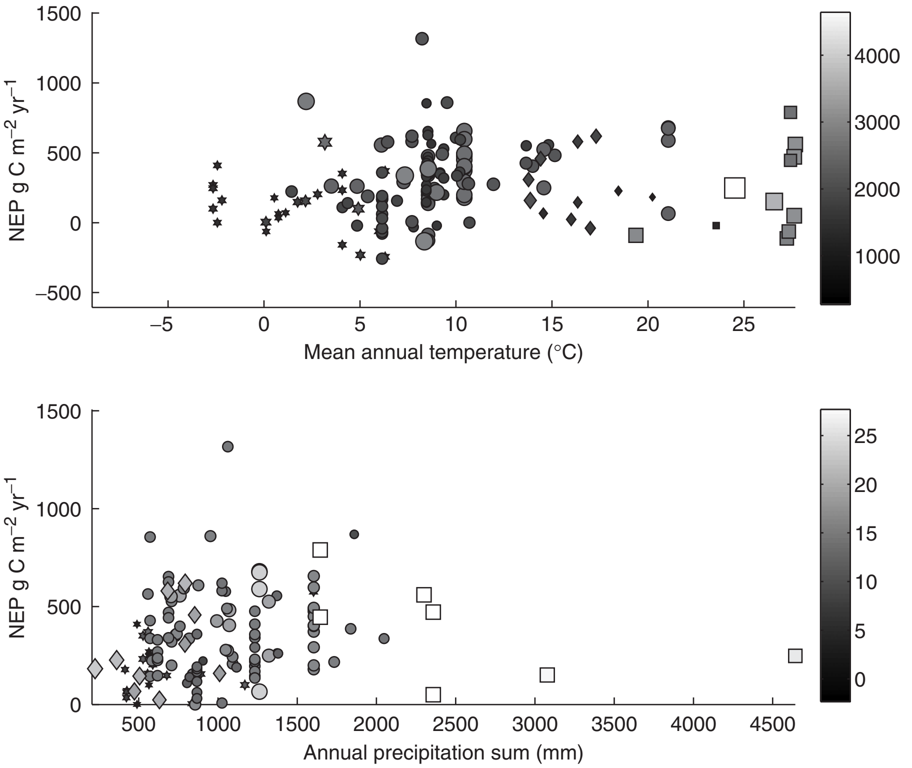

Fig. 5 The top panel shows the net ecosystem production (NEP) according to the mean annual temperature, the size and color of the marker is a measure for the annual precipitation sum (mm). The bottom panel shows the NEP according to the annual precipitation sum, the size and color of the marker is a measure for the mean annual temperature (°C). Stars, boreal; circles, temperate; diamonds, Mediterranean; and squares, tropical forests.

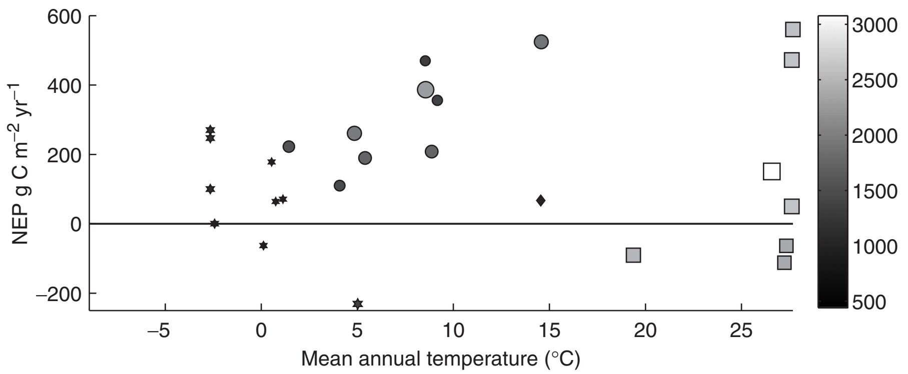

Fig. 6 Global relationship between net ecosystem production (NEP) and mean annual temperature in unmanaged forests. The size and color of the marker is a measure for the annual precipitation sum (mm). Stars, boreal; circles, temperate; diamonds, Mediterranean; and squares, tropical forests.

findings suggest that on the global scale GPP is mainly climate driven ($R^2 = 0.72$, $P < 0.01$) and only marginally sensitive to nonclimatic conditions. In contrast, the global pattern in NEP was found be insensitive to climatic conditions ($R^2 = 0.05$, $P = 0.03$) and was, therefore, expected to be mainly determined by nonclimatic conditions such as successional stage, management, site history and site disturbance. We hypothesize that different drivers determine the carbon fluxes at different spatial scales (i.e. the magnitude of NPP on the global scale can is likely driven by the climatic conditions, whereas the site level NPP is also determined by site quality and management).

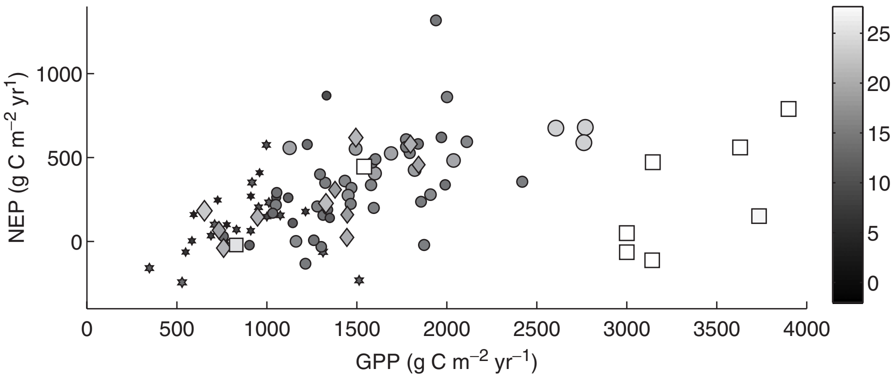

Fig. 7 Relationship between net ecosystem production (NEP) and gross primary production (GPP) across biomes. The size and color of the marker is a measure for the mean annual temperature (°C). Stars, boreal; circles, temperate; diamonds, Mediterranean; and squares, tropical forests.

Despite the difference in drivers between GPP and NEP, a linear relationship between GPP and NEP has been reported across terrestrial vegetations (Law *et al.*, 2002). If we confine our data set to a similar range in GPP as in Law *et al.* (2002; 600–2200 g C m^{-2} yr^{-1}), a similar relationship is observed (Fig. 7). However, increasing GPP beyond 2200 g C m^{-2} yr^{-1} does not result in a further increase of NEP (Fig. 7). Although below a GPP of 2200 g C m^{-2} yr^{-1} there is a tendency of higher NEP with higher GPP, this relationship has limited predictive power. At any GPP, the range of possible NEP values is so wide that it is even not possible to predict whether the forest will be a carbon source or sink ($R^2 = 0.28$ for a quadratic regression model, $P < 0.01$).

Effect of the growth strategy and water availability. The differences in CO_2 fluxes between growth strategies were tested individually for each flux in each biome (one-way ANOVA, assuming equal variances and using growth strategy as a factor). Out of the potential 42 tests (seven biomes × six fluxes), 19 tests could not be performed due to the absence of one of the growth strategies within the biome (i.e. no data available of deciduous forests in the humid tropics). In general, the fluxes between evergreen and deciduous forests did not differ within the same climate zones (ANOVA, $P > 0.15$; see Figs 8–10). Five exceptions were observed (ANOVA, $P \leq 0.10$): GPP and R_e are higher in evergreens compared with deciduous forests in the temperate humid zone, GPP and R_e are higher in deciduous forests in the boreal semiarid zone (based on few observations) and NEP is lower in deciduous than in evergreen mediterranean warm forests (based on few observations). Current statistical evidence, thus justifies merging growth strategies and hence limiting the stratification of biomes to the climatic zones. Nevertheless, we opted to present biomes that distinguish growth strategies to acknowledge other ecological differences and because 19 out of 42 tests could not be performed.

In general fluxes are lower in semi-arid ecosystems compared with humid ecosystems (Figs 3–5). In the temperate zone, this difference is significant at the 0.05 level for GPP, NEP, and R_h, while for NPP the difference is significant at the 0.10 level.

CO_2 balances

Where is the CO_2 going?. Eddy covariance studies have indicated uncertainties concerning the correct interpretation of CO_2 fluxes measured on calm nights (Goulden *et al.*, 1996; Malhi & Grace, 2000). These uncertainties are exceptionally important in tropical rain forests where typically about 80% of all nighttime data is collected during calm nights. The uncertainties are caused by CO_2 storage below the canopy, advective losses of CO_2 and higher random uncertainties during calm nights (Araujo *et al.*, 2002; Kruijt *et al.*, 2004; Richardson *et al.*, 2006) and it is often unclear how to deal with night-time flux measurements in tropical forests (however, see Saleska *et al.*, 2003). Two different approaches for replacing night-time measurements at low turbulence were reported to result in at least 100% difference of the annual NEP (Kruijt *et al.*, 2004). Consequently, the reported NEP's for tropical forests are likely to be an overestimate of the true CO_2 uptake. Based on the current estimates of NEP in tropical humid evergreen forests, the equivalent of 10% of the CO_2 influx by photosynthesis remains in the ecosystem (Fig. 8). Wood growth accounts for 50% of the carbon sink. However, the importance of woody biomass as a long-term sink of carbon in tropical humid forests is still under debate (cf. Phillips *et al.*, 1998; Clark, 2002;

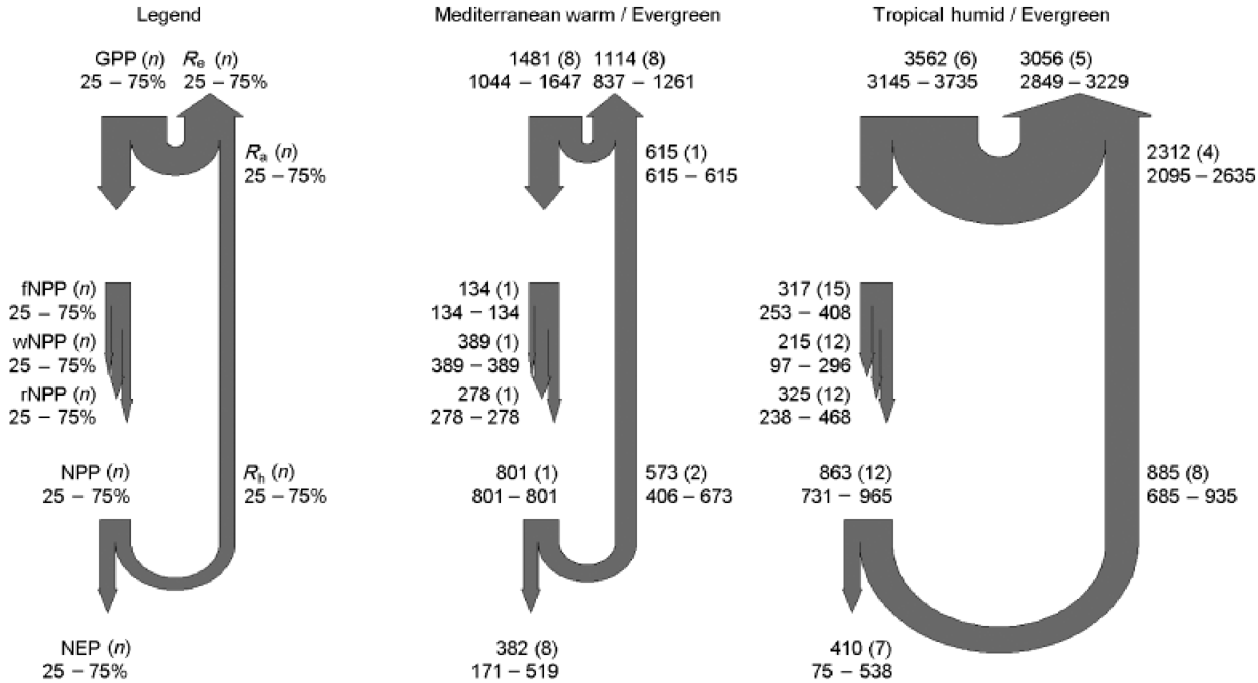

Fig. 8 Observed CO_2 balance for the mediterranean warm and tropical humid biome. These CO_2 balances were not closed and therefore the identities given by Eqns (1)–(4) do not apply. The width of the arrows is proportional to the fluxes and all units are in $g\,C\,m^{-2}\,yr^{-1}$, (n) refers to the number of observations; 25–75% refers to the 25th an 75th percentiles of the observations. Flux values were obtained from the same data but a different bootstrap-run and can therefore be slightly different from the values reported in Table 3.

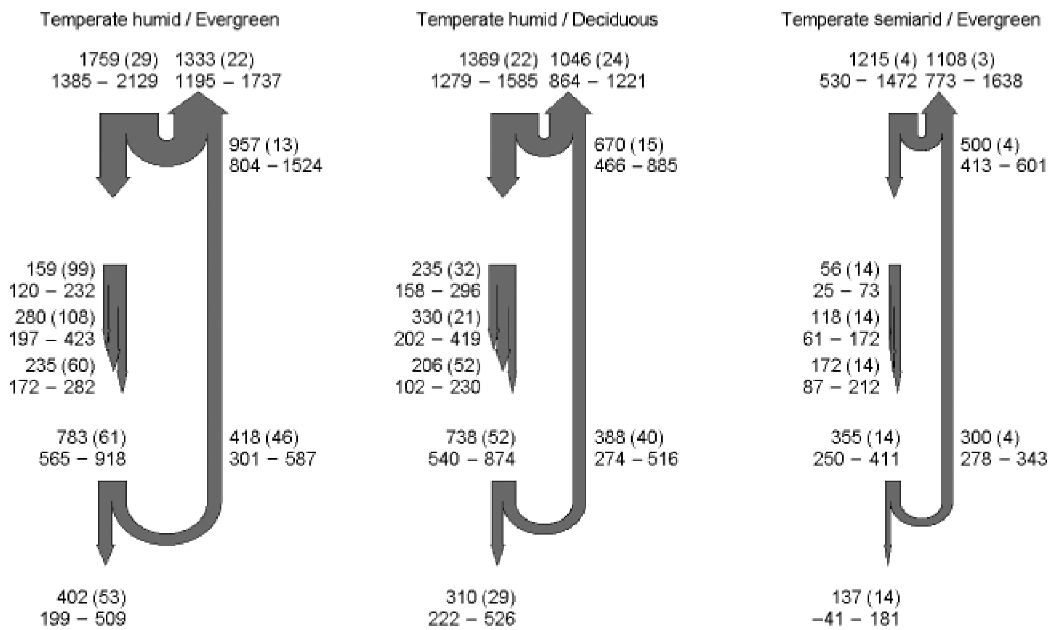

Fig. 9 Observed CO_2 balance for the temperate biomes. These CO_2 balances were not closed and therefore the identities given by Eqns (1)–(4) do not apply. The width of the arrows is proportional to the fluxes and all units are in $g\,C\,m^{-2}\,yr^{-1}$. The legend of the figures is given in Fig. 8. Flux values were obtained from the same data but a different bootstrap-run and can therefore be slightly different from the values reported in Table 3.

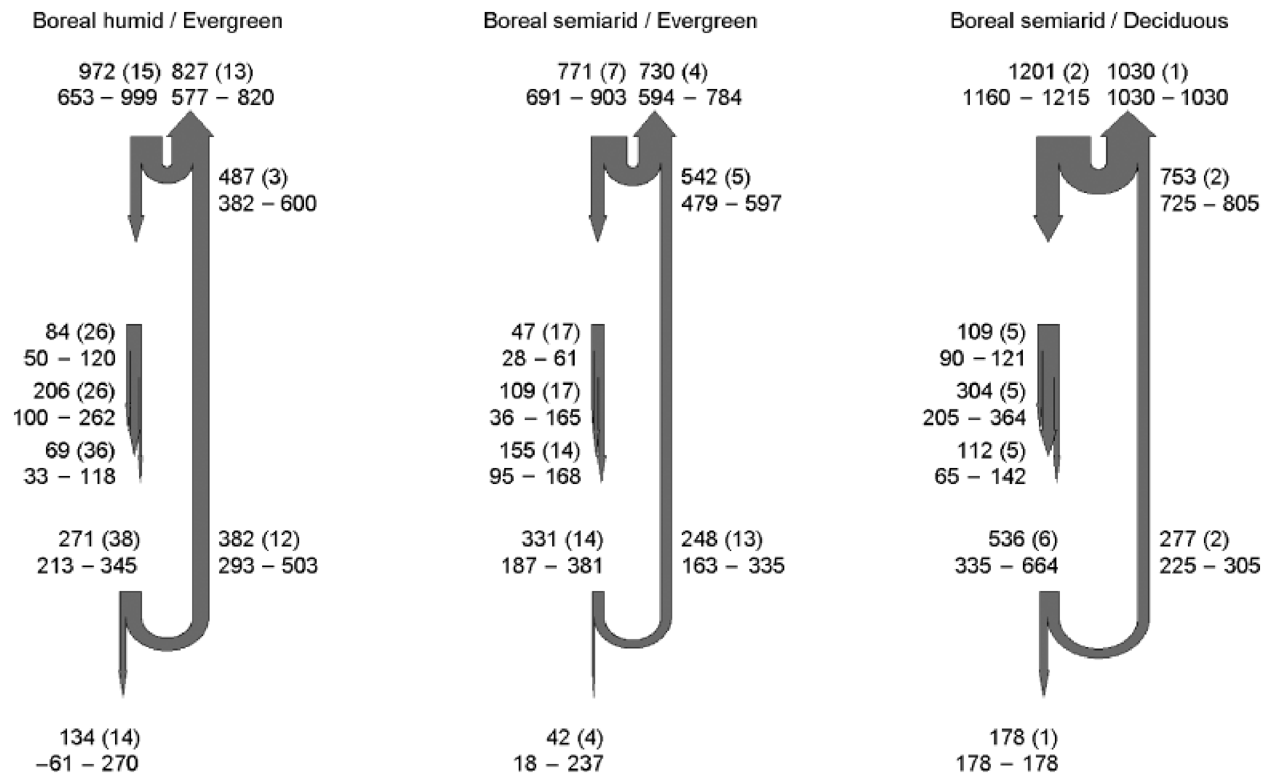

Fig. 10 Observed CO_2 balance for boreal biomes. These CO_2 balances were not closed and therefore the identities given by Eqns (1)–(4) do not apply. The width of the arrows is proportional to the fluxes and all units are in $g\,C\,m^{-2}\,yr^{-1}$. The legend of the figures is given in Fig. 8. Flux values were obtained from the same data but a different bootstrap-run and can therefore be slightly different from the values reported in Table 3.

Phillips *et al*., 2002). Even if the non-CO_2 losses amount to 15–20% of the NPP (Clark *et al*., 2001; Grace & Malhi, 2002; Richey *et al*., 2002), the sequestration of carbon in soils and organic matter pools is expected to be an important process in tropical humid forests. Despite the summer drought in Mediterranean warm forests, the equivalent of 25% of the CO_2 accumulated through photosynthesis remains in the ecosystem (Fig. 8). In this biome, wNPP is roughly equal to NEP, which suggests declining soil organic matter pools in response to land-use change or ecosystem perturbation.

Within the different temperate biomes, large differences were observed in absolute flux values (i.e. GPP, NPP, NEP; Fig. 9). In temperate humid evergreen forests the mean annual NEP is larger than the wNPP. Roughly 70% of the NEP accumulates in the woody biomass, and therefore sequestration of carbon in soils and organic matter pools is expected to be an important process. Temperate semiarid forests are close to a CO_2-neutral state, which means that an equal amount of CO_2 that was taken up by photosynthesis is released by auto- and heterotrophic respiration (Fig. 9). In temperate humid deciduous and temperate semiarid evergreen forests, wNPP and NEP are almost equal so accumulation of the entire annual NEP can occur in the woody biomass reducing the importance of the soil and organic matter pools for carbon sequestration.

The differences among the boreal biomes are smaller than the differences among the temperate biomes. In general, the boreal humid evergreen forests have higher absolute fluxes than the boreal semiarid evergreen forests. However, the boreal semiarid deciduous biome is more productive than its humid counterparts. In all three boreal biomes wNPP exceeds NEP, suggesting an important contribution of decomposition of historical carbon through land-use change or ecosystem perturbation.

Carbon use, expressed as the ratio of R_e over GPP (Table 3), is significantly different between temperate humid evergreen, temperate humid deciduous, and mediterranean warm forests in one group, boreal humid evergreen, boreal semiarid deciduous and tropical humid in a second group and boreal semiarid evergreen and temperate semiarid in a third group (ANOVA, $P<0.01$). High efficiencies, indicated by low R_e/GPP ratios were found in temperate humid and mediterranean forests. The variability in carbon use across forest biomes observed from our database is larger than the previously reported variability across forests, grasslands

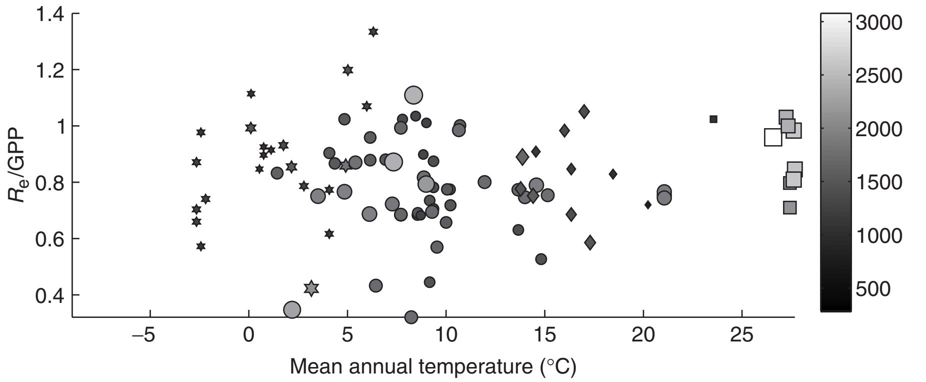

Fig. 11 Global patterns in R_e/gross primary production (GPP) according to the mean annual temperature and annual precipitation sum. The size and the color of the marker are measures for the absolute flux value. Stars, boreal; circles, temperate; diamonds, Mediterranean; and squares, tropical forests.

and tundra (Law *et al.*, 2002). As the drivers of NEP are not well understood it is not clear what determines these differences in carbon use but it is hypothesized that intensive managed (i.e. increasing wood production through thinning is among the causes of a more-efficient carbon use in forest biomes). We did not observe a global pattern in carbon use (Fig. 11).

Closing the CO_2 balance. In Figs 8–10, weighted mean CO_2-fluxes are plotted for different biomes without any further consideration. At intermediate temporal scales (years to decades) and in the absence of measurement and conceptual errors [Eqns (1)–(5) are to be used on the appropriate timescale], the theoretical relationships among the fluxes should hold. However, the figures indicate that this agreement is often poor. Therefore, closure of the CO_2 balance was enforced by adding an additional 'closure term.'

The closure terms are a numerical way to approach data quality and flux uncertainty on the biome-level. An underestimation of one flux (i.e. NPP can be accounted for by adding a closure term to NPP but also by decreasing R_a or GPP). Therefore, it is preferable to focus on the sum of the absolute values of the closure terms (Table 3), instead of individual closure terms (not shown). For all biomes, substantial correction terms (ranging from 10% to 60% of GPP) were needed to close the CO_2 balance (Table 3). There is no relationship between the relative amount of unallocated carbon and the mean annual temperature (Fig. 12) or annual precipitation sum (not shown).

Recall that the CO_2 balances for temperate humid evergreen, temperate humid deciduous and tropical humid evergreen forests were found to be robust against the influence of individual flux estimates (see 'Available data'). Despite robustness, 10–20% (Fig. 12) of the photosynthetic carbon uptake remains unallocated to a specific flux component, indicating that for these biomes better data in terms of accuracy and precision are needed rather than more data. Although the CO_2 balances for boreal humid evergreen and temperate semi-arid evergreen forests are reasonable robust (see 'Available data'), 45–60% of the carbon uptake remains unallocated in these ecosystems. More and better observations of the respiratory processes and lateral fluxes at the ecosystem scale (i.e. advection, VOC, DOC) would enable us to better close the CO_2 balances and to estimate regional and global carbon budgets more accurately than currently possible.

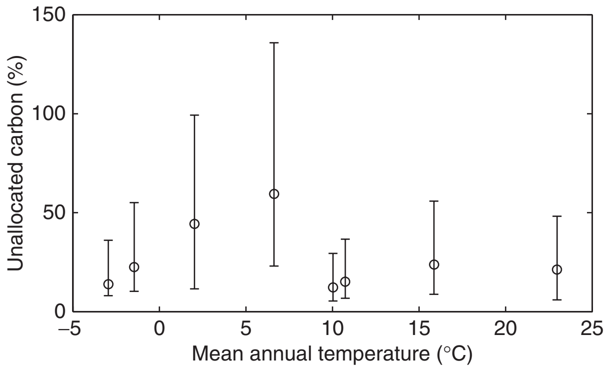

Fig. 12 Relationship between the unallocated carbon, calculated as the sum of the closure terms for gross primary production (GPP), net primary production (NPP), net ecosystem production (NEP), R_e, R_a and R_h and the mean annual temperature. Biomes from left to right: boreal semiarid deciduous, boreal semiarid evergreen, boreal humid evergreen, temperate semiarid evergreen, temperate humid evergreen, temperate humid deciduous, mediterranean warm evergreen, and tropical humid evergreen.

Conclusions

We have described a new global database of forest C fluxes and pools. This database, which quantifies CO_2 fluxes and pathways across a number of different levels of integration (from photosynthesis up to net ecosystem production), fills an important gap for model calibration, model validation and hypothesis testing at global and regional scales. The database contains 513 sites from eight major biomes. Estimates of the mean fluxes in temperate humid evergreen, temperate humid deciduous and tropical humid evergreen were found to be robust; in other biomes, small sample sizes and high variability among sampled sites resulted in less robust flux estimates. Closing the CO_2 balances required the introduction of closure terms. The value of the closure terms was taken as an indication for the existence of methodological and conceptual errors in the CO_2 balances. For all biomes, the correction terms needed to close biome-specific CO_2 balances are substantial, ranging from 10% to 60%. We believe that a better understanding of respiratory processes and lateral fluxes at the ecosystem scale is a prerequisite to closing CO_2 balances at the ecosystem level. This would enable us to estimate regional and global carbon budgets more accurately than currently possible. Carbon budgets of semiarid forests (boreal, temperate and tropical) would benefit most from additional data inputs.

The global patterns in GPP and NPP show clear relationships with mean annual temperature and annual precipitation. Primary production increases with increasing temperature and precipitation, but saturates beyond a threshold of 1500 mm precipitation for GPP and NPP or 10 °C mean annual temperature for NPP. Global patterns in NEP were not correlated with climatic variables. We hypothesize instead that variability in NEP is mainly determined by nonclimatic conditions such as successional stage, management, site history and site disturbance.

Availability of the database

Contributions or corrections to the database, as well as requests to use the database (subject to standard 'Fair Use' policies), should be directed to the corresponding author (S. L.).

Acknowledgements

We thank all site investigators, their funding agencies and the various regional flux networks (Afriflux, Ameriflux, AsiaFlux, CarboAfrica, CarboEurope-IP, ChinaFlux, Fluxnet-Canada, Ko-Flux, LBA, NECC, OzFlux, TCOS-Siberia, USCCC and Fluxnet) whose support is essential for obtaining the measurements without which the type of integrated analyses conducted in this article would not be possible. Data collection and processing was partly funded by CarboEurope-IP. The Research Foundation - Flanders (FWO-Vlaanderen) supported S.L. and B.G. with a post-doctoral fellowship and a research grant.

References

Amiro BD, Barr AG, Black TA *et al*. (2006) Carbon, energy and water fluxes at mature and disturbed forest sites, Saskatchewan, Canada. *Agricultural and Forest Meteorology*, **136**, 237–251.

Amthor JS (2000) The McCree-de Wit-Penning de Vries-Thornley respiration paradigms: 30 years later. *Annals of Botany*, **86**, 1–20.

Araujo AC, Nobre AD, Kruijt B *et al*. (2002) Comparative measurements of carbon dioxide fluxes from two nearby towers in a central Amazonian rainforest: The Manaus LBA site. *Journal of Geophysical Research-Atmospheres*, **107**, 8090–9019.

Baldocchi D (2003) Assessing the eddy covariance technique for evaluating carbon dioxide exchange rates of ecosystems: past, present and future. *Global Change Biology*, **9**, 479–492.

Baldocchi D, Falge E, Gu LH *et al*. (2001) FLUXNET: a new tool to study the temporal and spatial variability of ecosystem-scale carbon dioxide, water vapor, and energy flux densities. *Bulletin of the American Meteorological Society*, **82**, 2415–2434.

Black K, Bolger T, Davis P *et al*. (2007) Inventory and eddy covariance-based estimates of annual carbon sequestration in a Sitka spruce (*Picea sitchensis* (Bong.) Carr.) forest ecosystem. *European Journal of Forest Research*, **126**, 167–178.

Buchmann N, Schulze ED (1999) Net CO_2 and H_2O fluxes of terrestrial ecosystems. *Global Biogeochemical Cycles*, **13**, 751–760.

Chapin FS, Woodwell GM, Randerson JT *et al*. (2006) Reconciling carbon-cycle concepts, terminology and methodology. *Ecosystems*, **9**, 1041–1050.

Ciais P, Reichstein M, Viovy N *et al*. (2005) Europe-wide reduction in primary productivity caused bt the heat and drought in 2003. *Nature*, **437**, 529–533.

Clark DA (2002) Are tropical forests an important carbon sink? Reanalysis of the long-term plot data. *Ecological Applications*, **12**, 3–7.

Clark DA, Brown S, Kicklighter DW *et al*. (2001) Measuring net primary production in forests: concepts and field methods. *Ecological Applications*, **11**, 356–370.

Cramer W, Kicklighter DW, Bondeau A *et al*. (1999) Comparing global models of terrestrial net primary productivity (NPP): overview and key results. *Global Change Biology*, **5**, 1–15.

Falge E, Baldocchi D, Olson R *et al*. (2001) Gap filling strategies for defensible annual sums of net ecosystem exchange. *Agricultural and Forest Meteorology*, **107**, 43–69.

Global Soil Data Task (2000) *Global Soil Data Products CD-ROM (IGBP-DIS)*. International Geosphere-Biosphere Programme, Data and Information System, Potsdam, Germany. Oak Ridge National Laboratory Distributed Active Archive Center, Oak Ridge, TN, USA, http://www.daac.ornl.gov

Goulden ML, Munger JW, Fan SM *et al*. (1996) Measurements of carbon sequestration by long-term eddy covariance: methods and a critical evaluation of accuracy. *Global Change Biology*, **2**, 169–182.

Gower ST, Pongracic S, Landsberg JJ (1996) A global trend in belowground carbon allocation: can we use the relationship at smaller scales? *Ecology*, **77**, 1750–1755.

Grace J, Malhi Y (2002) Carbon dioxide goes with the flow. *Nature*, **416**, 594–595.

Griffis TJ, Black TA, Morgenstern K *et al.* (2003) Ecophysiological controls on the carbon balances of three southern boreal forests. *Agricultural and Forest Meteorology*, **117**, 53–71.

Guenther A, Hewitt CN, Erickson D *et al.* (1995) A global-model of natural volatile organic-compound emissions. *Journal of Geophysical Research-Atmospheres*, **100**, 8873–8892.

Hanson PJ, Edwards NT, Garten CT *et al.* (2000) Separating root and soil microbial contributions to soil respiration: a review of methods and observations. *Biogeochemistry*, **48**, 115–146.

Hanson PJ, Edwards NT, Tschaplinski TJ, Wullschleger SD, Joslin JD (2003) Estimating the net primary and net ecosystem production of a southeastern upland *Quercus* forest from an 8-year biometric record. In: *North American Temperate Deciduous Forest Responses to Changing Precipitation Regimes* (eds Hanson PJ, Wullschleger SD), pp. 472. Springer, New York.

Hollinger DY, Aber J, Dail B *et al.* (2004) Spatial and temporal variability in forest-atmosphere CO_2 exchange. *Global Change Biology*, **10**, 1689–1706.

Hollinger DY, Richardson AD (2005) Uncertainty in eddy covariance measurements and its application to physiological models. *Tree Physiology*, **25**, 873–885.

Jager HI, Hargrove WW, Brandt CC *et al.* (2000) Constructive contrasts between modeled and measured climate responses over a regional scale. *Ecosystems*, **3**, 396–411.

Janssens IA, Lankreijer H, Matteucci G *et al.* (2001) Productivity overshadows temperature in determining soil and ecosystem respiration across European forests. *Global Change Biology*, **7**, 269–278.

Keppler F, Hamilton JTG, BraB M *et al.* (2006) Methane emissions from terrestrial plants under aerobic conditions. *Nature*, **439**, 187.

Krinner G, Viovy N, de Noblet-Ducoudre N *et al.* (2005) A dynamic global vegetation model for studies of the coupled atmosphere–biosphere system. *Global Biogeochemical Cycles*, **19**, 1015.

Kruijt B, Elbers JA, von Randow C *et al.* (2004) The robustness of eddy correlation fluxes for Amazon rain forest conditions. *Ecological Applications*, **14**, S101–S113.

Law BE, Falge E, Gu L *et al.* (2002) Environmental controls over carbon dioxide and water vapor exchange of terrestrial vegetation. *Agricultural and Forest Meteorology*, **113**, 97–120.

Law BE, Turner D, Campbell J *et al.* (2004) Disturbance and climate effects on carbon stocks and fluxes across Western Oregon USA. *Global Change Biology*, **10**, 1429–1444.

Lieth HFH, Whittaker RH (1975) *Primary Productivity of the Biosphere*. Springer-Verlag, New York.

Malhi Y, Baldocchi DD, Jarvis PG (1999) The carbon balance of tropical, temperate and boreal forests. *Plant Cell and Environment*, **22**, 715–740.

Malhi Y, Grace J (2000) Tropical forests and atmospheric carbon dioxide. *Trends in Ecology and Evolution*, **15**, 332–337.

Mitchell TD, Jones PD (2005) An improved method of constructing a database of monthly climate observations and associated high-resolution grids. *International Journal of Climatology*, **25**, 693–712.

Olson RJ, Johnson KR, Zheng DL *et al.* (2001) Global and regional ecosystem modeling: database of model drivers and validation measurements. Oak Ridge National Laboratory, Oak Ridge, TN.

Oren RAM, Hsieh C-I, Stoy P *et al.* (2006) Estimating the uncertainty in annual net ecosystem carbon exchange: spatial variation in turbulent fluxes and sampling errors in eddy-covariance measurements. *Global Change Biology*, **12**, 883–896.

Papale D, Reichstein M, Aubinet M *et al.* (2006) Towards a standardized processing of net ecosystem exchange measured with eddy covariance technique: algorithms and uncertainty estimation. *Biogeosciences*, **3**, 571–583.

Penning de Vries FWT, Brunstin AHM, Vanlaar HH (1974) Products, requirements and efficiency of biosynthesis – quantitative approach. *Journal of Theoretical Biology*, **45**, 339–377.

Phillips OL, Malhi Y, Higuchi N *et al.* (1998) Changes in the carbon balance of tropical forests: evidence from long-term plots. *Science*, **282**, 439–442.

Phillips OL, Martinez RV, Arroyo L *et al.* (2002) Increasing dominance of large lianas in Amazonian forests. *Nature*, **418**, 770–774.

Raich JW, Nadelhoffer KJ (1989) Belowground carbon allocation in forest ecosystems: global trends. *Ecology*, **70**, 1346–1354.

Randerson JT, Chapin FS, Harden JW *et al.* (2002) Net ecosystem production: a comprehensive measure of net carbon accumulation by ecosystems. *Ecological Applications*, **12**, 937–947.

Reich PF, Eswaran H (2002) Global resources. In: *Encyclopedia of Soil Science* (ed. Lal R), pp. 607–611. Marcel Dekker, New York.

Reichstein M, Falge E, Baldocchi D *et al.* (2005) On the separation of net ecosystem exchange into assimilation and ecosystem respiration: review and improved algorithm. *Global Change Biology*, **11**, 1424–1439.

Reichstein M, Rey A, Freibauer A *et al.* (2003) Modeling temporal and large-scale spatial variability of soil respiration from soil water availability, temperature and vegetation productivity indices. *Global Biogeochemical Cycles*, **17**, 1104–1118.

Richardson AD, Hollinger DY (2005) Statistical modeling of ecosystem respiration using eddy covariance data: maximum likelihood parameter estimation, and Monte Carlo simulation of model and parameter uncertainty, applied to three simple models. *Agricultural and Forest Meteorology*, **131**, 191–208.

Richardson AD, Hollinger DY, Burba GG *et al.* (2006) A multi-site analysis of random error in tower-based measurements of carbon and energy fluxes. *Agricultural and Forest Meteorology*, **136**, 1–18.

Richey JE, Melack JM, Aufdenkampe AK *et al.* (2002) Outgassing from Amazonian rivers and wetlands as a large tropical source of atmospheric CO_2. *Nature*, **416**, 617–620.

Ryan MG, Hubbard RM, Pongracic S *et al.* (1996) Foliage, fine-root, woody-tissue and stand respiration in *Pinus radiata* in relation to nitrogen status. *Tree Physiology*, **16**, 333–343.

Saleska SR, Miller SD, Matross DM *et al.* (2003) Carbon in amazon forests: unexpected seasonal fluxes and disturbance-induced losses. *Science*, **302**, 1554–1557.

Schimel DS, House JI, Hibbard KA *et al.* (2001) Recent patterns and mechanisms of carbon exchange by terrestrial ecosystems. *Nature*, **414**, 169–172.

Schulze ED (2005) *Plant Ecology*. Springer-Verlag, Berlin.

Schulze ED, Heimann M (1998) Carbon and water exchange of terrestrial systems. In: *Asian Change in the Context of Global Change. IGBP Series*, Vol. 3 (eds Galloway JN, Melillo J), pp. 145–161. Cambridge University Press, Cambridge.

Schulze ED, Wirth C, Heimann M (2000) ''Kyoto forests'' and a broader perspective on management – response. *Science*, **290**, 1896–1896.

Schuur EAG (2003) Productivity and global climate revisited: the sensitivity of tropical forest growth to precipitation. *Ecology*, **84**, 1165–1170.

Scurlock JMO, Olson RJ (2002) Terrestrial net primary productivity – a brief history and a new worldwide database. *Environmental Reviews*, **10**, 91–109.

Tucker CJ, Pinzon JE, Brown ME *et al*. (2005) An extended AVHRR 8-km NDVI dataset compatible with MODIS and SPOT vegetation NDVI data. *International Journal of Remote Sensing*, **26**, 4485–4498.

Valentini R, Matteucci G, Dolman AJ *et al*. (2000) Respiration as the main determinant of carbon balance in European forests. *Nature*, **404**, 861–865.

Appendix A

Appendix A Data sources contained in the database.

Ameriflux (2006) *Ameriflux database*. http://public.ornl.gov/ameriflux/

Andrews JA, Harrison KG, Matamala R, Schlesinger WH (1999) Separation of root respiration from total soil respiration using carbon-13 labeling during free-air carbon dioxide enrichment (FACE). *Soil Science Society of America Journal*, **63**, 1429–1435.

Araujo AC, Nobre AD, Kruijt B *et al*. (2002) Comparative measurements of carbon dioxide fluxes from two nearby towers in a central Amazonian rainforest: The Manaus LBA site. *Journal of Geophysical Research-Atmospheres*, **107**, 8090–9019.

Arneth A, Kelliher FM, McSeveny TM, Byers JN (1998) Net ecosystem productivity, net primary productivity and ecosystem carbon sequestration in a *Pinus radiata* plantation subject to soil water deficit. *Tree Physiology*, **18**, 785–793.

Arneth A, Kelliher FM, McSeveny TM, Byers JN (1999) Assessment of annual carbon exchange in a water-stressed *Pinus radiata* plantation: an analysis based on eddy covariance measurements and an integrated biophysical model. *Global Change Biology*, **5**, 531–545.

Asensio D, Penuelas J, Ogaya R, Llusia J (2007) Seasonal soil and leaf CO_2 exchange rates in a Mediterranean holm oak forest and their responses to drought conditions. *Atmospheric Environment*, **41**, 2447–2455.

Aubinet M, Grelle A, Ibrom A *et al*. (2000) Estimates of the annual net carbon and water exchange of forests: The EUROFLUX methodology. *Advances in Ecological Research*, **30**, 113–175.

Barr AG, Black TA, Hogg EH, Griffis TJ, Morgenstern K, Kljun N, Theede A, Nesic Z (2007) Climatic controls on the carbon and water balances of a boreal aspen forest, 1994–2003. *Global Change Biology*, **13**, 561–576.

Barr AG, Griffis TJ, Black TA, Lee X, Staebler RM, Fuentes JD, Chen Z, Morgenstern K (2002) Comparing the carbon budgets of boreal and temperate deciduous forest stands. *Canadian Journal of Forest Research-Revue Canadienne De Recherche Forestiere*, **32**, 813–822.

Bascietto M, Hajny MT, Linder S, Masci A, Matteucci G, Montagnani L, Moors E, Mund M (2003) *Database of tree stands (Structure, age, biomass, LAI and NPP) of the FORCAST project*. http://www.daac.ornl.gov

Behera N, Joshi SK, Pati DP (1990) Root contribution to total soil metabolism in a tropical forest soil from Orissa, India. *Forest Ecology and Management*, **36**, 125–134.

Berbigier P, Bonnefond JM, Mellmann P (2001) CO_2 and water vapour fluxes for 2 years above Euroflux forest site. *Agricultural and Forest Meteorology*, **108**, 183–197.

Bergeron O, Margolis HA, Black TA, Coursolle C, Dunn AL, Barr AG, Wofsy SC (2007) Comparison of carbon dioxide fluxes over three boreal black spruce forests in Canada. *Global Change Biology*, **13**, 89–107.

Bergh J, Linder S (1999) Effects of soil warming during spring on photosynthetic recovery in boreal Norway spruce stands. *Global Change Biology*, **5**, 245–253.

Bhupinderpal S, Nordgren A, Lofvenius MO, Hogberg MN, Mellander PE, Hogberg P (2003) Tree root and soil heterotrophic respiration as revealed by girdling of boreal Scots pine forest: extending observations beyond the first year. *Plant, Cell, and Environment*, **26**, 1287–1296.

Black K, Bolger T, Davis P, Nieuwenhuis M, Reidy B, Saiz G, Tobin B, Osborne B (2007) Inventory and eddy covariance-based estimates of annual carbon sequestration in a Sitka spruce (*Picea sitchensis* (Bong.) Carr.) forest ecosystem. *European Journal of Forest Research*, **126**, 167–178.

Black K, Tobin B, Saiz G, Byrne KA, Osborne B (2004) Improved estimates of biomass expansion factors for Sitka spruce. *Irish Forestry*, **61**, 50–65.

Black TA, DenHartog G, Neumann HH *et al*. (1996) Annual cycles of water vapour and carbon dioxide fluxes in and above a boreal aspen forest. *Global Change Biology*, **2**, 219–229.

Bolstad PV, Davis KJ, Martin J, Cook BD, Wang W (2004) Component and whole-system respiration fluxes in northern deciduous forests. *Tree Physiology*, **24**, 493–504.

Bond-Lamberty B, Wang C, Gower ST, Norman J (2002) Leaf area dynamics of a boreal black spruce fire chronosequence. *Tree Physiology*, **22**, 993–1001.

Bond-Lamberty B, Wang CK, Gower ST (2004) Contribution of root respiration to soil surface CO_2 flux in a boreal black spruce chronosequence. *Tree Physiology*, **24**, 1387–1395.

Bowden RD, Nadelhoffer KJ, Boone RD, Melillo JM, Garrison JB (1993) Contributions of aboveground litter, belowground litter, and root respiration to total soil respiration in a temperature mixed hardwood forest. *Canadian Journal of Forest Research-Revue Canadienne De Recherche Forestiere*, **23**, 1402–1407.

Buchmann N (2000) Biotic and abiotic factors controlling soil respiration rates in *Picea abies* stands. *Soil Biology & Biochemistry*, **32**, 1625–1635.

Burton AJ, Pregitzer KS, Crawford JN, Zogg GP, Zak DR (2004) Simulated chronic NO_3- deposition reduces soil respiration in northern hardwood forests. *Global Change Biology*, **10**, 1080–1091.

Calfapietra C, Gielen B, Sabatti M, De Angelis P, Miglietta F, Scarascia-Mugnozza G, Ceulemans R (2003) Do above-ground growth dynamics of poplar change with time under CO_2 enrichment? *New Phytologist*, **160**, 305–318.

Campbell JL, Sun OJ, Law BE (2004) Disturbance and net ecosystem production across three climatically distinct forest landscapes. *Global Biogeochemical Cycles*, **18**, GB4017.

CarboEurope-IP (2006) *CarboEurope-IP database*. http://gaia.agraria.unitus.it/cpz/login.asp

Carrara A, Kowalski AS, Neirynck J, Janssens IA, Yuste JC, Ceulemans R (2003) Net ecosystem CO_2 exchange of mixed forest in Belgium over 5 years. *Agricultural and Forest Meteorology*, **119**, 209–227.

Carswell FE, Costa AL, Palheta M *et al*. (2002) Seasonality in CO_2 and H_2O flux at an eastern Amazonian rain forest. *Journal of Geophysical Research-Atmospheres*, **107**, 8076.

Chambers JQ, Tribuzy ES, Toledo LC *et al*. (2004) Respiration from a tropical forest ecosystem: partitioning of sources and low carbon use efficiency. *Ecological Applications*, **14**, S72–S88.

Clark DA (1998) *NPP Tropical Forest*. Oak Ridge National Laboratory Distributed Active Archive Center, Oak Ridge, Tennessee, USA, http://www.daac.ornl.gov

Clark DA, Brown S, Kicklighter DW, Chambers JQ, Thomlinson JR, Ni J, Holland EA (2001) Net primary production in tropical forests: an evaluation and synthesis of existing field data. *Ecological Applications*, **11**, 371–384.

Clark KL, Gholz HL, Castro MS (2004) Carbon dynamics along a chronosequence of slash pine plantations in north Florida. *Ecological Applications*, **14**, 1154–1171.

Clark KL, Gholz HL, Moncrieff JB, Cropley F, Loescher HW (1999) Environmental controls over net exchanges of carbon dioxide from contrasting Florida ecosystems. *Ecological Applications*, **9**, 936–948.

Cleveland CC, Townsend AR (2006) Nutrient additions to a tropical rain forest drive substantial soil carbon dioxide losses to the atmosphere. *Proceedings of The National Academy of Sciences of The United States of America*, **103**, 10316–10321.

Coles JRP, Yavitt JB (2004) Linking belowground carbon allocation to anaerobic CH_4 and CO_2 production in a forested peatland, New York state. *Geomicrobiology Journal*, **21**, 445–455.

Comeau PG, Kimmins JP (1999) *NPP Boreal Forest*. Oak Ridge National Laboratory Distributed Active Archive Center, Oak Ridge, Tennessee, USA, http://www.daac.ornl.gov

Cronan CS (2003) Belowground biomass, production, and carbon cycling in mature Norway spruce, Maine, USA. *Canadian Journal of Forest Research-Revue Canadienne De Recherche Forestiere*, **33**, 339–350.

Cronan CS, Grigal DF (1995) Use of calcium aluminum atios as indicators of stress in forest ecosystems. *Journal of Environmental Quality*, **24**, 209–226.

Curtis PS, Hanson PJ, Bolstad P, Barford C, Randolph JC, Schmid HP, Wilson KB (2002) Biometric and eddy-covariance based estimates of annual carbon storage in five eastern North American deciduous forests. *Agricultural and Forest Meteorology*, **113**, 3–19.

Davidson EA, Savage K, Bolstad P *et al*. (2002) Belowground carbon allocation in forests estimated from litterfall and IRGA-based soil respiration measurements. *Agricultural and Forest Meteorology*, **113**, 39–51.

DeAngelis DL, Gardner RH, Shugart HH (1981) Productivity of forest ecosystems studied during the IBP: the woodlands data set. In: *Dynamics of forest ecosystems* (ed. Reichle DE). Cambridge University Press, Cambridge.

DeLucia EH, Hamilton JG, Naidu SL *et al*. (1999) Net primary production of a forest ecosystem with experimental CO_2 enrichment. *Science*, **284**, 1177–1179.

Desai AR, Bolstad PV, Cook BD, Davis KJ, Carey EV (2005) Comparing net ecosystem exchange of carbon dioxide between an old-growth and mature forest in the upper Midwest, USA. *Agricultural and Forest Meteorology*, **128**, 33–55.

Dorr H, Munnich KO (1987) Annual variation in soil respiration in selected areas of the temperate zone. *Tellus B*, **39**, 114–121.

Dunn AL, Barford CC, Wofsy SC, Goulden ML, Daube BC (2007) A long-term record of carbon exchange in a boreal black spruce forest: means, responses to interannual variability, and decadal trends. *Global Change Biology*, **13**, 577–590.

Edwards NT, Harris WF (1977) Carbon cycling in a mixed deciduous forest floor. *Ecology*, **58**, 431–435.

Ehman JL, Schmid HP, Grimmond CSB, Randolph JC, Hanson PJ, Wayson CA, Cropley FD (2002) An initial intercomparison of micrometeorological and ecological inventory estimates of carbon exchange in a mid-latitude deciduous forest. *Global Change Biology*, **8**, 575–589.

Eliasson PE, McMurtrie RE, Pepper DA, Stromgren M, Linder S, Agren GI (2005) The response of heterotrophic CO_2 flux to soil warming. *Global Change Biology*, **11**, 167–181.

Epron D, Farque L, Lucot E, Badot PM (1999) Soil CO_2 efflux in a beech forest: dependence on soil temperature and soil water content. *Annals of Forest Science*, **56**, 221–226.

Epron D, Le Dantec V, Dufrene E, Granier A (2001) Seasonal dynamics of soil carbon dioxide efflux and simulated rhizosphere respiration in a beech forest. *Tree Physiology*, **21**, 145–152.

Epron D, Nouvellon Y, Deleporte P *et al*. (2006) Soil carbon balance in a clonal Eucalyptus plantation in Congo: effects of logging on carbon inputs and soil CO_2 efflux. *Global Change Biology*, **12**, 1021–1031.

Esser G, Lieth HFH, Scurlock JMO, Olson RJ (1997) Worldwide estimates and bibliography of net primary productivity derived from pre-1982. Publications ORNL Technical Memorandum TM-13485. Oak Ridge National Laboratory, 132 pp.

Ewel KC, Cropper WP, Gholz HL (1987) Soil CO_2 evolution in Florida slash pine plantations.2. importance of root respiration. *Canadian Journal of Forest Research-Revue Canadienne De Recherche Forestiere*, **17**, 330–333.

Fahey TJ, Hughes JW (1994) Fine-root dynamics in a northern hardwood forest ecosystem, Hubbard Brook experimental forest, Nh. *Journal of Ecology*, **82**, 533–548.

Fahey TJ, Tierney GL, Fitzhugh RD, Wilson GF, Siccama TG (2005) Soil respiration and soil carbon balance in a northern hardwood forest ecosystem. *Canadian Journal of Forest Research-Revue Canadienne De Recherche Forestiere*, **35**, 244–253.

Falge E, Baldocchi D, Tenhunen J *et al*. (2002) Seasonality of ecosystem respiration and gross primary production as derived from FLUXNET measurements. *Agricultural and Forest Meteorology*, **113**, 53.

Fluxnet (2006) *Fluxnet database*. http://www.fluxnet.ornl.gov/fluxnet/index.cfm

Fredeen AL, Waughtal JD, Pypker TG (2007) When do replanted sub-boreal clearcuts become net sinks for CO_2? *Forest Ecology and Management*, **239**, 210.

Gaumont-Guay D, Black TA, Griffis TJ, Barr AG, Morgenstern K, Jassal RS, Nesic Z (2006) Influence of temperature and drought on seasonal and interannual variations of soil, bole and ecosystem respiration in a boreal aspen stand. *Agricultural and Forest Meteorology*, **140**, 203–219.

Giardina CP, Binkley D, Ryan MG, Fownes JH, Senock RS (2004) Belowground carbon cycling in a humid tropical forest decreases with fertilization. *Oecologia*, **139**, 545–550.

Giardina CP, Ryan MG, Binkley D, Fownes JH (2003) Primary production and carbon allocation in relation to nutrient supply in a tropical experimental forest. *Global Change Biology*, **9**, 1438–1450.

Gielen B, Calfapietra C, Lukac M *et al*. (2005) Net carbon storage in a poplar plantation (POPFACE) after three years of free-air CO_2 enrichment. *Tree Physiology*, **25**, 1399–1408.

GKSS (2001) *Multi-decadal atmospheric modeling for Europe*. GKSS, Frauke Freser, http://www.daac.ornl.gov

Global_Soil_Data_Task (2000) *Global Soil Data Products CD-ROM (IGBP-DIS)*. International Geosphere-Biosphere Programme, Data and Information System, Potsdam, Germany. Oak Ridge National Laboratory Distributed Active Archive Center, Oak Ridge, Tennessee, USA, http://www.daac.ornl.gov

Goulden ML, Miller SD, da Rocha HR, Menton MC, de Freitas HC, Figueira A, de Sousa CAD (2004) Diel and seasonal patterns of tropical forest CO_2 exchange. *Ecological Applications*, **14**, S42–S54.

Goulden ML, Wofsy SC, Harden JW *et al*. (1998) Sensitivity of boreal forest carbon balance to soil thaw. *Science*, **279**, 214–217.

Gower ST, Krankina O, Olson RJ, Apps M, Linder S, Wang C (2001) Net primary production and carbon allocation patterns of boreal forest ecosystems. *Ecological Applications*, **11**, 1395–1411.

Gower ST, Vogel JG, Norman JM, Kucharik CJ, Steele SJ, Stow TK (1997) Carbon distribution and aboveground net primary production in aspen, jack pine, and black spruce stands in Saskatchewan and Manitoba, Canada. *Journal of Geophysical Research-Atmospheres*, **102**, 29029–29041.

Grace J (2004) *CARBO-AGE Age related dynamics of carbon exchange in European forests*. Contract EVK2-CT-1999-00045, Final Report. University of Edinburgh.

Greco S, Baldocchi DD (1996) Seasonal variations of CO_2 and water vapour exchange rates over a temperate deciduous forest. *Global Change Biology*, **2**, 183–197.

Griffis TJ, Black TA, Gaumont-Guay D, Drewitt GB, Nesic Z, Barr AG, Morgenstern K, Kljun N (2004) Seasonal variation and partitioning of ecosystem respiration in a southern boreal aspen forest. *Agricultural and Forest Meteorology*, **125**, 207–223.

Grimm U, Fassbender HW (1999) *NPP tropical forest*. Oak Ridge National Laboratory Distributed Active Archive Center, Oak Ridge, Tennessee, USA, http://www.daac.ornl.gov

Guan DX, Wu JB, Zhao XS, Han SJ, Yu GR, Sun XM, Jin CJ (2006) CO_2 fluxes over an old, temperate mixed forest in northeastern China. *Agricultural and Forest Meteorology*, **137**, 138–149.

Hamilton JG, DeLucia EH, George K, Naidu SL, Finzi AC, Schlesinger WH (2002) Forest carbon balance under elevated CO_2. *Oecologia*, **131**, 250–260.

Hanson PJ, Edwards NT, Tschaplinski TJ, Wullschleger SD, Joslin JD (2003) Estimating the net primary and net ecosystem production of a southeastern upland *Quercus* forest from an 8-year biometric record. In: *North American temperate deciduous forest responses to changing precipitation regimes* (eds Hanson PJ and Wullschleger, SD). Springer, New York.

Harmon ME, Bible K, Ryan MG, Shaw DC, Chen H, Klopatek J, Li X (2004) Production, respiration, and overall carbon balance in an old-growth Pseudotsuga-tsuga forest ecosystem. *Ecosystems*, **7**, 498–512.

Havas P (1999) *NPP Boreal Forest*. Oak Ridge National Laboratory Distributed Active Archive Center, Oak Ridge, Tennessee, USA, http://www.daac.ornl.gov

Haynes BE, Gower ST (1995) Belowground carbon allocation in unfertilized and fertilized red pine plantations in northern Wisconsin. *Tree Physiology*, **15**, 317–325.

Hirano T, Hirata R, Fujinuma Y *et al*. (2003) CO_2 and water vapor exchange of a larch forest in northern Japan. *Tellus Series B-Chemical and Physical Meteorology*, **55**, 244–257.

Hirano T, Segah H, Harada T, Limin S, June T, Hirata R, Osaki M (2007) Carbon dioxide balance of a tropical peat swamp forest in Kalimantan, Indonesia. *Global Change Biology*, **13**, 412–425.

Hogberg P, Nordgren A, Buchmann N *et al*. (2001) Large-scale forest girdling shows that current photosynthesis drives soil respiration. *Nature*, **411**, 789–792.

Hollinger DY, Aber J, Dail B *et al*. (2004) Spatial and temporal variability in forest-atmosphere CO_2 exchange. *Global Change Biology*, **10**, 1689–1706.

Humphreys ER, Black TA, Morgenstern K, Cai TB, Drewitt GB, Nesic Z, Trofymow JA (2006) Carbon dioxide fluxes in coastal Douglas-fir stands at different stages of development after clearcut harvesting. *Agricultural and Forest Meteorology*, **140**, 6–22.

Hutyra LR, Munger JW, Saleska SR *et al*. (2006) Seasonal controls on the exchange of carbon and water in an Amazonian rainforest. *Journal of geophysical Research*, **112**, G03008.

Irvine J, Law BE (2002) Contrasting soil respiration in young and old-growth ponderosa pine forests. *Global Change Biology*, **8**, 1183–1194.

Ito A, Oikawa T (2002) A simulation model of the carbon cycle in land ecosystems (Sim-CYCLE): a description based on dry-matter production theory and plot-scale validation. *Ecological Modelling*, **151**, 143–176.

Ito A, Saigusa N, Murayama S, Yamamoto S (2005) Modeling of gross and net carbon dioxide exchange over a cool-temperate deciduous broad-leaved forest in Japan: Analysis of seasonal and interannual change. *Agricultural and Forest Meteorology*, **134**, 122–134.

Janssens IA, Crookshanks M, Taylor G, Ceulemans R (1998) Elevated atmospheric CO_2 increases fine root production, respiration, rhizosphere respiration and soil CO_2 efflux in Scots pine seedlings. *Global Change Biology*, **4**, 871–878.

Jordan CF, Cuevas E, Medina E (1999) *NPP Tropical Forest*. Oak Ridge National Laboratory Distributed Active Archive Center, Oak Ridge, Tennessee, USA, http://www.daac.ornl.gov

JRC (2006) *FAPAR database*. Global Environmental Monitoring (GEM) Unit, Institute for Environment and Sustainability (IES), EC Joint Research Centre (JRC), Ispra, Italy. http://fapar.jrc.it/WWW/Data/Pages/FAPAR_Home/FAPAR_Home.php, http://www.daac.ornl.gov

Kalyn AL, Van Rees KCJ (2006) Contribution of fine roots to ecosystem biomass and net primary production in black spruce, aspen, and jack pine forests in Saskatchewan. *Agricultural and Forest Meteorology*, **140**, 236–243.

Khomik M, Arain MA, McCaughey JH (2006) Temporal and spatial variability of soil respiration in a boreal mixedwood forest. *Agricultural and Forest Meteorology*, **140**, 244–256.

Kidwell KB (1997) *NOAA global vegetation index user's guide*. U.S. Department of Commerce, National Oceanic and Atmospheric Administration, National Environmental Satellite, Data, and Information Service, National Climatic Data Center, Climate Services Division, Satellite Services Branch.

Kimball JS, Thornton PE, White MA, Running SW (1997) Simulating forest productivity and surface-atmosphere carbon exchange in the BOREAS study region. *Tree Physiology*, **17**, 589–599.

Kira T, Manokaran N, Appanah S (1998) *NPP Tropical Forest*. Oak Ridge National Laboratory Distributed Active Archive Center, Oak Ridge, Tennessee, USA, http://www.daac.ornl.gov

Knohl A, Schulze ED, Kolle O, Buchmann N (2003) Large carbon uptake by an unmanaged 250-year-old deciduous forest in Central Germany. *Agricultural and Forest Meteorology*, **118**, 151–167.

Kolari P, Pumpanen J, Rannik Ü, Ilvesniemi H, Hari P, Berninger F (2004) Carbon balance of different aged Scots pine forests in Southern Finland. *Global Change Biology*, **10**, 1106–1119.

Kowalski AS, Loustau D, Berbigier P *et al*. (2004) Paired comparisons of carbon exchange between undisturbed and regenerating stands in four managed forests in Europe. *Global Change Biology*, **10**, 1707–1723.

Kowalski S, Sartore M, Burlett R, Berbigier P, Loustau D (2003) The annual carbon budget of a French pine forest (*Pinus pinaster*) following harvest. *Global Change Biology*, **9**, 1051–1065.

Krakina (1999) *NPP Boreal Forest*. Oak Ridge National Laboratory Distributed Active Archive Center, Oak Ridge, Tennessee, USA, http://www.daac.ornl.gov

Krinner G, Viovy N, de Noblet-Ducoudre N *et al*. (2005) A dynamic global vegetation model for studies of the coupled atmosphere-biosphere system. *Global Biogeochemical Cycles*, **19**, GB1015.

Kutsch W, Eschenbach C, Dilly O *et al*. (2001a) The Carbon Cycle of Contrasting Landscape Elements of the Bornhöved District. In: *Ecosystem Approaches to Landscape Management in Central Europe. Ecological Studies*, Vol. 147 (ed. Tenhunen J), pp. 75–95. Springer-Verlag, Berlin, Heidelberg.

Kutsch WL, Liu CJ, Hormann G, Herbst M (2005) Spatial heterogeneity of ecosystem carbon fluxes in a broadleaved forest in Northern Germany. *Global Change Biology*, **11**, 70–88.

Kutsch WL, Staack A, Wojtzel J, Middelhoff U, Kappen L (2001b) Field measurements of root respiration and total soil respiration in an alder forest. *New Phytologist*, **150**, 157–168.

Lagergren F, Eklundh L, Grelle A, Lundblad M, Molder M, Lankreijer H, Lindroth A (2005) Net primary production and light use efficiency in a mixed coniferous forest in Sweden. *Plant, Cell, and Environment*, **28**, 412–423.

Lai C-T, Katul G, Butnor J, Ellsworth D, Oren R (2002) Modelling night time ecosystem respiration by a constrained source optimization method. *Global Change Biology*, **8**, 124–141.

Lavigne MB, Boutin R, Foster RJ, Goodine G, Bernier PY, Robitaille G (2003) Soil respiration responses to temperature are controlled more by roots than by decomposition in balsam fir ecosystems. *Canadian Journal of Forest Research-Revue Canadienne De Recherche Forestiere*, **33**, 1744–1753.

Law BE, Falge E, Gu L *et al*. (2002) Environmental controls over carbon dioxide and water vapor exchange of terrestrial vegetation. *Agricultural and Forest Meteorology*, **113**, 97–120.

Law BE, Kelliher FM, Baldocchi DD, Anthoni PM, Irvine J, Moore D, Van Tuyl S (2001a) Spatial and temporal variation in respiration in a young ponderosa pine forests during a summer drought. *Agricultural and Forest Meteorology*, **110**, 27–43.

Law BE, Ryan MG, Anthoni PM (1999) Seasonal and annual respiration of a ponderosa pine ecosystem. *Global Change Biology*, **5**, 169–182.

Law BE, Thornton PE, Irvine J, Anthoni PM, Van Tuyl S (2001b) Carbon storage and fluxes in ponderosa pine forests at different developmental stages. *Global Change Biology*, **7**, 755–777.

Law BE, Turner D, Campbell J, Sun OJ, Van Tuyl S, Ritts WD, Cohen WB (2004) Disturbance and climate effects on carbon stocks and fluxes across Western Oregon USA. *Global Change Biology*, **10**, 1429-1444.

Law BE, Waring RH, Anthoni PM, Aber JD (2000) Measurements of gross and net ecosystem productivity and water vapour exchange of a *Pinus ponderosa* ecosystem, and an evaluation of two generalized models. *Global Change Biology*, **6**, 155–168.

Lee MS, Nakane K, Nakatsubo T, Koizumi H (2003) Seasonal changes in the contribution of root respiration to total soil respiration in a cool-temperate deciduous forest. *Plant and Soil*, **255**, 311–318.

Lee MS, Nakane K, Nakatsubo T, Mo WH, Koizumi H (2002) Effects of rainfall events on soil CO_2 flux in a cool temperate deciduous broad-leaved forest. *Ecological Research*, **17**, 401–409.

Li YQ, Xu M, Sun OJ, Cui WC (2004) Effects of root and litter exclusion on soil CO_2 efflux and microbial biomass in wet tropical forests. *Soil Biology & Biochemistry*, **36**, 2111–2114.

Linder S (1998) *NPP Boreal Forest*. Oak Ridge National Laboratory Distributed Active Archive Center, Oak Ridge, Tennessee, USA, http://www.daac.ornl.gov

Linder S, Agren GI (1998) *NPP Boreal Forest*. Oak Ridge National Laboratory Distributed Active Archive Center, Oak Ridge, Tennessee, USA, http://www.daac.ornl.gov

Lloyd JON, Shibistova O, Zolotoukhine D *et al*. (2002) Seasonal and annual variations in the photosynthetic productivity and carbon balance of a central Siberian pine forest. *Tellus B*, **54**, 590–610.

Loescher HW, Oberbauer SF, Gholz HL, Clark DB (2003) Environmental controls on net ecosystem-level carbon exchange and productivity in a Central American tropical wet forest. *Global Change Biology*, **9**, 396–412.

Lugo AE (1992) Comparison of tropical tree plantations with secondary forests of similar age. *Ecological Monographs*, **62**, 1–41.

Maass M, Martinez-Yrizar A (2001) *NPP Tropical Forest*. Oak Ridge National Laboratory Distributed Active Archive Center, Oak Ridge, Tennessee, USA, http://www.daac.ornl.gov

Maier CA, Albaugh TJ, Allen HL, Dougherty PM (2004) Respiratory carbon use and carbon storage in mid-rotation loblolly pine (*Pinus taeda* L.) plantations: the effect of site resources on the stand carbon balance. *Global Change Biology*, **10**, 1335–1350.

Maier CA, Kress LW (2000) Soil CO_2 evolution and root respiration in 11 year-old loblolly pine (*Pinus taeda*) plantations as affected by moisture and nutrient availability. *Canadian Journal of Forest Research-Revue Canadienne De Recherche Forestiere*, **30**, 347–359.

Malhi Y, Baldocchi DD, Jarvis PG (1999) The carbon balance of tropical, temperate and boreal forests. *Plant, Cell, and Environment*, **22**, 715–740.

Malhi Y, Nobre AD, Grace J, Kruijt B, Pereira MGP, Culf A, Scott S (1998) Carbon dioxide transfer over a Central Amazonian rain forest. *Journal of Geophysical Research-Atmospheres*, **103**, 31593–31612.

Markkanen T, Rannik Ü, Keronen P, Suni T, Vesala T (2001) Eddy covariance fluxes over a boreal Scots pine forest. *Boreal Environment Research*, **6**, 65–78.

Martin JG, Kloeppel BD, Schaefer TL, Kimbler DL, McNulty SG (1998) Aboveground biomass and nitrogen allocation of ten deciduous southern Appalachian tree species. *Canadian Journal of Forest Research-Revue Canadienne De Recherche Forestiere*, **28**, 1648–1659.

Mateus J, Rodrigues AM, Pita GP (2006) Seasonal evolution of Evapotranspiration (regime) and carbon assimilation over a Eucalyptus Globulus plantation. *Silva Lusitana*, **14**, 135–147.

McCaughey JH, Pejam MR, Arain MA, Cameron DA (2006) Carbon dioxide and energy fluxes from a boreal mixedwood forest ecosystem in Ontario, Canada. *Agricultural and Forest Meteorology*, **140**, 79–96.

McDowell NG, Balster NJ, Marshall JD (2001) Belowground carbon allocation of Rocky Mountain Douglas-fir. *Canadian Journal of Forest Research-Revue Canadienne De Recherche Forestiere*, **31**, 1425–1436.

Medlyn BE, Berbigier P, Clement R *et al*. (2005) Carbon balance of coniferous forests growing in contrasting climates: Model-based analysis. *Agricultural and Forest Meteorology*, **131**, 97–124.

Mialet-Serra I, Clement A, Sonderegger N, Roupsard O, Jourdan C, Labouisse JP, Dingkuhn N (2005) Assimilate storage in vegetative organs of coconut (*Cocos nucifera*). *Experimental Agriculture*, **41**, 161–174.

Miller SD, Goulden ML, Menton MC, da Rocha HR, de Freitas HC, Figueira A, de Sousa CAD (2004) Biometric and micrometeorological measurements of tropical forest carbon balance. *Ecological Applications*, **14**, S114–S126.

Milyukova IM, Kolle O, Varlagin AV, Vygodskaya NN, Schulze ED, Lloyd J (2002) Carbon balance of a southern taiga spruce stand in European Russia. *Tellus Series B-Chemical and Physical Meteorology*, **54**, 429–442.

Misson L, Tang JW, Xu M, McKay M, Goldstein A (2005) Influences of recovery from clear-cut, climate variability, and thinning on the carbon balance of a young ponderosa pine plantation. *Agricultural and Forest Meteorology*, **130**, 207–222.

Mitchell TD, Jones PD (2005) An improved method of constructing a database of monthly climate observations and associated high-resolution grids. *International Journal of Climatology*, **25**, 693–712.

Mo W, Lee MS, Uchida M, Inatomi M, Saigusa N, Mariko S, Koizumi H (2005) Seasonal and annual variations in soil respiration in a cool-temperate deciduous broad-leaved forest in Japan. *Agricultural and Forest Meteorology*, **134**, 81–94.

Mollicone D, Matteucci G, Köble R, Masci A, Chiesi M, Smits PC (2003) A model-based approach for estimation of carbon sinks in European forests. In: *Fluxes of Carbon Water and Energy of European Forests*. *Ecological Applications*, Vol. 163 (ed. Valentini R), pp. 179–206. Springer Verlag, Berlin.

Moncrieff JB, Fang C (1999) A model for soil CO_2 production and transport 2: application to a Florida *Pinus elliotte* plantation. *Agricultural and Forest Meteorology*, **95**, 237–256.

Morgenstern K, Black TA, Humphreys ER *et al*. (2004) Sensitivity and uncertainty of the carbon balance of a Pacific Northwest Douglas-fir forest during El Niño/La Niña cycle. *Agricultural and Forest Meteorology*, **123**, 201–219.

Mund M, Kummetz E, Hein M, Bauer GA, Schulze ED (2002) Growth and carbon stocks of a spruce forest chronosequence in central Europe. *Forest Ecology and Management*, **171**, 275-296.

Munger JW, Barford C, Wofsy S (2004) Exchanges between the forest and the atmosphere. In: *Forest Landscape Dynamics in Forests in Time: The Environmental Consequences of 1,000 years of Change in New England* (eds Foster D, Aber J). Yale University Press, Yale.

Murty D, McMurtrie RE, Ryan MG (1996) Declining forest productivity in aging forest stands: A modeling analysis of alternative hypotheses. *Tree Physiology*, **16**, 187–200.

Nagy NT, Janssens IA, Yuste JC, Carrara A, Ceulemans R (2006) Footprint-adjusted net ecosystem CO_2 exchange and corresponding carbon balance components of a mixed temperate forest. *Agricultural and Forest Meteorology*, **139**, 344–360.

Nakai Y, Kitamura K, Suzuki S, Abe S (2003) Year-long carbon dioxide exchange above a broadleaf deciduous forest in Sapporo, Northern Japan. *Tellus Series B-Chemical and Physical Meteorology*, **55**, 305–312.

Nakane K (1980) Comparative studies of cycling of soil organic carbon in three primeval moist forests. *Japanese Journal of Ecology*, **30**, 155–172.

Nakane K (1995) Soil carbon cycling in a Japanese cedar (*Cryptomeria japonica*) plantation. *Forest Ecology and Management*, **72**, 185–197.

Nakane K, Tsubota H, Yamamoto M (1984) Cycling of soil carbon in a Japanese red pine forest. I. Before a clear-felling. *Botanical Magazine Tokyo*, **97**, 39–60.

Nakane K, Tsubota H, Yamamoto M (1986) Cycling of soil carbon in a Japanese red pine forest II. Changes occurring in the first year after a clear-felling. *Ecological Research*, **1**, 47–58.

Nakane K, Yamamoto M, Tsubota H (1983) Estimation of root respiration rate in a mature forest ecosystem. *Japanese Journal of Ecology*, **33**, 397–408.

Norby RJ, Hanson PJ, O'Neill EG *et al*. (2002) Net primary productivity of a CO_2-enriched deciduous forest and the implications for carbon storage. *Ecological Applications*, **12**, 1261–1266.

Nye PH, Greenland DJ (1998) *NPP Tropical Forest*. Oak Ridge National Laboratory Distributed Active Archive Center, Oak Ridge, Tennessee, USA, http://www.daac.ornl.gov

O'Connell KEB, Gower ST, Norman JM (2003) Net ecosystem production of two contrasting boreal black spruce forest communities. *Ecosystems*, **6**, 248–260.

Ohashi M, Gyokusen K, Saito A (2000) Contribution of root respiration to total soil respiration in a Japanese cedar (*Cryptomeria japonica* D. Don) artificial forest. *Ecological Research*, **15**, 323–333.

Ohtsuka T, Akiyama T, Hashimoto Y *et al*. (2005) Biometric based estimates of net primary production (NPP) in a cool-temperate deciduous forest stand beneath a flux tower. *Agricultural and Forest Meteorology*, **134**, 27–38.

Ollinger SV, Smith ML (2005) Net primary production and canopy nitrogen in a temperate forest landscape: An analysis using imaging spectroscopy, modeling and field data. *Ecosystems*, **8**, 760–778.

Olson RJ, Scurlock JMO, Prince SD, Zheng DL, Johnson KR (2001) *NPP Multi-Biome*. Oak Ridge National Laboratory Distributed Active Archive Center, Oak Ridge, Tennessee, USA, http://www.daac.ornl.gov

Oren RAM, Hsieh C-I, Stoy P, Albertson J, McCarthy HR, Harrell P, Katul GG (2006) Estimating the uncertainty in annual net ecosystem carbon exchange: spatial variation in turbulent fluxes and sampling errors in eddy-covariance measurements. *Global Change Biology*, **12**, 883–896.

Pereira JS, Pita GP, Carneira M *et al*. (2003) Full carbon balance in an eucalypt plantation in Portugal. *Comparative Biochemistry and Physiology*, **134**, S177.

Pilegaard K, Hummelshoj P, Jensen NO, Chen Z (2001) Two years of continuous CO_2 eddy-flux measurements over a Danish beech forest. *Agricultural and Forest Meteorology*, **107**, 29–41.

Powell TL, Bracho R, Li JH, Dore S, Hinkle CR, Drake BG (2006) Environmental controls over net ecosystem carbon exchange of scrub oak in central Florida. *Agricultural and Forest Meteorology*, **141**, 19–34.

Reichstein M, Rey A, Freibauer A *et al*. (2003) Modeling temporal and large-scale spatial variability of soil respiration from soil water availability, temperature and vegetation productivity indices. *Global Biogeochemical Cycles*, **17**, 1104–1118.

Reichstein M, Tenhunen JD, Roupsard O, Ourcival JM, Rambal S, Dore S, Valentini R (2002) Ecosystem respiration in two Mediterranean evergreen Holm Oak forests: drought effects and decomposition dynamics. *Functional Ecology*, **16**, 27–39.

Rodeghiero M, Cescatti A (2006) Indirect partitioning of soil respiration in a series of evergreen forest ecosystem. *Plant and Soil*, **284**, 7–22.

Rodrigues AM, Pita GP, Mateus J (2005) Turbulent fluxes of carbon dioxide and water vapour over an eucalyptus forest in Portugal. *Silvae Lusitana*, **13**, 169–180.

Roser C, Montagnani L, Schulze ED *et al*. (2002) Net CO_2 exchange rates in three different successional stages of the ''Dark Taiga'' of central Siberia. *Tellus B*, **54**, 642–654.

Roupsard O, Bonnefond JM, Irvine M *et al*. (2006) Partitioning of energy and evapo-transpiration above and below a tropical palm canopy (*Cocos nucifera* L.). *Agricultural and Forest Meteorology*, **139**, 252–268.

Ruess RW, Hendrick RL, Burton AJ, Pregitzer KS, Sveinbjornsson B, Allen ME, Maurer GE (2003) Coupling fine root dynamics with ecosystem carbon cycling in black spruce forests of interior Alaska. *Ecological Monographs*, **73**, 643–662.

Ruess RW, VanCleve K, Yarie J, Viereck LA (1996) Contributions of fine root production and turnover to the carbon and nitrogen cycling in taiga forests of the Alaskan interior. *Canadian Journal of Forest Research-Revue Canadienne De Recherche Forestiere*, **26**, 1326–1336.

Running SW, Gower ST (1991) Forest-Bgc, a general-model of forest ecosystem processes for regional applications.2. Dynamic carbon allocation and nitrogen budgets. *Tree Physiology*, **9**, 147–160.

Runyon J, Waring RH, Goward SN, Welles JM (1994) Environmental limits on net primary production and light-use efficiency across the Oregon transect. *Ecological Applications*, **4**, 226–237.

Ryan MG (1991) A simple method for estimating gross carbon budgets for vegetation in forest ecosystems. *Tree Physiology*, **9**, 255–266.

Ryan MG, Hubbard RM, Pongracic S, Raison RJ, McMurtrie RE (1996) Foliage, fine-root, woody-tissue and stand respiration in *Pinus radiata* in relation to nitrogen status. *Tree Physiology*, **16**, 333–343.

Ryan MG, Lavigne MB, Gower ST (1997) Annual carbon cost of autotrophic respiration in boreal forest ecosystems in relation to species and climate. *Journal of Geophysical Research-Atmospheres*, **102**, 28871–28883.

Ryan MG, Waring RH (1992) Maintenance respiration and stand development in a sub-alpine lodgepole pine forest. *Ecology*, **73**, 2100–2108.

Saigusa N, Yamamoto S, Murayama S, Kondo H (2005) Interannual variability of carbon budget components in an AsiaFlux forest site estimated by long-term flux measurements. *Agricultural and Forest Meteorology*, **134**, 4–16.

Saigusa N, Yamamoto S, Murayama S, Kondo H, Nishimura N (2002) Gross primary production and net ecosystem exchange of a cool-temperate deciduous forest estimated by the eddy covariance method. *Agricultural and Forest Meteorology*, **112**, 203–215.

Saiz G, Byrne KA, Butterbach-Bahl K, Kiese R, Blujdeas V, Farrell EP (2006) Stand age-related effects on soil respiration in a first rotation Sitka spruce chronosequence in central Ireland. *Global Change Biology*, **12**, 1007–1020.

Saleska SR, Miller SD, Matross DM *et al*. (2003) Carbon in amazon forests: unexpected seasonal fluxes and disturbance-induced losses. *Science*, **302**, 1554–1557.

Schmid HP, Grimmond CSB, Cropley F, Offerle B, Su HB (2000) Measurements of CO_2 and energy fluxes over a mixed hardwood forest in the mid-western United States. *Agricultural and Forest Meteorology*, **103**, 357–374.

Schulze E-D (2000) The carbon and nitrogen cycle in forest ecosystems. In: *Carbon and Nitrogen Cycling in European Forest Ecosystems*. *Ecological Studies*, Vol. 142 (ed. Schulz E-D), pp. 500. Spinger, Berlin.

Schulze ED, Lloyd J, Kelliher FM *et al*. (1999) Productivity of forests in the Eurosiberian boreal region and their potential to act as a carbon sink – a synthesis. *Global Change Biology*, **5**, 703–722.

Schuur EAG (2005) *NPP Tropical Forest*. Oak Ridge National Laboratory Distributed Active Archive Center, Oak Ridge, Tennessee, USA, http://www.daac.ornl.gov

Steele SJ, Gower ST, Vogel JG, Norman JM (1997) Root mass, net primary production and turnover in aspen, jack pine and black spruce forests in Saskatchewan and Manitoba, Canada. *Tree Physiology*, **17**, 577–587.

Subke JA (2002) *Forest floor CO_2 fluxes in temperate forest ecosystems. An investigation of spatial and temporal patterns and abiotic controls*. PhD Thesis.

Subke JA, Hahn V, Battipaglia G, Linder S, Buchmann N, Cotrufo MF (2004) Feedback interactions between needle litter decomposition and rhizosphere activity. *Oecologia*, **139**, 551–559.

Sulzman EW, Brant JB, Bowden RD, Lajtha K (2005) Contribution of aboveground litter, belowground litter, and rhizosphere respiration to total soil CO_2 efflux in an old growth coniferous forest. *Biogeochemistry*, **73**, 231–256.

Sun OJ, Campbell J, Law BE, Wolf V (2004) Dynamics of carbon stocks in soils and detritus across chronosequences of different forest types in the Pacific Northwest, USA. *Global Change Biology*, **10**, 1470–1481.

Tagesson T, Lindroth A (2007) High soil carbon efflux rates in several ecosystems in southern Sweden. *Boreal Environment Research*, **12**, 65–80.

Tate KR, Ross DJ, Obrien BJ, Kelliher FM (1993) Carbon storage and turnover, and respiratory activity, in the litter and soil of an old-growth southern beech (Nothofagus) forest. *Soil Biology & Biochemistry*, **25**, 1601–1612.

Thierron V, Laudelout H (1996) Contribution of root respiration to total CO_2 efflux from the soil of a deciduous forest. *Canadian Journal of Forest Research*, **26**, 1142–1148.

Trumbore SE, Chadwick OA, Amundson R (1996) Rapid exchange between soil carbon and atmospheric carbon dioxide driven by temperature change. *Science*, **272**, 393–396.

Tucker CJ, Pinzon JE, Brown ME, Slayback DA, Pak EW, Mahoney R, Vermote EF, El Saleous N (2005) An extended AVHRR 8-km NDVI dataset compatible with MODIS and SPOT vegetation NDVI data. *International Journal Of Remote Sensing*, **26**, 4485–4498.

Urbanski S, Barford C, wofsy S *et al*. (2007) Factors controlling CO_2 exchange on time scales from hourly to decadal at Harvard Forest. *Journal of Geophysical research-Biogeoscience*, **112**, G02020.

Valentini R, DeAngelis P, Matteucci G, Monaco R, Dore S, Mugnozza GES (1996) Seasonal net carbon dioxide exchange of a beech forest with the atmosphere. *Global Change Biology*, **2**, 199–207.

Valentini R, Matteucci G, Dolman AJ *et al*. (2000) Respiration as the main determinant of carbon balance in European forests. *Nature*, **404**, 861–865.

Vogel JG, Valentine DW, Ruess RW (2005) Soil and root respiration in mature Alaskan black spruce forests that vary in soil organic matter decomposition rates. *Canadian Journal of Forest Research-Revue Canadienne De Recherche Forestiere*, **35**, 161–174.

Wang C, Yang J (2007) Rhizospheric and heterotrophic components of soil respiration in six Chinese temperate forests. *Global Change Biology*, **13**, 123–131.

Wang KY, Kellomaki S, Zha TS, Peltola H (2004) Component carbon fluxes and their contribution to ecosystem carbon exchange in a pine forest: an assessment based on eddy covariance measurements and an integrated model. *Tree Physiology*, **24**, 19–34.

Wang Y, Amundson R, Niu XF (2000) Seasonal and altitudinal variation in decomposition of soil organic matter inferred from radiocarbon measurements of soil CO_2 flux. *Global Biogeochemical Cycles*, **14**, 199–211.

Williams M, Rastetter EB, Fernandes DN, Goulden ML, Shaver GR, Johnson LC (1997) Predicting gross primary productivity in terrestrial ecosystems. *Ecological Applications*, **7**, 882–894.

Williams M, Schwarz PA, Law BE, Irvine J, Kurpius MR (2005) An improved analysis of forest carbon dynamics using data assimilation. *Global Change Biology*, **11**, 89–105.

Wilson KB, Baldocchi DD (2001) Comparing independent estimates of carbon dioxide exchange over 5 years at a deciduous forest in the southeastern United States. *Journal of Geophysical Research-Atmospheres*, **106**, 34167–34178.

Wirth C, Czimczik CI, Schulze ED (2002) Beyond annual budgets: carbon flux at different temporal scales in fire-prone Siberian Scots pine forests. *Tellus Series B-Chemical and Physical Meteorology*, **54**, 611–630.

Wofsy SC, Goulden ML, Munger JW, Fan SM, Bakwin PS, Daube BC, Bassow SL, Bazzaz FA (1993) Net exchange of CO_2 in a midlatitude forest. *Science*, **260**, 1314–1317.

Wu JB, Guan DX, Wang M, Pei TF, Han SJ, Jin CJ (2006) Year-round soil and ecosystem respiration in a temperate broad-leaved Korean Pine forest. *Forest Ecology and Management*, **223**, 35–44.

Xu L, Baldocchi DD (2004) Seasonal variation in carbon dioxide exchange over a Mediterranean annual grassland in California. *Agricultural and Forest Meteorology*, **123**, 79.

Yan J, Wang Y, Zhou G, Zhang D (2006) Estimates of soil respiration and net primary production of three forests at different succession stages in South China. *Global Change Biology*, **12**, 810–821.

Yanai RD, Park BB, Hamburg SP (2006) The vertical and horizontal distribution of roots in northern hardwood stands of varying age. *Canadian Journal of Forest Research-Revue Canadienne De Recherche Forestiere*, **36**, 450–459.

Yuste JC, Konopka B, Janssens IA, Coenen K, Xiao CW, Ceulemans R (2005) Contrasting net primary productivity and carbon distribution between neighboring stands of Quercus robur and Pinus sylvestris. *Tree Physiology*, **25**, 701–712.

Zha TS, Xing ZS, Wang KY, Kellomaki S, Barr AG (2007) Total and component carbon fluxes of a Scots pine ecosystem from chamber measurements and eddy covariance. *Annals Of Botany*, **99**, 345–353.

Zhang JH, Han SJ, Yu GR (2006) Seasonal variation in carbon dioxide exchange over a 200-year-old Chinese broad-leaved Korean pine mixed forest. *Agricultural and Forest Meteorology*, **137**, 150–165.

Appendix B

Table B1 Overview of the information contained in the database

Plot information		
Plot name	Text	Name of the plot
Biome	Text	Biome according to US Department of Agriculture (1999)
Growth strategy	Text	Evergreen, deciduous or mixed
Growth form	Text	Needle-leaved, broadleaved or mixed
Tree species	Text	Dominant tree species
Tree species	Text	Co-dominant tree species
Latitude	Number	Latitude in decimal degrees
Longitude	Number	Longitude in decimal degrees
Elevation	Number	Elevation above sea level in m
Management	Text	Relevant information on management and disturbance
Observed stand characteristics		
Basal area	Number	Basal area in $m^{-2}\,ha^{-1}$
Diameter	Number	Diameter at breast height in m
Height	Number	Mean tree height in m
Density	Number	Stand density in number of trees.ha^{-1}
Age	Number	Age of the dominant trees in years
LAI	Number	Maximal LAI in $m^2\,m^{-2}$
Method	Text	Description of the method used to determine LAI
Observed stand biomass		
Foliar biomass	Number	Foliar biomass in $g\,C\,m^{-2}$
Branch biomass	Number	Branch biomass in $g\,C\,m^{-2}$
Stem biomass	Number	Stem biomass in $g\,C\,m^{-2}$
Stump biomass	Number	Stump biomass in $g\,C\,m^{-2}$
Coarse root biomass	Number	Coarse root biomass in $g\,C\,m^{-2}$
Fine root biomass	Number	Fine root biomass in $g\,C\,m^{-2}$
Aboveground biomass	Number	Total aboveground biomass in $g\,C\,m^{-2}$
Belowground biomass	Number	Total belowground biomass in $g\,C\,m^{-2}$
Observed stand climate		
Temperature	Number	Mean annual temperature in °C
Precipitation	Number	Total annual precipitation in mm
Evaporation	Number	Total annual evaporation in mm
APAR	Number	Total annual absorbed radiation in $MJ\,m^{-2}$
PAR	Number	Total annual incident radiation in $MJ\,m^{-2}$
IPAR	Number	Total annual intercepted radiation in $MJ\,m^{-2}$
Observed flux estimate		
GPP	Number	Ecosystem GPP in $g\,C\,m^{-2}\,yr^{-1}$
NEP	Number	Ecosystem NEP in $g\,C\,m^{-2}\,yr^{-1}$
R_e	Number	Ecosystem Re $g\,C\,m^{-2}\,yr^{-1}$
NPP wood	Number	NPP of the stems/wood $g\,C\,m^{-2}\,yr^{-1}$
NPP foliage	Number	NPP of the foliage $g\,C\,m^{-2}\,yr^{-1}$
NPP branch	Number	NPP of the branches $g\,C\,m^{-2}\,yr^{-1}$
NPP stumps	Number	NPP of the stumps $g\,C\,m^{-2}\,yr^{-1}$
NPP coarse	Number	NPP of the coarse roots $g\,C\,m^{-2}\,yr^{-1}$
NPP fine	Number	NPP of the fine roots $g\,C\,m^{-2}\,yr^{-1}$
NPP repro	Number	NPP of the reproductive organs $g\,C\,m^{-2}\,yr^{-1}$
NPP herbi	Number	NPP of the herbivory $g\,C\,m^{-2}\,yr^{-1}$
NPP under	Number	NPP of the understory $g\,C\,m^{-2}\,yr^{-1}$
NPP VOC	Number	NPP of the VOC's $g\,C\,m^{-2}\,yr^{-1}$
NPP exudates	Number	NPP of the root exudates $g\,C\,m^{-2}\,yr^{-1}$
R_s	Number	Total soil respiration $g\,C\,m^{-2}\,yr^{-1}$
R_a	Number	Autotrophic respiration $g\,C\,m^{-2}\,yr^{-1}$
R_h	Number	Heterotrophic respiration $g\,C\,m^{-2}\,yr^{-1}$
Methodology	Text	Description of the different methodologies that were used to estimate the fluxes
Site climate and environment		
Temperature	Number	Monthly mean annual temperature in °C (CRU, 2006)
Precipitation	Number	Monthly precipitation sum in mm CRU (2006)
Air humidity	Number	Monthly air humidity CRU (2006)
Cloud cover	Number	Monthly average cloud cover (%) CRU (2006)
Number of wet days	Number	Monthly sum of wet days CRU (2006)
Long wave radiation (1)	Number	Monthly absorbed downward longwave radiation in $W\,m^{-2}$ Krinner *et al.* (2005)
Long wave radiation (2)	Number	Monthly net surface longwave radiation in $W\,m^{-2}$ Krinner *et al.* (2005)
Solar radiation	Number	Monthly solar radiation in $W\,m^{-2}$ Krinner *et al.* (2005)
Soil moisture	Number	Monthly soil moisture in mm Krinner *et al.* (2005)
Dry deposition	Number	Mean monthly dry deposition of N $g\,N\,m^{-2}$ $month^{-1}$ Krinner *et al.* (2005)
Wet deposition	Number	Mean monthly wet deposition of N $g\,N\,m^{-2}$ $month^{-1}$ Krinner *et al.* (2005)
NH*x* deposition	Number	Mean monthly NHx deposition of N $g\,N\,m^{-2}$ $month^{-1}$ Krinner *et al.* (2005)
NDVI	Number	Mean 14-day NDVI Tucker *et al.* (2005)

EXHIBIT EGC-2

Global Ecology and Biogeography, (Global Ecol. Biogeogr.) (2014) **23**, 297–310

Global Ecology and Biogeography
A Journal of Macroecology

RESEARCH PAPER

Carbon stock and density of northern boreal and temperate forests

Martin Thurner[1*], Christian Beer[1,2], Maurizio Santoro[3], Nuno Carvalhais[1,4], Thomas Wutzler[1], Dmitry Schepaschenko[5], Anatoly Shvidenko[5], Elisabeth Kompter[1], Bernhard Ahrens[1], Shaun R. Levick[1] and Christiane Schmullius[6]

[1]Max Planck Institute for Biogeochemistry (MPI-BGC), Hans-Knöll-Straße 10, D-07745 Jena, Germany, [2]Department of Applied Environmental Science (ITM) and the Bolin Centre for Climate Research, Stockholm University, SE-106 91 Stockholm, Sweden, [3]Gamma Remote Sensing, Worbstraße 225, CH-3073 Gümligen, Switzerland, [4]Universidade Nova de Lisboa, Faculdade de Ciências e Tecnologia (FCT), 2829-516 Caparica, Portugal, [5]International Institute for Applied Systems Analysis (IIASA), Schlossplatz 1, A-2361 Laxenburg, Austria, [6]Friedrich-Schiller-University (FSU), Institute of Geography, Earth Observation, Grietgasse 6, D-07743 Jena, Germany

*Correspondence: Martin Thurner, Max Planck Institute for Biogeochemistry (MPI-BGC), Hans-Knöll-Straße 10, D-07745 Jena, Germany.
E-mail: mthurn@bgc-jena.mpg.de

ABSTRACT

Aim To infer a forest carbon density map at 0.01° resolution from a radar remote sensing product for the estimation of carbon stocks in Northern Hemisphere boreal and temperate forests.

Location The study area extends from 30° N to 80° N, covering three forest biomes – temperate broadleaf and mixed forests (TBMF), temperate conifer forests (TCF) and boreal forests (BFT) – over three continents (North America, Europe and Asia).

Methods This study is based on a recently available growing stock volume (GSV) product retrieved from synthetic aperture radar data. Forest biomass and spatially explicit uncertainty estimates were derived from the GSV using existing databases of wood density and allometric relationships between biomass compartments (stem, branches, roots, foliage). We tested the resultant map against inventory-based biomass data from Russia, Europe and the USA prior to making intercontinent and interbiome carbon stock comparisons.

Results Our derived carbon density map agrees well with inventory data at regional scales (r^2 = 0.70–0.90). While 40.7 ± 15.7 petagram of carbon (Pg C) are stored in BFT, TBMF and TCF contain 24.5 ± 9.4 Pg C and 14.5 ± 4.8 Pg C, respectively. In terms of carbon density, we found 6.21 ± 2.07 kg C m^{-2} retained in TCF and 5.80 ± 2.21 kg C m^{-2} in TBMF, whereas BFT have a mean carbon density of 4.00 ± 1.54 kg C m^{-2}. Indications of a higher carbon density in Europe compared with the other continents across each of the three biomes could not be proved to be significant.

Main conclusions The presented carbon density and corresponding uncertainty map give an insight into the spatial patterns of biomass and stand as a new benchmark to improve carbon cycle models and carbon monitoring systems. In total, we found 79.8 ± 29.9 Pg C stored in northern boreal and temperate forests, with Asian BFT accounting for 22.1 ± 8.3 Pg C.

Keywords

Boreal forest, carbon density map, carbon monitoring, forest biomass, forest carbon stocks, global carbon cycle, growing stock volume, SAR remote sensing, temperate forest.

INTRODUCTION

Terrestrial vegetation plays an important role within the global carbon cycle and hence the earth system, as it sequesters atmospheric carbon dioxide and is thus able to mitigate global warming (Denman *et al.*, 2007; Bonan, 2008). Biomass dynamics reflect the potential of vegetation to act as a carbon sink over the long term, as they integrate photosynthesis, autotrophic respiration and litterfall fluxes. However, the interannual variability of carbon fluxes remains relatively unexplored (Wolf *et al.*,

DOI: 10.1111/geb.12125
http://wileyonlinelibrary.com/journal/geb

2011), mainly due to the absence of consistent spatial information on biomass (Bellassen *et al.*, 2011). Lack of knowledge about the initial condition of vegetation biomass is one important reason for the large discrepancies in the projected land carbon sink between coupled climate–carbon cycle models (Friedlingstein *et al.*, 2006; Hurtt *et al.*, 2010).

Forest cover and forest structure provide additional important feedbacks on biophysical properties and processes like albedo and evapotranspiration. Thus, improving our knowledge about the state of the world's forests is also important for understanding their influence on energy and water fluxes. Beside their ecological importance, forests are also of great social, economic (Bonan, 2008) and even political value in terms of the Reducing Emissions from Deforestation and Degradation (REDD) scheme (UN-REDD, 2011). Despite their relevance, forests are at risk due to deforestation and degradation processes. Although reforestation is expected to have exceeded deforestation in boreal and temperate forests in the period between 1990 and 2010, logging, fires and insects can have a significant impact in these biomes at regional scales (FAO, 2010).

Current estimates of the carbon stock for boreal and temperate forests are usually based upon upscaling of often sparse forest inventory data to national estimates. Such approaches involve a poor spatial resolution and high remaining uncertainty (Boudreau *et al.*, 2008). Previous studies show important divergences in estimated carbon stocks and densities of temperate and boreal forests (e.g. Saugier *et al.*, 2001; Pan *et al.*, 2011). Although there are discrepancies in the methods used for estimating biomass, and in the forest area and biomass compartments considered, these large differences highlight the need to improve our knowledge of the current state of non-tropical forests.

As forest inventories are always limited, especially in remote areas, remote sensing can serve as a very useful tool for monitoring the state and also the dynamics of forest ecosystems. While biomass maps based on remote sensing data recently became available for the tropics (Saatchi *et al.*, 2011; Baccini *et al.*, 2012), spatially explicit datasets on forest carbon stocks in the Northern Hemisphere have been rare and inconsistent up to now. Remote sensing has shown the potential to overcome this shortcoming and biomass has already been successfully mapped using light detection and ranging (LiDAR; e.g. Lefsky *et al.*, 2002; Boudreau *et al.*, 2008) and synthetic aperture radar (SAR; e.g. Ranson *et al.*, 1997; Wagner *et al.*, 2003; Neumann *et al.*, 2012) data. However, these studies either do not cover the whole extent of temperate and boreal forests in a single product, rely on using classifications with an early biomass saturation and/or are highly dependent on inventory data.

The availability of extensive observations by the Envisat Advanced Synthetic Aperture Radar (ASAR) has boosted the development of an algorithm to retrieve forest growing stock volume (GSV) (Santoro *et al.*, 2011, 2013). The major innovation of this retrieval algorithm, referred to as the BIOMASAR algorithm, is that it does not require reference data to calibrate the model linking the remote sensing observation with the output variable, i.e. the GSV. Recently, a dataset of GSV estimates covering the Northern Hemisphere between 30° N and 80° N, and thus including the boreal and temperate forests of North America, Europe and Asia, was generated with the BIOMASAR algorithm at a spatial resolution of 0.01° (Santoro *et al.*, in prep.). While forestry and remote sensing scientists tend to quantify 'biomass' in terms of GSV, scientists working on the carbon cycle and climate modelling, as well as national carbon monitoring systems (involved in REDD), require information on how much carbon is stored in vegetation expressed in mass units, and comprising in addition estimates of carbon in other tree compartments such as branches and roots. This allows for comparison with the carbon pools usually implemented in dynamic global vegetation models (DGVMs; e.g. Moorcroft *et al.*, 2001; Beer *et al.*, 2006; Randerson *et al.*, 2009) on the one hand and for assessment of national forest resources (e.g. DeFries *et al.*, 2002; Grainger, 2009) on the other.

Many studies have inferred biomass from GSV by applying so-called biomass expansion factors, which were empirically derived for a certain species or region (e.g. Somogyi *et al.*, 2008; Teobaldelli *et al.*, 2009; Guo *et al.*, 2010). In contrast, this study intends to derive biomass from GSV using information on wood density and the allometric relation between biomass compartments. At the same time, these relations should be consistently applicable over the whole study area. This approach allows for a division between biomass compartments (stem, branches, roots, foliage), which can provide useful information for applications requiring such detailed data.

The aims for this study are (1): to infer a consistent forest carbon map from recently available remote sensing GSV data, (2) to provide spatially explicit uncertainty estimates to the biomass map, (3) to estimate the total carbon stocks in Northern Hemisphere boreal and temperate forests, (4) to evaluate the derived product against independent datasets, and finally (5) to demonstrate the potential of multitemporal Envisat ASAR data to consistently map biomass at a moderate resolution covering large areas.

MATERIALS AND METHODS

GSV data

This study is based on GSV estimates obtained with the BIOMASAR algorithm from large numbers of observations by the ASAR instrument on board the Envisat satellite (Santoro *et al.*, 2011). Forest GSV refers to the volume of tree stems per unit area and is measured in $m^3\ ha^{-1}$. The GSV estimated from the SAR data is determined by (1) the wavelength of the ASAR instrument (5.6 cm) and (2) the structural and dielectric properties of the forest. Objects with a size smaller than the wavelength are transparent to ASAR; similarly, objects with frozen water are transparent. By combining in a weighted approach individual GSV estimates from primarily winter-time ASAR data, the GSV estimation procedure extracts the maximum in terms of signal related to GSV in the radar data (Santoro *et al.*, 2011). Stumps are accounted for in the ASAR GSV estimate as long as they are seen by ASAR, i.e. their size is larger than the wavelength and they are standing. GSV estimates might also contain a necromass component if this is directly sensed by the radar. However, these aspects have not been quantified so far.

Spatially explicit GSV data with a resolution of 0.01° were obtained for North America, Europe and Asia covering the latitudes between 30° N and 80° N. The multitemporal SAR dataset was acquired between October 2009 and February 2011, thus containing information on the state of the vegetation structure in the year 2010. GSV was mapped without saturation up to 300 m^3 ha^{-1}. Above this level the retrieved GSV was characterized by a tendency to saturate, i.e. increasing underestimation for increasing GSV (Santoro *et al.*, unpublished data). However, less than 1% of the pixels in the study area had a GSV above this value. The uncertainty of GSV estimates was quantified to be 10% (Santoro *et al.*, 2011). The BIOMASAR algorithm retrieves GSV regardless of the vegetation type. To ensure that the biomass estimates reported here correspond to a forest type of vegetation, non-forested areas were masked out beforehand according to the GLC2000 land-use/land-cover map (JRC, 2003; see Appendix S1 in Supporting Information).

Additional datasets

In addition to GSV, the Global Wood Density Database (Chave *et al.*, 2009; Zanne *et al.*, 2009) and the JRC GHG-AFOLU Biomass Compartment Database (JRC, 2009) were used in this study. While the Global Wood Density Database contains information on wood density, the JRC Biomass Compartment Database includes measurements of the absolute amount of biomass in different compartments, both over a wide range of species and sufficiently covering the study area. The Global Wood Density Database consists of more than 16,000 entries, covering more than 8000 tree species. The JRC Biomass Compartment Database also gives additional information on latitude/longitude, tree age, diameter, height and density amongst other things.

As there is no detailed tree species map available covering the whole study area, information contained in those databases had to be aggregated to the level of leaf types (broadleaf, needleleaf deciduous, needleleaf evergreen forest). GLC2000 could be further used to distinguish between leaf types. GLC2000 assigns one of 22 different land-cover classes to each pixel. These classes were summarized to broadleaf, needleleaf deciduous, needleleaf evergreen, mixed forest and non-forest (for details see Appendix S1). GLC2000 was reprojected using nearest neighbour resampling to 0.01° in order to match the resolution of the GSV map.

Derivation of total forest carbon from GSV

In a first step, stem biomass (SB) was derived from GSV using information on wood density (WD) from the Global Wood Density Database (Fig. 1) as follows:

$$SB = GSV \times WD. \quad (1)$$

All the entries for different tree species contained in the database were summarized to tree genera and leaf types. In the absence of a global tree species map, no weighting according to the occurrence of tree species could be implemented. Investigations concentrated on the most common genera in boreal and temperate forests, including *Abies*, *Acer*, *Alnus*, *Betula*, *Fagus*, *Fraxinus*, *Larix*, *Picea*, *Pinus*, *Populus*, *Quercus*, *Tilia* and *Tsuga*. For each pixel of the GSV map stem biomass was calculated following equation (1). Mean wood density per leaf type has been applied according to the leaf type distribution derived from the GLC2000 land-cover map.

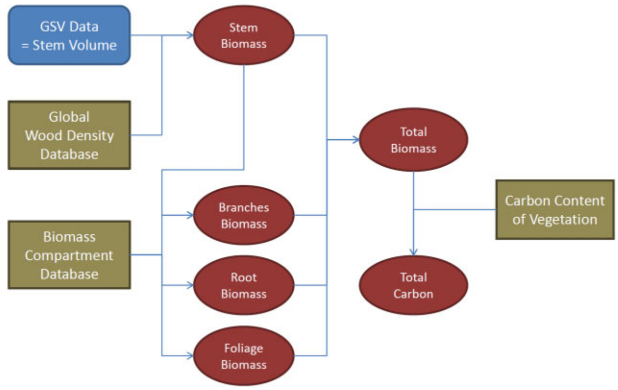

Figure 1 Processing algorithm.

In a second step, allometric relationships at leaf type level between stem biomass and the other required biomass compartments (BC; including branches, foliage, roots) were derived by fitting root functions to the Biomass Compartment Database. Nonlinear models of the following form were fitted using generalized least square regression (Pinheiro & Bates, 2000):

$$BC = a \times SB^{1/b}. \quad (2)$$

The model form is similar to the allometric relationships used by Zianis *et al.* (2005) and Wutzler *et al.* (2008), although we used stem biomass instead of tree diameter as a predictor. Branch, root and foliage biomass were calculated in this manner. These relationships were applied to the stem biomass map leading to maps of the other biomass compartments. The coefficients a and b in equation (2) were also derived for each leaf type. Then, the GLC2000 land-cover map was applied again to estimate biomass compartments for the different leaf types. *Abies*, *Alnus*, *Betula*, *Fagus*, *Larix*, *Picea*, *Pinus*, *Populus*, *Quercus* and *Tsuga* could be included in this analysis. Unfortunately, for *Acer*, *Fraxinus* and *Tilia* there was not sufficient information (at least 10 database entries) on root biomass available in the database.

Finally, total biomass (TB) was inferred as the sum of the biomass compartments stem, branches (BB), root (RB) and foliage biomass (FB):

$$TB = SB + BB + RB + FB. \quad (3)$$

The carbon content in vegetation varies between leaf type and biomes (Thomas & Martin, 2012); however, variations between plant tissues are of minor importance. This was taken into account here:

$$\mathrm{TC} = 0.488\mathrm{TB} \quad (4)$$

for temperate/boreal broadleaf tree species and

$$\mathrm{TC} = 0.508\mathrm{TB} \quad (5)$$

for temperate/boreal needleleaf tree species.

Uncertainty analysis

In addition to the total carbon density map, an uncertainty estimate was derived for each pixel. Here we refer to uncertainty in terms of the standard deviation of the biomass value. All the steps of the processing algorithm contribute to the overall uncertainty. Factors adding uncertainty to the final product include: (1) uncertainty of the BIOMASAR GSV estimates; (2) uncertainty of GLC2000 land-use/land-cover classification; (3) uncertainty of wood density data; (4) uncertainty of biomass compartment data; (5) uncertainty of the carbon content in vegetation.

The relative error of GSV estimates related to the retrieval algorithm was quantified by Santoro *et al.* (2011) to be on average 10%. The uncertainty of GLC2000 land cover could not be accounted for in this analysis. It is assumed to slightly affect the spatial distribution of uncertainties, but to have only a minor effect on their overall range. The land-cover classification potentially introduces uncertainty by applying a wood density or an allometric relation for the wrong leaf type. The standard deviation of wood density for different leaf types, containing its variance between species, could be used to quantify its uncertainty. The uncertainty introduced by the relationship between biomass compartments, which is caused by the variation of allometric functions within leaf types, was estimated from the variance of residuals of the model fit. It was estimated by applying a generalized model (Pinheiro & Bates, 2000; Zuur *et al.*, 2009). This kind of model allowed an increase of the variance of residuals with increasing covariate, in this case the stem biomass. Hence an increasing uncertainty in branch, root and foliage biomass could be modelled with increasing stem biomass. The uncertainty of the carbon content of vegetation was considered negligible compared with the magnitude of the other uncertainties.

Error propagation was implemented following Taylor (1997). We applied a Gaussian error propagation (GEP) approach. Its use in ecological studies has been demonstrated by Lo (2005) for a similar example. It was found to be especially beneficial when implying step-by-step calculations or different scales, both of which are relevant to this study.

Uncertainty of stem biomass (u_{SB}) can be calculated from the relative error of GSV (u_{GSV} = 10% GSV) and the standard deviation of wood density (u_{WD}). These uncertainties can be assumed to be independent and random:

$$u_{\mathrm{SB}} = \sqrt{\left(\frac{dSB}{dGSV}\cdot u_{\mathrm{GSV}}\right)^2 + \left(\frac{dSB}{dWD}\cdot u_{\mathrm{WD}}\right)^2} = \sqrt{(WD\cdot u_{\mathrm{GSV}})^2 + (GSV\cdot u_{\mathrm{WD}})^2} \quad (6)$$

Here dSB/dGSV denotes the partial derivative of SB with respect to GSV. The uncertainty of branches biomass (u_{BB}) for given stem biomass consists of the propagated uncertainty of stem biomass and the uncertainty of the fitted relationship between those two variables ($u_{\mathrm{BB}=f(\mathrm{SB})}$, cf. Taylor, 1997, p. 190), which is caused by the uncertainty of the Biomass Compartment Database. Again, these uncertainties can be assumed to be independent and random:

$$u_{BB} = \sqrt{\left(\frac{\mathrm{dBB}}{\mathrm{dSB}}\cdot u_{\mathrm{SB}}\right)^2 + u^2_{\mathrm{BB}=f(\mathrm{SB})}} = \sqrt{\left(\frac{a}{b}\cdot \mathrm{SB}^{\frac{1}{b}-1}\cdot u_{\mathrm{SB}}\right)^2 + u^2_{\mathrm{BB}=f(\mathrm{SB})}} \quad (7)$$

The derivatives are evaluated at given stem biomass and estimated model parameters. The uncertainty of the allometric function can be derived from the generalized model. We are interested in the uncertainty introduced by the influence of species, climate, tree age and other possible factors on this allometric relation. The variance of the residuals is expressed in dependence of the residual standard error (RSE) and rising with the power of the absolute value of the covariate (SB). The parameter δ is fitted by the model (Pinheiro & Bates, 2000; Zuur *et al.*, 2009):

$$u^2_{\mathrm{BB}=f(\mathrm{SB})} = \mathrm{RSE}^2 \times |\mathrm{SB}|^{2\delta} \quad (8)$$

The uncertainty of root (u_{RB}) and foliage (u_{FB}) biomass can be derived in the same way.

As the uncertainties of the biomass compartments cannot be considered to be independent (they are all calculated out of stem biomass; i.e. if the uncertainty in stem biomass increases, the uncertainty in the other biomass compartments will also increase), the uncertainty in their sum (u_{TB}) has to be calculated as the sum of the original uncertainties:

$$u_{\mathrm{TB}} = u_{\mathrm{SB}} + u_{\mathrm{BB}} + u_{\mathrm{RB}} + u_{\mathrm{FB}}. \quad (9)$$

Finally, the uncertainty of total biomass was propagated in order to derive the uncertainty of total carbon, assuming negligible uncertainty of carbon content:

$$u_{\mathrm{TC}} = \frac{\mathrm{dTC}}{\mathrm{dTB}} u_{\mathrm{TB}} = 0.488 u_{\mathrm{TB}} \quad (10)$$

for temperate/boreal broadleaf tree species and

$$u_{\mathrm{TC}} = \frac{\mathrm{dTC}}{\mathrm{dTB}} u_{\mathrm{TB}} = 0.508 u_{\mathrm{TB}} \quad (11)$$

for temperate/boreal needleleaf tree species.

Evaluation

The carbon map we produced was evaluated against different independent datasets, covering an exhaustive range of ecosystems and forest structures. For intercomparison, Russian forest enterprise data (Shvidenko *et al.*, 2010; Schepaschenko *et al.*, 2011), the United States National Biomass and Carbon Dataset for the year 2000 (NBCD2000; Kellndorfer *et al*., 2010; Kellndorfer *et al*., 2012) and European national statistics (EFI, 2005) were used. The intercomparison was implemented at a regional level (Russian forest enterprises, US counties, European countries) to ensure that the biomass values in the two datasets refer to the forest structure, i.e. are of the same scale.

The Russian land-cover dataset produced by the International Institute for Applied Systems Analysis (IIASA; Shvidenko *et al*., 2010; Schepaschenko *et al*., 2011) is based on integration of forest inventory data and other relevant information. The dataset contains detailed forest characteristics (species composition, age, GSV, biomass etc.) at 1-km resolution. Intercomparison was performed for approximately 1600 forest enterprises with an average area of 9132.3 km^2, ranging from 2.8 to 550,074.0 km^2. While forest enterprises are usually small in densely populated territories in European Russia, they cover very large areas in remote territories of Siberia.

NBCD2000 (Kellndorfer *et al*., 2012) was produced by the Woods Hole Research Center (WHRC) and can be seen as a benchmark map covering the conterminous United States. Combining United States Department of Agriculture (USDA) Forest Service Forest Inventory and Analysis (FIA; USDA, 2012) and remote sensing data [interferometric SAR (InSAR) data from the Shuttle Radar Topography Mission (SRTM) and optical Landsat data], a high-resolution (30 m) raster dataset of aboveground wood carbon was derived (Kellndorfer *et al*., 2010, 2012). Aggregated biomass values could be compared for more than 3000 counties with an average area of 2405.7 km^2, ranging from 0.8 to 52,109.4 km^2. The comparison at the level of forest enterprises, counties or countries ensures a comparison to original forest inventory data and is not affected by the spatial variability introduced by other remote sensing data into the reference datasets.

Estimation of boreal and temperate forest carbon stock and density

Based on the new total carbon density map, boreal and temperate forest carbon stock and carbon density were estimated across three continents – North America, Europe and Asia. Biomes were extracted according to Olson *et al*. (2001), including boreal forests (BFT), temperate broadleaf/mixed forests (TBMF) and temperate conifer forests (TCF). Continental boundaries were defined according to ESRI (2008). The land-cover map GLC2000 was used as a forest mask in order to specify forest area. GLC2000 considers a pixel containing more than 15% tree cover as forest (JRC, 2003). When deriving biomass estimates at a coarser spatial scale, the actual area of each grid cell was explicitly taken into account, assuming the earth to be a perfect sphere. The carbon stock and its corresponding uncertainty of biomes and continents were calculated as the sum of the absolute biomass and uncertainties of the corresponding pixel values, respectively. In order to derive the carbon density and its uncertainty per biome and continent, the carbon stock and its uncertainty were divided by the covered area.

Table 1 Wood density mean and standard deviation obtained from the Global Wood Density Database for different leaf types.

Forest leaf type	Broadleaf	Needleleaf deciduous	Needleleaf evergreen
Mean wood density (g cm^{-3})	0.570	0.464	0.411
Standard deviation of wood density (g cm^{-3})	0.150	0.057	0.066

RESULTS AND DISCUSSION

Wood density

The mean values and standard deviations of wood density for different leaf types are summarized in Table 1. Corresponding boxplots show the median values and quartiles not only across leaf types but also in more detail across tree genera (Fig. 2). As the differences between mean and median values are negligible, the mean values can be considered to describe the distributions of wood density sufficiently well. Thus, they were used to calculate stem biomass following equation (1). When summarized to leaf types, the wood density of broadleaf trees in particular varies considerably between tree species. In this processing step, the uncertainty introduced by the Global Wood Density Database is relatively large for broadleaf trees. In terms of their mean value, broadleaf trees have the highest wood density and thus a higher biomass per volume, followed by needleleaf deciduous and needleleaf evergreen trees.

Allometric relationships

The allometric relationships between branch, root and foliage biomass to stem biomass were found to be best modelled as a root function (Fig. 3). While an increasing stem biomass is able to support the growth of more branches and also leaves, at the same time more biomass has to be allocated to roots in order to supply water and nutrients for increasing maintenance and growth needs. These findings are consistent with the pipe model (Shinozaki *et al*., 1964). Increasing competition for resources with increasing stand biomass is responsible for the nonlinearity of the relationship. The database contained trees with a stem biomass up to about 400 t ha^{-1}. While broadleaf trees were found to be able to support higher branch biomass, needleleaf evergreen trees were found to have higher foliage biomass compared with the other leaf types. However, at a 95% confidence interval, these findings were not significant, except a significantly higher multiplier in the allometric relation between foliage and stem biomass for needleleaf evergreen trees compared with broadleaf trees. The modelled relationship of root biomass to stem biomass was not significantly different between leaf types. Relative uncertainty introduced in this processing step is highest for inferring foliage biomass from stem biomass, especially for needleleaf deciduous trees with low stem biomass values.

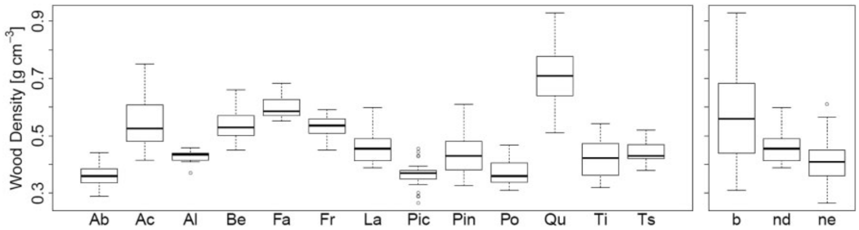

Figure 2 Variance in wood density (g cm^{-3}) measurements contained in the Global Wood Density Database across tree genera (left: Ab, *Abies*; Ac, *Acer*; Al, *Alnus*; Be, *Betula*; Fa, *Fagus*; Fr, *Fraxinus*; La, *Larix*; Pic, *Picea*; Pin, *Pinus*; Po, *Populus*; Qu, *Quercus*; Ti, *Tilia*; Ts, *Tsuga*) and leaf types (right: b, broadleaf; nd, needleleaf deciduous; ne, needleleaf evergreen). The box–whisker plots show the median and the interquartile range of values. The whiskers extend up to the most extreme data point which is no more than 1.5 times the interquartile range away from the box. Outliers are drawn as circles.

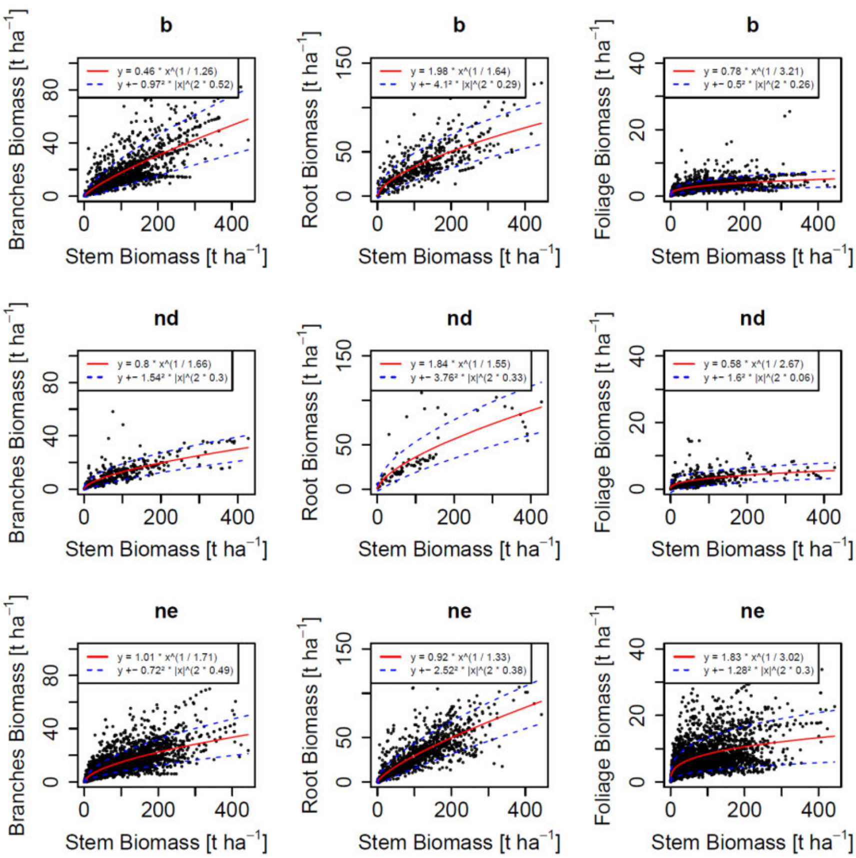

Figure 3 Fitted allometric relationships between stem, branch, root and foliage biomass (t ha^{-1}) using the Biomass Compartment Database [b, broadleaf; nd, needleleaf deciduous; ne, needleleaf evergreen; central solid line, functional relationship; upper and lower bound (dashed), uncertainty bound (standard deviation of the residuals)].

Carbon density map

Most of the forests with the highest carbon content per area (> 8 kg C m^{-2}) are situated along the Rocky Mountains in north-west Canada and the USA, the European mountains (both mostly temperate coniferous forest), European Russia, southern central Siberia (temperate broadleaf and mixed forests, southern boreal forests) and Japan (mostly temperate broadleaf and mixed forests; Fig. 4). In the boreal zone, forest carbon decreases to the north along a latitudinal gradient. The spatial patterns give information on potential carbon loss due to disturbances or potential availability of wood to humans. Corresponding relative uncertainty is most often between 20 and 40%, especially in the high-biomass areas. The lowest relative uncertainties are estimated in the high-biomass areas of north-west Canada and the USA, central Siberia, most European mountain ranges and Japan. The relative uncertainty of this modelling approach increases in the northern taiga, where there is very low biomass.

The individual biomass compartment maps are presented in detail in Appendix S2. The differences in spatial patterns follow the distributions of leaf types in GLC2000 and can be explained by the differences between leaf types in modelled compartment relationships (Fig. 3). The relative uncertainty of stem carbon (Appendix S2) is below 20% in most areas, except for broadleaf trees where the high variation in wood density causes higher

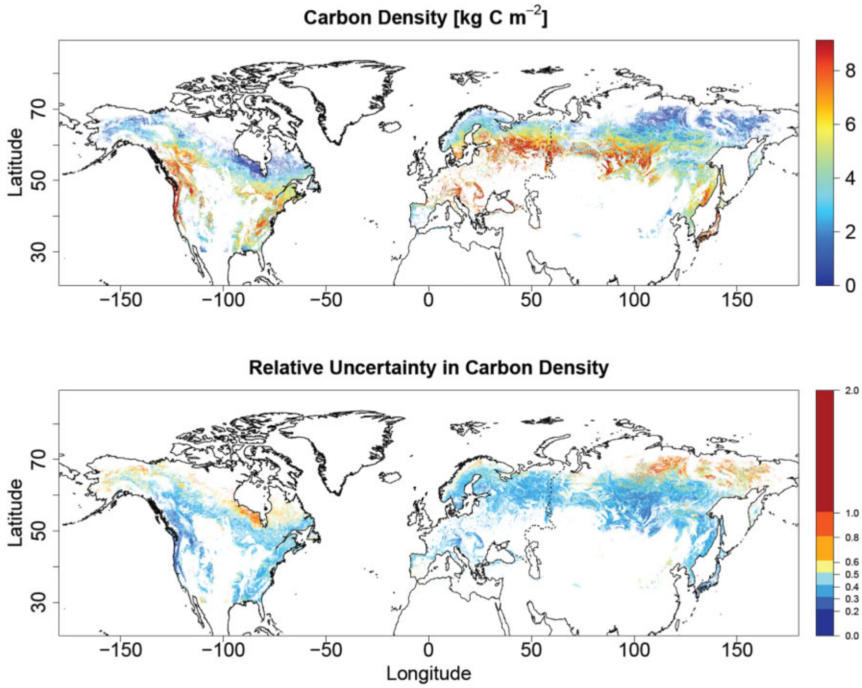

Figure 4 Spatial distribution of total forest carbon density (tree stems + branches + roots + foliage) in Northern Hemisphere boreal and temperate forests and its corresponding relative uncertainty (a value of 1 means 100% uncertainty). Non-forest is masked out according to the GLC2000 land-use/land-cover map (JRC, 2003). The dashed black line indicates the boundary between Europe and Asia (data from ESRI, 2008) used for the estimation of continental carbon stocks in this study.

uncertainties. Modelling of branch, and particularly root and foliage carbon, introduces additional uncertainty (Appendix S2), which is highest (in relative terms) in low-biomass areas (mostly the northern taiga). But as the total carbon map is dominated by stem biomass, while the other compartments account only for a small proportion of total carbon, the overall relative uncertainty of the final map (Fig. 4) is within a very satisfactory range.

For Russia, the estimated carbon density at forest enterprise level agrees well with IIASA data ($r^2 = 0.78$, RMSE = 1.13 kg C m^{-2}, Fig. 5a). In an additional investigation no significant differences in this relationship were found for different bioclimatic zones in Russia (Appendix S3). For the USA, the comparison of aggregated values at county level shows strong agreement with the WHRC NBCD 2000 dataset ($r^2 = 0.90$, RMSE = 0.54 kg C m^{-2}, Fig. 5b). For European countries, evaluation results are comparable ($r^2 = 0.70$, RMSE = 0.87 kg C m^{-2}, Fig. 5c). While there is no systematic error apparent from the intercomparison in Russia, our product might slightly underestimate high carbon densities, as can be seen from the evaluation results for US and European data.

Boreal and temperate forest carbon stock and carbon density

In 2010, the boreal and temperate forests of the Northern Hemisphere (30 to 80° N) stored about 79.8 ± 29.9 Pg C (Table 2) and their mean carbon density was 4.76 ± 1.78 kg C m^{-2} of forest area (Table 3). Most of the forest carbon in the Northern Hemisphere is stored in BFT (40.7 ± 15.7 Pg C), while TBMF and TCF account for 24.5 ± 9.4 Pg C and 14.5 ± 4.8 Pg C, respectively (Table 2). In terms of carbon density, 6.21 ± 2.07 kg C m^{-2} are retained in TCF and 5.80 ± 2.21 kg C m^{-2} in TBMF, whereas we found a mean carbon density of 4.00 ± 1.54 kg C m^{-2} in BFT

Table 2 Estimated mean and uncertainty of total forest carbon for North America, Europe and Asia across three different biomes. Uncertainty denotes the aggregated uncertainty (i.e. standard deviation) of each pixel belonging to the specific biome and continent.

Total forest carbon (Pg C)	North America	Europe	Asia	Sum of three continents
TBMF	9.7 ± 3.8	8.6 ± 3.1	6.2 ± 2.4	24.5 ± 9.4
TCF	10.1 ± 3.3	1.5 ± 0.5	2.9 ± 1.1	14.5 ± 4.8
BFT	8.9 ± 3.7	9.8 ± 3.6	22.1 ± 8.3	40.7 ± 15.7
Sum of three biomes	28.7 ± 10.8	19.9 ± 7.3	31.2 ± 11.8	79.8 ± 29.9

TBMF, temperate broadleaf and mixed forests; TCF, temperate conifer forests; BFT, boreal forests/taiga.

Table 3 Estimated mean and uncertainty of carbon density for North America, Europe and Asia across three different biomes. Uncertainty denotes the aggregated uncertainty (i.e. standard deviation) of each pixel belonging to the specific biome and continent.

Carbon density (kg C m^{-2} forest)	North America	Europe	Asia	Mean of three continents
TBMF	5.42 ± 2.14	6.70 ± 2.46	5.38 ± 2.05	5.80 ± 2.21
TCF	6.42 ± 2.07	7.60 ± 2.62	5.13 ± 1.86	6.21 ± 2.07
BFT	2.99 ± 1.26	5.47 ± 2.04	4.07 ± 1.53	4.00 ± 1.54
Mean of three biomes	4.53 ± 1.71	6.08 ± 2.24	4.36 ± 1.64	4.76 ± 1.78

TBMF, temperate broadleaf and mixed forests; TCF, temperate conifer forests; BFT, boreal forests/taiga.

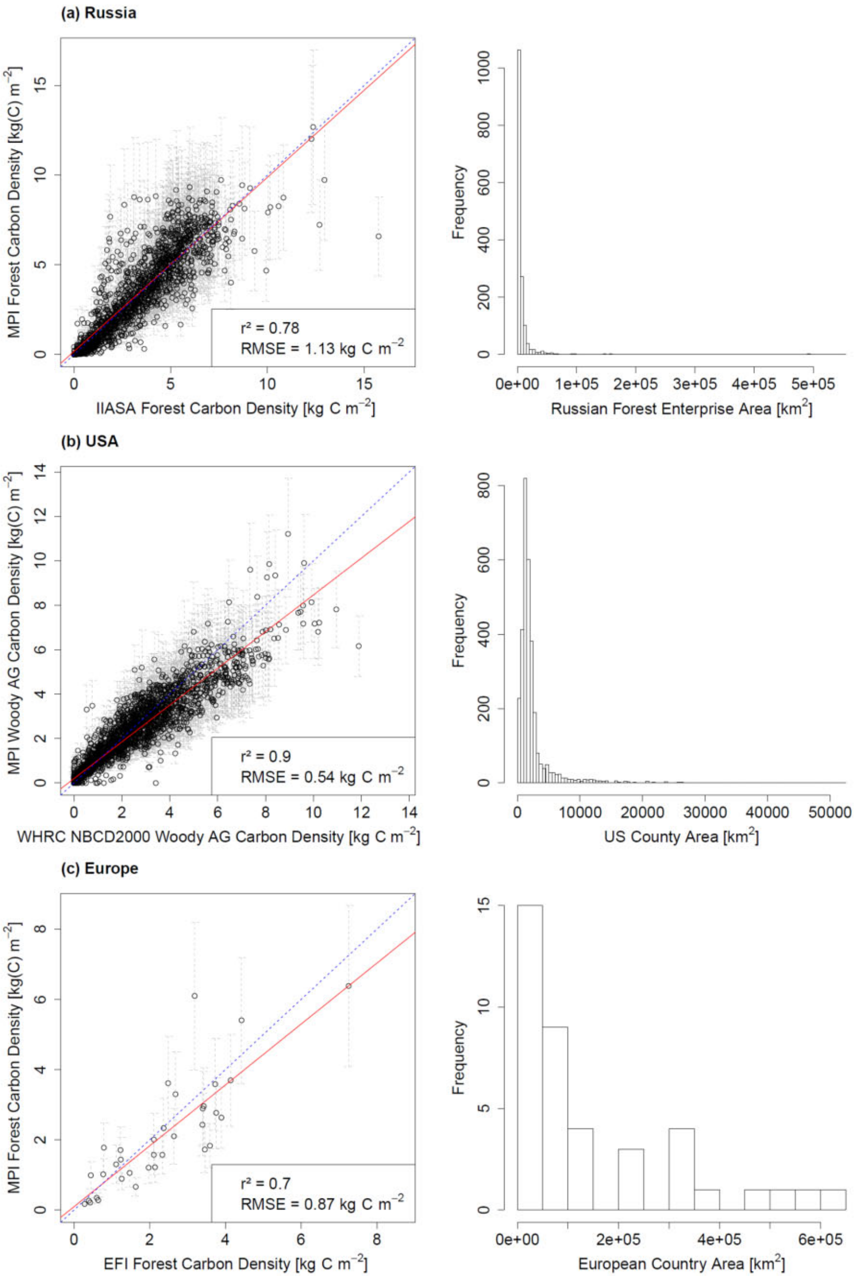

Figure 5 Intercomparison of carbon density data from this study (MPI) and (a) IIASA forest enterprise, (b) WHRC NBCD2000 US county, and (c) EFI European country carbon density data. The dotted line is the 1-to-1 line. The solid line is the linear regression line. Please note: here carbon density is calculated per total (enterprise/county/country) area, not per forest area, due to differences in the estimated forest area between products. Corresponding histograms show the spatial scale at which evaluation took place.

(Table 3). The uncertainty of these estimates is the sum of the uncertainties of all 0.01° pixels and is within the range of 30–40%.

Forest biome carbon stock and density values were also obtained more detailed for North America, Europe and Asia (see Tables 2 & 3 and Fig. 6). Asian BFT account for the largest carbon stock within the investigated biomes. Concerning carbon density, TBMF were found to have a higher carbon density than TCF in Asia, in contrast to the other two continents. European forests exhibit a higher carbon density across all the three biomes compared with North America and Asia. Due to the conservative approach of estimating uncertainty implemented in this study, many of these findings are not significant at the 95% confidence interval. However, some of the reported results are significant. Carbon stocks (Table 2) in TCF are significantly smaller in Europe and Asia than in North America. On the other hand, carbon stocks in BFT are significantly higher in Asia than in Europe and North America. In Europe, there is significantly less carbon stored in TCF than in TBMF and BFT, while in Asia carbon stocks were found to be significantly higher in BFT than in TBMF and TCF. Carbon density (Table 3) is significantly higher in European versus North American BFT. In North America, carbon density was found to be significantly higher in TBMF and TCF than in BFT.

While European forest carbon stocks are relatively small compared with those of the other continents, the carbon density is higher in Europe across all the three biomes compared with North America and Asia (Fig. 6, see also Tables 2 & 3). These patterns are also visible in Fig. 7, which shows carbon density per

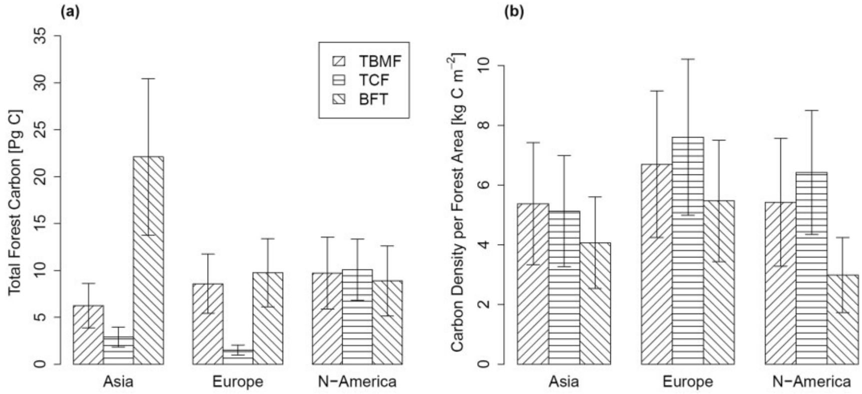

Figure 6 (a) Total carbon stored in Northern Hemisphere forests (TBMF, temperate broadleaf and mixed forests; TCF, temperate conifer forests; BFT, boreal forests/taiga) and (b) their corresponding carbon density.

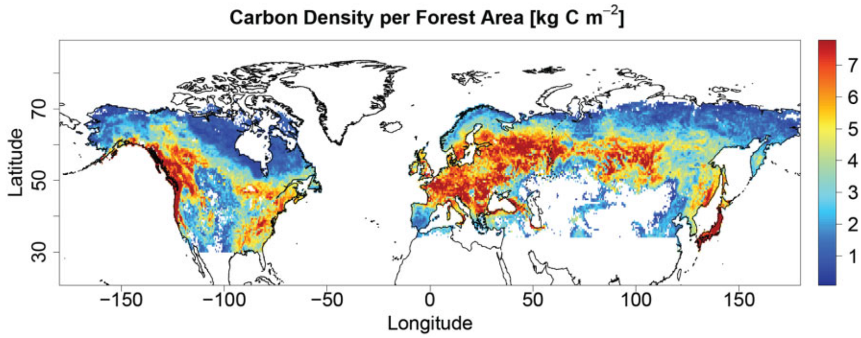

Figure 7 Spatial distribution of carbon density per forest area in Northern Hemisphere boreal and temperate forests (aggregated to 0.5° resolution). The dashed black line indicates the boundary between Europe and Asia (data from ESRI, 2008) used for the estimation of continental carbon stocks in this study.

Table 4 Total forest carbon values reported in other studies. Pan *et al.* (2011) distinguished between continents and biomes. Goodale *et al.* (2002) and Liski *et al.* (2003) distinguished between continents only. Saugier *et al.* (2001) distinguished between biomes only.

Other studies	Total forest carbon (Pg C)	North America	Europe	Asia	Sum of three continents	Saugier *et al.* (2001)§
Pan *et al.* (2011)*	TBMF + TCF	**19.4**	**10.5**	**8.3**	38.2	139
	BFT	**14.0**	**12.1**	**27.9**	53.9	57
	Sum of three biomes	**33.4**	**22.6**	**36.2**	92.1	196
Goodale *et al.* (2002)†	Sum of three biomes	31.3	52.2		83.5	
Liski *et al.* (2003)‡	Sum of three biomes	31	49		80	

TBMF, temperate broadleaf and mixed forests; TCF, temperate conifer forests; BFT, boreal forests/taiga.
*Forest total living biomass from 2007; understorey vegetation may be excluded if very small compared with total biomass; excluding Australia, New Zealand and 'other countries'.
†Live vegetation from 1990; including understorey vegetation.
‡Woody biomass on forest and other wooded land in temperate and boreal forests; including dead trees; including shrubs and bushes; from early/mid 1990s; China, Korea and Japan excluded.
§Carbon in living phytomass; including understorey vegetation; based on different studies.

forest area aggregated to a regional scale (0.5° pixel size). Carbon stocks per area of forest are estimated to be high in central Europe, for example (Fig. 7), while relative to total land the carbon density is small (Fig. 4) since the European landscape is dominated by agricultural areas. Average biomass density is higher in Europe, probably due to the influence of favourable climatic conditions, forest management activities and protected areas. Such information is important, for example for a comparison with process-oriented ecosystem models, such as DGVMs, which are often operated at coarser spatial resolutions like 0.5°.

The obtained forest carbon stock and density values were compared against estimates reported in the literature (Tables 4 & 5), although differences in the method for estimating biomass, the forest area and biomass compartments considered and in the time of investigation limit a direct comparison with other studies. The inclusion of understorey and green forest floor vegetation in literature values in particular might contribute substantially to some disagreements with our reported values, particularly in boreal forests (Schepaschenko *et al.*, 1998; Shvidenko *et al.*, 2007). Furthermore, differences in the

Table 5 Carbon density values calculated from other studies. Pan *et al.* (2011) distinguished between continents and biomes. Goodale *et al.* (2002) and Liski *et al.* (2003) distinguished between continents only. Saugier *et al.* (2001) distinguished between biomes only.

Other studies	Carbon density (kg C m^{-2} forest)	North America	Europe	Asia	Mean of three continents	Saugier *et al.* (2001)§
Pan *et al.* (2011)*	TBMF + TCF	**7.55**	**7.27**	**4.47**	6.51	13.35
	BFT	**6.10**	**5.28**	**4.12**	4.76	4.15
	Mean of three biomes	**6.87**	**6.05**	**4.20**	5.35	8.13
Goodale *et al.* (2002)†	Mean of three biomes	4.46	3.88		4.07	
Liski *et al.* (2003)‡	Mean of three biomes	4.3	4.3		4.3	

TBMF, temperate broadleaf and mixed forests; TCF, temperate conifer forests; BFT, boreal forests/taiga.
*Forest total living biomass and forest area data from 2007; understorey vegetation may be excluded if very small compared with total biomass; excluding Australia, New Zealand and 'other countries'.
†Live vegetation and total forest and woodland area from 1990; including understorey vegetation.
‡Woody biomass on forest and other wooded land in temperate and boreal forests; including dead trees; including shrubs and bushes; from early/mid 1990s; China, Korea and Japan excluded.
§Carbon in living phytomass; including understorey vegetation; based on different studies; using biome area instead of forest area.

definition of GSV between forest inventory and Envisat ASAR data, primarily concerning the inclusion of trees of certain diameters, stumps and necromass, can potentially lead to a bias in the estimated biomass. However, the validation of remote sensing-based biomass against inventory-based estimates showed no clear bias (Santoro *et al.*, 2011). Therefore, we assume the effects of GSV definition to be small compared with other sources of uncertainty. The shift in time between our product and other studies can further contribute to differences, since forest carbon stocks might have been affected significantly, for example by fires, insects (Kurz *et al.*, 2008) or climate change (Allen *et al.*, 2010), in the meantime.

Estimated temperate forest carbon stocks agree well with recently published results by Pan *et al.* (2011), who used a different biomass estimation method based mainly on forest inventory data. The value reported by Saugier *et al.* (2001) for temperate forests seems to be far too high in light of our study. The estimated value for boreal forests is a bit lower than those of Pan *et al.* (2011) and Saugier *et al.* (2001), but at least the value from Pan *et al.* (2011) is within the range of uncertainty of this study. Carbon stocks derived by Goodale *et al.* (2002) and Liski *et al.* (2003) for North America and Eurasia were very close to the results of this study, and were well below the uncertainty margin.

We confirm higher carbon densities in temperate forests compared with boreal forests as already reported by Pan *et al.* (2011) and Saugier *et al.* (2001). Values estimated for boreal forests agree well with these studies; however Saugier *et al.* (2001) dramatically overestimate temperate forest carbon density. While all the densities stated by Pan *et al.* (2011) for European and Asian boreal and temperate forests are within the uncertainty of the values calculated in this study, Pan *et al.* (2011) reported much higher carbon densities in North America, especially for boreal forests. Carbon densities calculated by Goodale *et al.* (2002) and Liski *et al.* (2003) are close to our estimates in North America, but lower in Eurasia.

Outlook

A comparison of different sets of predictors for the modelling of allometric relationships has shown that the applied algorithm could be further improved by the availability of a consistent global tree species map. For example modelling of branch biomass out of stem biomass using a generalized additive model (GAM) (Hastie & Tibshirani, 1990; Wood, 2006; for a detailed description of methods see Appendix S4) was significantly improved in terms of adjusted R^2, root mean square error (RMSE) and Akaike's information criterion (AIC) (Akaike, 1974) when information on tree genus was taken into account (Fig. 8). In contrast, the approach used in this study could only make use of leaf type information in addition to the stem biomass. Results were similar for root and foliage biomass.

The Global Wood Density Database and the Biomass Compartment Database could be explored by tree genus and not by leaf type only. There is a need for a global tree species map comparable to the tree species map covering Europe available from JRC (Köble & Seufert, 2001). Further investigations could explore improvements in the derivation of a biomass map making use of such more detailed information. The consideration of different climate zones could further improve modelling of allometric relationships (Fig. 8). This would require more extensive and standardized measurements of biomass compartments, covering all important tree species across all the different climate zones. In contrast, tree age and tree density did not have much effect on GAM results. Such improvements would lead to a better biomass estimate and to a reduction in the uncertainty of the resulting total carbon map.

It should be noted that the uncertainty estimate given has to be interpreted as an upper bound. As discussed in Taylor (1997), the calculation of the uncertainty of the sum of biomass compartments as the sum of their uncertainties (equation 9) might also lead to an overestimation of the error in the case of dependent variables. A direct estimation of total biomass (as the sum

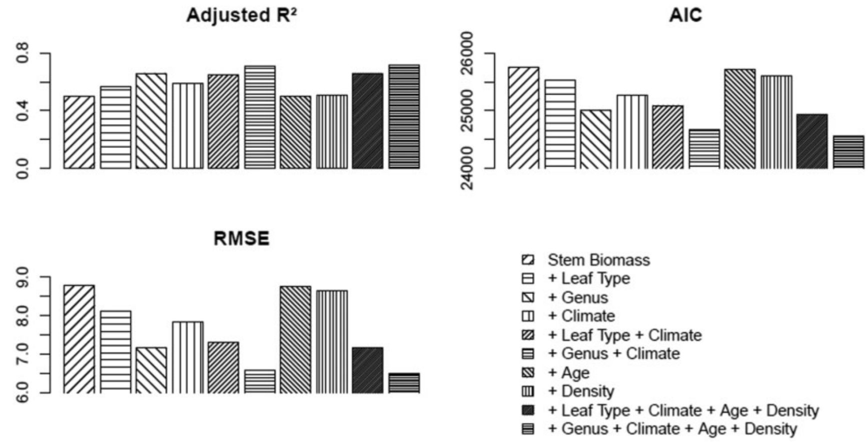

Figure 8 Generalized additive model (GAM) results modelling branch biomass using different sets of predictors (AIC, Akaike's information criterion; RMSE, root mean square error; for a detailed description of methods see Appendix S4).

of compartments) from stem biomass based on the Global Biomass Compartment Database would decrease the uncertainty estimate but lead to an inconsistency between the estimated biomass compartments and the total biomass. Nevertheless, the application of GEP allowed for a conservative uncertainty estimate over a large dataset. Its benefits for ecological studies have already been illustrated by Lo (2005). However, uncertainty estimation due to land cover and of the GSV product should be further improved.

Land-cover information is essential for our method of estimating the biomass at the 0.01° pixel size level since the leaf type determines the applied wood density and the parameters used for the allometric equation (equation 2). Therefore, assuming a pixel size of 0.01° × 0.01° to be covered by a single leaf type is a simplification in our study which we cannot avoid because the underlying GSV map also comes with this pixel size. At a higher level of aggregation, land-cover uncertainty directly translates into forest area uncertainty which is used to estimate total carbon stocks at a continental scale. In general, two types of uncertainty are important here: First, there is no information about forest area within a 0.01° land-cover pixel and second, misclassification leads to uncertainty in forest area at the continental scale. The subpixel uncertainty (first type) effect on carbon stock estimates is considered to be small. In case of a pixel that is classified as forest but in reality contains only minor tree coverage, the GSV estimate at the same scale will be also small. The effects of the second type of uncertainty are also considered to be small since forest misclassifications most often occur in heterogeneous landscapes (Mayaux *et al.*, 2006), where areas of sparse forests with low carbon stocks are usually situated. In this respect, using GLC2000 has the advantage of using a low threshold (15%) of tree cover for forest classification (JRC, 2003). In doing so, we make sure to include most forest areas.

The evaluation results indicate that the accuracy of the presented carbon density map is comparable to upscaled forest inventory data at a regional scale. This highlights the potential of remote sensing data to complement biomass inventories. Although Envisat ASAR data are not optimal and other SAR datasets exist that might lead to improved estimates, only Envisat ASAR data are available globally and are free to users. At a finer resolution of about 1 km, a direct comparison to other data remains problematic. Forest inventory data represent the stand scale and upscaling is also highly uncertain (Gibbs *et al.*, 2007; Saatchi *et al.*, 2007, 2011). Upscaling forest inventory data by high-resolution airborne LiDAR data is the most promising type of product for the evaluation of the small-scale variability of biomass (Patenaude *et al.*, 2004; Saatchi *et al.*, 2011). Such products are being processed currently and should be used in the near future. This will help to also understand if a resolution of 0.01° is also sufficient in spatially heterogeneous European forests or if a finer-scale mapping is required in patchy forest ecosystems.

CONCLUSION

In this study we have presented a biomass map originating from one consistent remote sensing and modelling approach, covering all the extratropical regions of the Northern Hemisphere in a single product with a moderate spatial resolution. This map, together with the spatially explicit quantification of its uncertainty, updates current estimates of the carbon currently stored in the forests of North America, Europe and Asia. Together with recent results of Saatchi *et al.* (2011) or Baccini *et al.* (2012), for example, it can be of great value for a wide range of users, spanning from global climate modellers to national carbon monitoring systems. Evaluation results have shown that this product can serve as a new benchmark regarding spatially explicit and consistent biomass and carbon mapping with moderate spatial resolution. The forest carbon density dataset (total carbon and single compartments) and its corresponding uncertainty are available at the BIOMASAR project website (http://www.biomasar.org) and at the GEOCARBON Data Portal (http://www.bgc-jena.mpg.de/geodb/projects/Home.php).

In the Northern Hemisphere, boreal and temperate forest carbon stocks were found to be almost equal in magnitude. Temperate forests have a higher carbon density than boreal forests. However, due to our conservative uncertainty estimate these findings could be proved to be significant only for North America. Despite higher carbon densities across boreal and temperate forest biomes in Europe when compared with the other continents these are still within its confidence intervals. While our results confirm the temperate forest carbon given in Pan *et al.* (2011), there seems to be less carbon stored in boreal forests than previously estimated (Saugier *et al.*, 2001; Pan *et al.*, 2011), although such a comparison with other studies is problematic due to the different methods employed. We consider an earlier estimate of temperate forest biomass (Saugier *et al.*, 2001) to be unrealistically high. In the future, a regular repetition of consistent biomass estimation from remote sensing data may also help to improve our knowledge on disturbance, deforestation, degradation and regrowth processes in addition to the current state. The lack of continuity of most remote sensing missions is a disadvantage since it implies an additional cross-calibration step between GSV or biomass datasets obtained from different sensors and, therefore, retrieval approaches. The availability of a global tree species map as well as more comprehensive allometric biomass databases would further reduce the uncertainties of the results.

ACKNOWLEDGEMENTS

This study is supported by the European Space Agency (ESA) within the Support to Science Element (STSE) project BIOMASAR (ESRIN contract no. 21892/08/I-EC). The global land-cover map GLC2000 from the Joint Research Centre (JRC), the Global Wood Density Database and the JRC GHG-AFOLU Biomass Compartment Database contributed significantly to this work. For providing reference data on biomass, we want to acknowledge the United States National Biomass and Carbon Dataset for the year 2000 (NBCD2000, provided by Josef Kellndorfer) and the European Forest Institute (EFI).

REFERENCES

Akaike, H. (1974) A new look at the statistical model identification. *IEEE Transactions on Automatic Control*, **19**, 716–723.

Allen, C.D., Macalady, A.K., Chenchouni, H., Bachelet, D., McDowell, N., Vennetier, M., Kitzberger, T., Rigling, A., Breshears, D.B., Hogg, E.H., Gonzalez, P., Fensham, R., Zhang, Z., Castro, J., Demidova, N., Lim, J.-H., Allard, G., Running, S.W., Semerci, A. & Cobb, N. (2010) A global overview of drought and heat-induced tree mortality reveals emerging climate change risks for forests. *Forest Ecology and Management*, **259**, 660–684.

Baccini, A., Goetz, S.J., Walker, W.S., Laporte, N.T., Sun, M., Sulla-Menashe, D., Hackler, J., Beck, P.S.A., Dubayah, R., Friedl, M.A., Samanta, S. & Houghton, R. (2012) Estimated carbon dioxide emissions from tropical deforestation improved by carbon-density maps. *Nature Climate Change*, **2**, 182–185.

Beer, C., Lucht, W., Schmullius, C. & Shvidenko, A. (2006) Small net carbon dioxide uptake by Russian forests during 1981–1999. *Geophysical Research Letters*, **33**, L15403. doi:10.1029/2006GL026919.

Bellassen, V., Delbart, N., Le Maire, G., Luyssaert, S., Ciais, P. & Viovy, N. (2011) Potential knowledge gain in large-scale simulations of forest carbon fluxes from remotely sensed biomass and height. *Forest Ecology and Management*, **261**, 515–530.

Bonan, G.B. (2008) Forests and climate change: forcings, feedbacks, and the climate benefits of forests. *Science*, **320**, 1444–1449.

Boudreau, J., Nelson, R., Margolis, H., Beaudoin, A., Guindon, L. & Kimes, D. (2008) Regional aboveground forest biomass using airborne and spaceborne LiDAR in Québec. *Remote Sensing of Environment*, **112**, 3876–3890.

Chave, J., Coomes, D., Jansen, S., Lewis, S.L., Swenson, N.G. & Zanne, A.E. (2009) Towards a worldwide wood economics spectrum. *Ecology Letters*, **12**, 351–366.

DeFries, R.S., Houghton, R.A., Hansen, M.C., Field, C.B., Skole, D. & Townshend, J. (2002) Carbon emissions from tropical deforestation and regrowth based on satellite observations for the 1980s and 1990s. *Proceedings of the National Academy of Sciences USA*, **99**, 14256–14261.

Denman, K.L., Brasseur, G., Chidthaisong, A., Ciais, P., Cox, P.M., Dickinson, R.E., Hauglustaine, D., Heinze, C., Holland, E., Jacob, D., Lohmann, U., Ramachandran, S., da Silva Dias, P.L., Wofsy, S.C. & Zhang, X. (2007) Couplings between changes in the climate system and biogeochemistry. *Climate change 2007: the physical science basis. Contribution of Working Group I to the Fourth Assessment Report of the Intergovernmental Panel on Climate Change* (ed. by S. Solomon, D. Qin, M. Manning, Z. Chen, M. Marquis, K.B. Averyt, M. Tignor and H.L. Miller), 499–588. Cambridge University Press, Cambridge.

EFI (2005) *LTFRA database*. European Forest Institute. Available at: http://www.efi.int/portal/virtual_library/databases/ (accessed 8 June 2012).

ESRI (2008) *Continents shapefile*. Baruch Geoportal. Baruch College. City University of New York. Available at: <http://www.baruch.cuny.edu/geoportal/data/esri/esri_intl.htm (accessed 7 December 2012).

FAO (2010) *Global Forest Resources Assessment 2010. Main report*. FAO Forestry Paper 163. Food and Agriculture Organization, Rome.

Friedlingstein, P., Cox, P., Betts, R. *et al.* (2006) Climate–carbon cycle feedback analysis: results from the C(4)MIP model intercomparison. *Journal of Climate*, **19**, 3337–3353.

Gibbs, H.K., Brown, S., Niles, J.O. & Foley, J.A. (2007) Monitoring and estimating tropical forest carbon stocks: making REDD a reality. *Environmental Research Letters*, **2**, 045023. doi:10.1088/1748-9326/2/4/045023.

Goodale, C.L., Apps, M.J., Birdsey, R.A., Field, C.B., Heath, L.S., Houghton, R.A., Jenkins, J.C., Kohlmaier, G.H., Kurz, W., Liu, S.R., Nabuurs, G.J., Nilsson, S. & Shvidenko, A.Z. (2002) Forest carbon sinks in the Northern Hemisphere. *Ecological Applications*, **12**, 891–899.

Grainger, A. (2009) Towards a new global forest science. *International Forestry Review*, **11**, 126–133.

Guo, Z., Fang, J., Pan, Y. & Birdsey, R. (2010) Inventory-based estimates of forest biomass carbon stocks in China: a comparison of three methods. *Forest Ecology and Management*, **259**, 1225–1231.

Hastie, T.J. & Tibshirani, R.J. (1990) *Generalized additive models*. Chapman & Hall/CRC, Boca Raton, FL.

Hurtt, G.C., Fisk, J., Thomas, R.Q., Dubayah, R., Moorcroft, P.R. & Shugart, H.H. (2010) Linking models and data on vegetation structure. *Journal of Geophysical Research*, **115**, G00E10. doi:10.1029/2009JG000937.

JRC (2003) *Global Land Cover 2000 database*. European Commission. Joint Research Centre. Available at: http://bioval.jrc.ec.europa.eu/products/glc2000/glc2000.php (accessed 3 July 2012).

JRC (2009) *The Biomass Compartment Database of the GHG-AFOLU project of the European Commission*. Joint Research Centre. Available at: http://afoludata.jrc.ec.europa.eu/index.php/public_area/biomass_compartments (accessed 6 January 2012).

Kellndorfer, J., Walker, W., LaPoint, E. & Kirsch, K. (2010) Statistical fusion of LiDAR, InSAR, and optical remote sensing data for forest stand height characterization: a regional-scale method based on LVIS, SRTM, Landsat ETM+, and ancillary data sets. *Geophysical Research Letters*, **115**, G00E08.

Kellndorfer, J., Walker, W., LaPoint, E., Bishop, J., Cormier, T., Fiske, G., Hoppus, M., Kirsch, K. & Westfall, J. (2012) *NACP aboveground biomass and carbon baseline data (NBCD 2000)*, USA 2000 data set. ORNL DAAC, Oak Ridge, TN. Available at: http://daac.ornl.gov (accessed 7 November 2012)

Köble, R. & Seufert, G. (2001) Novel maps for forest tree species in Europe. *Proceedings of the 8th European Symposium on the Physico-Chemical Behaviour of Air Pollutants: 'A Changing Atmosphere!'*, Torino, Italy, 17–20 September 2001.

Kurz, W.A., Dymond, C.C., Stinson, G., Rampley, G.J., Neilson, E.T., Carroll, A.L., Ebata, T. & Safranyik, L. (2008) Mountain pine beetle and forest carbon feedback to climate change. *Nature*, **452**, 987–990.

Lefsky, M.A., Cohen, W.B., Harding, D.J., Parker, G.G., Acker, S.A. & Gower, S.T. (2002) Lidar remote sensing of aboveground biomass in three biomes. *Global Ecology and Biogeography*, **11**, 393–399.

Liski, J., Korotkov, A.V., Prins, C.F.L., Karjalainen, T., Victor, D.G. & Kauppi, P.E. (2003) Increased carbon sink in temperate and boreal forests. *Climatic Change*, **61**, 89–99.

Lo, E. (2005) Gaussian error propagation applied to ecological data: post-ice-storm-downed woody biomass. *Ecological Monographs*, **75**, 451–466.

Mayaux, P., Eva, H., Gallego, J., Strahler, A.H., Herold, M., Agrawal, S., Naumov, S., De Miranda, E.E., Di Bella, C.M., Ordoyne, C., Kopin, Y. & Roy, P. (2006) Validation of the global land cover 2000 map. *IEEE Transactions on Geoscience and Remote Sensing*, **44**, 1728–1739.

Moorcroft, P.R., Hurtt, G.C. & Pacala, S.W. (2001) A method for scaling vegetation dynamics: the ecosystem demography model (ED). *Ecological Monographs*, **71**, 557–585.

Neumann, M., Saatchi, S.S., Ulander, L.M.H. & Fransson, J.E.S. (2012) Assessing performance of L- and P-Band polarimetric interferometric SAR data in estimating boreal forest aboveground biomass. *IEEE Transactions on Geoscience and Remote Sensing*, **50**, 714–726.

Olson, D.M., Dinerstein, E., Wikramanayake, E.D., Burgess, N.D., Powell, G.V.N., Underwood, E.C., D'Amico, J.A., Itoua, I., Strand, H.E., Morrison, J.C., Loucks, C.J., Allnutt, T.F., Ricketts, T.H., Kura, Y., Lamoreux, J.F., Wettengel, W.W., Hedao, P. & Kassem, K.R. (2001) Terrestrial ecoregions of the world: a new map of life on Earth. *Bioscience*, **51**, 933–938.

Pan, Y., Birdsey, R.A., Fang, J., Houghton, R., Kauppi, P.E., Kurz, W.A., Phillips, O.L., Shvidenko, A., Lewis, S.L., Canadell, J.G., Ciais, P., Jackson, R.B., Pacala, S.W., McGuire, A.D., Piao, S., Rautiainen, A., Sitch, S. & Hayes, D. (2011) A large and persistent carbon sink in the world's forests. *Science*, **333**, 988–993.

Patenaude, G., Hill, R.A., Milne, R., Gaveau, D.L.A., Briggs, B.B.J. & Dawson, T.P. (2004) Quantifying forest above ground carbon content using LiDAR remote sensing. *Remote Sensing of Environment*, **93**, 368–380.

Pinheiro, J. & Bates, D. (2000) *Mixed-effects models in S and S-PLUS*. Springer, New York.

Randerson, J.T., Hoffman, F.M., Thornton, P.E., Mahowald, N.M., Lindsay, K., Lee, Y.-H., Nevison, C.D., Doney, S.C., Bonan, G., Stöckli, R., Covey, C., Running, S.W. & Fung, I.Y. (2009) Systematic assessment of terrestrial biogeochemistry in coupled climate–carbon models. *Global Change Biology*, **15**, 2462–2484.

Ranson, K.J., Sun, G., Lang, R.H., Chauhan, N.S., Cacciola, R.J. & Kilic, O. (1997) Mapping of boreal forest biomass from spaceborne synthetic aperture radar. *Journal of Geophysical Research*, **102**, 29599–29610.

Saatchi, S.S., Houghton, R.A., Alvala, R.C.D., Soares, J.V. & Yu, Y. (2007) Distribution of aboveground live biomass in the Amazon Basin. *Global Change Biology*, **13**, 816–837.

Saatchi, S.S., Harris, N.L., Brown, S., Lefsky, M., Mitchard, E.T., Salas, W., Zutta, B.R., Buermann, W., Lewis, S.L., Hagen, S., Petrova, S., White, L., Silman, M. & Morel, A. (2011) Benchmark map of forest carbon stocks in tropical regions across three continents. *Proceedings of the National Academy of Sciences USA*, **108**, 9899–9904.

Santoro, M., Beer, C., Cartus, O., Schmullius, C., Shvidenko, A., McCallum, I., Wegmüller, U. & Wiesmann, A. (2011) Retrieval of growing stock volume in boreal forest using hyper-temporal series of Envisat ASAR ScanSAR backscatter measurements. *Remote Sensing of Environment*, **115**, 490–507.

Santoro, M., Cartus, O., Fransson, J.E.S., Shvidenko, A., McCallum, I., Hall, R.J., Beaudoin, A., Beer, C. & Schmullius, C. (2013) Estimates of forest growing stock volume for Sweden, Central Siberia and Québec using Envisat Advanced Synthetic Aperture Radar backscatter data. *Remote Sensing*, **5**, 4503–4532.

Saugier, B., Roy, J. & Mooney, H.A. (2001) Estimations of global terrestrial productivity: converging toward a single number?

Terrestrial global productivity (ed. by J. Roy, B. Saugier and H.A. Mooney), pp. 543–557. Academic Press, San Diego, CA.

Schepaschenko, D., Shvidenko, A. & Nilsson, S. (1998) Phytomass (live biomass) and carbon of Siberian forests. *Biomass and Bioenergy*, **14**, 21–31.

Schepaschenko, D., McCallum, I., Shvidenko, A., Fritz, S., Kraxner, F. & Obersteiner, M. (2011) A new hybrid land cover dataset for Russia: a methodology for integrating statistics, remote sensing and *in situ* information. *Journal of Land Use Science*, **6**, 245–259.

Shinozaki, K., Yoda, K., Hozumi, K. & Kira, T. (1964) A quantitative analysis of plant form – the pipe model theory. I. Basic analyses. *Japanese Journal of Ecology*, **14**, 97–105.

Shvidenko, A., Schepaschenko, D., Nilsson, S. & Bouloui, Y. (2007) Semi-empirical models for assessing biological productivity of northern Eurasian forests. *Ecological Modelling*, **204**, 163–179.

Shvidenko, A., Schepaschenko, D., McCallum, I. & Nilsson, S. (2010) Can the uncertainty of full carbon accounting of forest ecosystems be made acceptable to policymakers? *Climatic Change*, **103**, 137–157.

Somogyi, Z., Teobaldelli, M., Federici, S., Matteucci, G., Pagliari, V., Grassi, G. & Seufert, G. (2008) Allometric biomass and carbon factors database. *iForest – Biogeosciences and Forestry*, **1**, 107–113.

Taylor, J.R. (1997) *An introduction to error analysis. The study of uncertainties in physical measurements*. University Science Books, Sausalito, CA.

Teobaldelli, M., Somogyi, Z., Migliavacca, M. & Usoltsev, V.A. (2009) Generalized functions of biomass expansion factors for conifers and broadleaved by stand age, growing stock and site index. *Forest Ecology and Management*, **257**, 1004–1013.

Thomas, S.C. & Martin, A.R. (2012) Carbon content of tree tissues: a synthesis. *Forests*, **3**, 332–352.

UN-REDD (2011) *UN-REDD Programme. Support to National REDD+ Action*. Global Programme Framework 2011–2015. Adopted as of 9 August 2011. The United Nations Collaborative Programme on Reducing Emissions from Deforestation and Forest Degradation in Developing Countries.

USDA (2012) *Forest inventory and analysis national program*. United States Department of Agriculture. Available at: http://www.fia.fs.fed.us/ (accessed 7 November 2012).

Wagner, W., Luckman, A., Vietmeier, J., Tansey, K., Balzter, H., Schmullius, C., Davidson, M., Gaveau, D., Gluck, M., Le Toan, T., Quegan, S., Shvidenko, A., Wiesmann, A. & Yu, J.J. (2003) Large-scale mapping of boreal forest in Siberia using ERS tandem coherence and JERS backscatter data. *Remote Sensing of Environment*, **85**, 125–144.

Wolf, A., Ciais, P., Bellassen, V., Delbart, N., Field, C.B. & Berry, J.A. (2011) Forest biomass allometry in global land surface models. *Global Biogeochemical Cycles*, **25**, GB3015. doi:10.1029/2010GB003917.

Wood, S.N. (2006) *Generalized additive models: an introduction with R*. Chapman & Hall/CRC Press, Boca Raton, FL.

Wutzler, T., Wirth, C. & Schumacher, J. (2008) Generic biomass functions for common beech (*Fagus sylvatica*) in central Europe: predictions and components of uncertainty. *Canadian Journal of Forest Research*, **38**, 1661–1675.

Zanne, A.E., Lopez-Gonzalez, G., Coomes, D.A., Ilic, J., Jansen, S., Lewis, S.L., Miller, R.B., Swenson, N.G., Wiemann, M.C. & Chave, J. (2009) *Data from: towards a worldwide wood economics spectrum*. Dryad Digital Repository. Available at: http://datadryad.org/handle/10255/dryad.234 (accessed 2 November 2011).

Zianis, D., Muukkonen, P., Mäkipää, R. & Mencuccini, M. (2005) Biomass and stem volume equations for tree species in Europe. *Silva Fennica Monographs*, **4**, 63.

Zuur, A.F., Ieno, E.N., Walker, N.J., Saveliev, A.A. & Smith, G.M. (2009) *Mixed effects models and extensions in ecology with R*. Springer, New York.

SUPPORTING INFORMATION

Additional supporting information may be found in the online version of this article at the publisher's web-site.

Appendix S1 GLC2000 classes and their aggregation to leaf types.

Appendix S2 Spatial distribution of biomass compartment carbon density in Northern Hemisphere boreal and temperate forests and its corresponding relative uncertainty.

Appendix S3 Intercomparison of this study's (MPI) and IIASA forest enterprise carbon density data for different bioclimatic zones in Russia.

Appendix S4 Modelling of branch, root and foliage biomass out of stem biomass and other predictors using generalized additive models.

BIOSKETCH

Martin Thurner is a PhD student at Max Planck Institute for Biogeochemistry in Jena, Germany. His main research interest is to improve climate carbon cycle models by the integration of remote sensing data.

Editor: Josep Penuelas

EXHIBIT EGC-3

Percentage of Hours Burning Oil (2017, Selected Months)

	Winter	
	Jan	Feb
Manchester Street		
Unit 9	0%	0%
Unit 10	0%	0%
Unit 11	0%	0%
Ocean State Power		
Unit 1	-	0.07%
Unit 2	-	0.06%
Pawtucket Power		
Unit 1	-	-

Percentage of Hours Burning Oil (2016, Selected Months)

	Winter			Summer	
	Jan	Feb	Dec	Jul	Aug
Manchester Street					
Unit 9	0%	0%	0%	0%	0%
Unit 10	0%	0%	0%	0%	0%
Unit 11	0.03%	0%	0%	0%	0%
Ocean State Power					
Unit 1	0%	0%	0%	0%	0%
Unit 2	0%	0%	0%	0%	0%
Pawtucket Power					
Unit 1	-	0%	50%	0%	0%

Percentage of Hours Burning Oil (2015, Selected Months)

	Winter			Summer	
	Jan	Feb	Dec	Jul	Aug
Manchester Street					
Unit 9	0%	-	0%	0%	0%
Unit 10	16%	67%	0%	0%	0%
Unit 11	15%	77%	0%	0%	0%
Ocean State Power					
Unit 1	35%	44%	0%	0%	0%
Unit 2	32%	71%	0%	0%	0%
Pawtucket Power					
Unit 1	100%	95%	0%	0%	2%

Percentage of Hours Burning Oil (2014, Selected Months)

	Winter			Summer	
	Jan	Feb	Dec	Jul	Aug
Manchester Street					
Unit 9	37%	16%	0%	0%	0%
Unit 10	0%	37%	0%	0%	0%
Unit 11	51%	17%	0%	0%	0%
Ocean State Power					
Unit 1	0%	0%	0%	0%	0%
Unit 2	0%	0%	0%	0%	0%
Pawtucket Power					
Unit 1	-	-	0%	0%	0%

Percentage of Hours Burning Oil (2013, Selected Months)

	Winter			Summer	
	Jan	Feb	Dec	Jul	Aug
Manchester Street					
Unit 9	4%	17%	10%	0%	0%
Unit 10	4%	19%	0%	0%	0%
Unit 11	0%	0%	33%	0%	0%
Ocean State Power					
Unit 1	0%	0%	0%	0%	0%
Unit 2	0%	-	0%	0%	0%
Pawtucket Power					
Unit 1	-	-	-	0%	0%

Note: Dash means did not operate during the month.

Source: EPA CEMS